People's Democratic Republic of Algeria
Ministry of Higher Education and Scientific Research
University 20 August 1955 – Skikda

Ref :D012125036D

Faculty of Technology
Department of Electrical Engineering
Automatic Laboratory of Skikda

Thesis

For the Degree of

Doctor of Philosophy

Domain: Science and Technology

Section: Automatic

Specialty: Diagnosis and Systems Supervisory

Presented by

Alima Chaouche

Theme

Advanced control for biological reactors of water treatment.

Presented publicly on:

The jury composed

Président	**Pr. Lachouri Abderrazak**	**Full Professor**	**University of Skikda Alegria.**
Supervisor	**Pr. Ramdani Messaoud**	**Full Professor**	**University of Annaba Alegria.**
Co-supervisor	**Pr. Mehennaoui Lamine**	**Full Professor**	**University of Skikda Alegria.**
Examiners	**Pr. Guechi El Hadi**	**Full Professor**	**University of Skikda Alegria.**
	Pr. Kourd Yahia	**Full Professor**	**University of Souk Ahras Ageria.**
	Pr. Gherbi Sofiane	**Full Professor**	**University of Annaba Alegria.**
	Pr. Bouden Toufik	**Full Professor**	**University of Jijel Alegria.**

Year 2025

République Algérienne Démocratique et Populaire
Ministère de l'Enseignement Supérieur et de la Recherche Scientifique
Université 20 Août 1955 - Skikda

Ref :D012125036D

Faculté de Technologie
Département de Génie Electrique
Laboratoire LRES Skikda

THÈSE

En vue de l'obtention du diplôme de

Doctorat En Science

Domaine : Science et Technologie

Filière : Automatique

Spécialité : Diagnostic et Surveillance des systèmes

Présentée par

Chaouche Alima

Thème

Commande avancée des réacteurs biologiques de traitement des eaux

Soutenue publiquement le
Devant le jury composé de :

Président	**Pr. Lachouri Abderrazak**	**Professeur**	Université 20 août 1955 - Skikda.
Encadreur	**Pr. Ramdani Messaoud**	**Professeur**	Université Badji Mokhtar - Annaba
Co-Encadreur	**Pr. Mehennaoui Lamine**	**Professeur**	Université 20 août 1955 - Skikda.
Examinateurs	**Pr. Guechi El Hadi**	**Professeur**	Université 20 août 1955 - Skikda.
	Pr. Kourd Yahia	**Professeur**	Université Souk Ahras.
	Pr. Gherbi Sofiane	**Professeur**	Université Badji Mokhtar-Annaba.
	Pr. Bouden Toufik	**Professeur**	Université de Jijel.

Année 2025

Abstract

This thesis addresses the development of robust control and unknown input estimation methods for complex dynamic systems, with a particular focus on the biological treatment of wastewater by activated sludge. The primary goal is to develop advanced theoretical and methodological tools to enhance the monitoring and control of industrial processes characterized by nonlinear dynamics, parametric uncertainties, and fault occurrences.

The first part presents the biological wastewater treatment process and its ASM1 mathematical model. To overcome the complexity limiting real-time applications, a reduced model tailored to sequencing batch reactors (SBR) is introduced, facilitating the design of observers and control strategies.

The second part lays the theoretical groundwork on singular and linear parameter varying (LPV) systems, examining their structural properties such as regularity, controllability, and observability along side stability analysis via parameter dependent Lyapunov functions. The use of linear matrix inequalities (LMIs) for robust system analysis and controller synthesis is also detailed.

A key contribution of this thesis is the formulation of three novel unknown input estimation algorithms for a class of nonlinear systems combining LPV components and purely Lipschitz nonlinearities. Each algorithm is designed according to the distribution of unknown inputs within the system, enabling the estimation of the maximum possible unknown inputs unlike existing approaches which address only specific cases. Prior to introducing these algorithms, a general H_∞ observer design methodology based on LMIs is developed for nonlinear descriptor systems with nonlinear outputs. This approach exploits a tailored Lyapunov function to avoid the differentiation of disturbances, resulting in less conservative LMI conditions. The reduction in conservatism is attributed to the specific Lyapunov function structure, a judicious application of Youngs inequality, and a reformulation of the Lipschitz condition.

Finally, two advanced control strategies for dissolved oxygen regulation in activated sludge processes are proposed: a neural network-based model predictive control (NNMPC) optimized via metaheuristic algorithms such as Particle Swarm Optimization (PSO) and Genetic Algorithms (GA), and a fault-tolerant dynamic output feedback control (DOFFTC) strategy. The DOFFTC leverages our unknown input estimation algorithm for LPV/nonlinear Lipschitz systems, formulated through linear matrix inequality (LMI) constraints, to actively estimate and compensate for dynamic sensor faults. Independently implemented and validated on the BSM1 benchmark within MATLAB/Simulink, this approach demonstrates significant improvements in robustness, fault resilience, and overall control accuracy. The proposed DOFFTC offers an advanced and reliable solution for the sus-

tainable and efficient management of wastewater treatment processes.

Keywords: Fault-Tolerant Control, Singular Systems, Unknown Input Observers,Linear Parameter Variable models, Wastewater Treatment, $\mathcal{H}_\infty$ Robust Control, Unknown Input Estimation, Nonlinear Dynamical Systems, Activated Sludge Systems, Linear Matrix Inequalities (LMI), Lyapunov Methods, Fault Detection.

Résumé

Cette thèse traite du développement de méthodes de contrôle robuste et d'estimation des entrées inconnues pour des systèmes dynamiques complexes, avec un accent particulier sur le traitement biologique des eaux usées par boues activées. L'objectif principal est de développer des outils théoriques et méthodologiques avancés pour améliorer la surveillance et le contrôle des procédés industriels caractérisés par des dynamiques non linéaires, des incertitudes paramétriques et la survenue de défauts.

La première partie présente le procédé de traitement biologique des eaux usées ainsi que son modèle mathématique ASM1. Pour surmonter la complexité limitant les applications en temps réel, un modèle réduit adapté aux réacteurs séquentiels à batch (SBR) est proposé, facilitant la conception des observateurs et des stratégies de contrôle.

La deuxième partie établit les fondements théoriques des systèmes singuliers et des systèmes à paramètres variables linéaires (LPV), en examinant leurs propriétés structurelles telles que la régularité, la contrôlabilité et lobservabilité ainsi que lanalyse de stabilité via des fonctions de Lyapunov dépendantes des paramètres. L'utilisation des inégalités matricielles linéaires (LMI) pour lanalyse robuste et la synthèse des contrôleurs est également présentée en détaille.

Une contribution majeure de cette thèse est le développement de trois nouveaux algorithmes d'estimation des entrées inconnues pour une classe de systèmes non linéaires combinant des parties LPV et des non-linéarités purement Lipschitz. Chaque algorithme est conçu en fonction de la distribution des entrées inconnues dans le système, permettant ainsi d'estimer le maximum possible d'entrées inconnues contrairement aux méthodes existantes qui ne considèrent que des cas particuliers. Avant d'introduire ces algorithmes, une méthodologie générale de conception d'observateur H_∞ basée sur les LMI est développée pour des systèmes descripteurs non linéaires à sorties non linéaires. Cette approche utilise une fonction de Lyapunov spécifique pour éviter la différentiation des perturbations, ce qui conduit à des conditions LMI moins conservatrices. La réduction de la conservatisme est attribuée à la structure spécifique de la fonction de Lyapunov, à une application judicieuse de l'inégalité de Young, et à une reformulation de la condition de Lipschitz.

Deux stratégies de commande avancées pour la régulation de l'oxygène dissous dans les procédés de boues activées sont finalement proposées : une commande prédictive basée sur les réseaux de neurones (NNMPC), optimisée par des algorithmes méta-heuristiques tels que l'optimisation par essaim de particules (PSO) et les algorithmes génétiques (GA), ainsi qu'une stratégie de commande tolérante aux défauts par retour dynamique de la sortie (DOFFTC). La stratégie DOFFTC s'appuie sur notre algorithme d'estimation d'entrées inconnues pour les systèmes LPV/non linéaires de type Lipschitz, formulé à l'aide de contraintes sous forme d'inégalités matricielles linéaires (LMI), afin d'estimer et de

compenser activement les défauts dynamiques des capteurs. Mise en œuvre de façon indépendante et validée sur le benchmark BSM1 dans lenvironnement MATLAB/Simulink, cette approche montre des améliorations significatives en matière de robustesse, de résilience face aux défauts, et de précision globale de la commande. La stratégie DOFFTC proposée constitue une solution avancée et fiable pour une gestion durable et efficace des procédés de traitement des eaux usées.

Mots-clés : Commande Tolérante aux Défauts, Systèmes Singuliers, Observateurs d'Entrées Inconnues, Modèles LPV, Traitement des Eaux Usées, Inégalités Matricielles Linéaires (LMI), Commande Robuste $\mathcal{H}_\infty$, Systèmes Dynamiques Non Linéaires, Systèmes à Boues Activées, Méthodes de Lyapunov, Détection de Défauts.

ملخص

تتناول هذه الأطروحة تطوير طرق التحكم المتين وتقدير المدخلات المجهولة للأنظمة الديناميكية المعقدة، مع تركيز خاص على المعالجة البيولوجية لمياه الصرف الصحي باستخدام الحمأة المنشطة. ويتمثل الهدف الرئيسي في تطوير أدوات نظرية ومنهجية متقدمة من شأنها أن تُحسِّن مراقبة والتحكم في العمليات الصناعية التي تتسم بديناميكيات غير خطية، وعدم يقين في المعاملات، واحتمال حدوث الأعطال الخاص بها.

الجزء الأول يقدِّم عملية المعالجة البيولوجية لمياه الصرف الصحي وكذلك نموذجها الرياضيASM1 وللتغلب على التعقيد الذي يحدَ من التطبيقات في الزمن الحقيقي، تم اقتراح نموذج مبسَط مكيَف مع المفاعلات الدورية المتسلسلة (SBR) مما يسهل تصميم المراقب واستراتيجيات التحكم.

يتناول هذا الجزء الأسس النظرية للأنظمة الشاذة (Systémes singuliers) والأنظمة ذات المعاملات المتغيرة خطيًا (LPV)، ويتم فيه دراسة الخصائص البنيوية لهذه الأنظمة، مثل خاصية الانتظام، وقابلية التحكم، وقابلية الملاحظة. كما يُعرض تحليل الاستقرار بالاعتماد على دوال ليابونوف المرتبطة بالمعاملات. علاوة على ذلك، يقدَّم استخدام المتباينات المصفوفية الخطية (LMI) كأداة فعّالة للتحليل المتين وتصميم وحدات التحكم، مع شرحٍ مفصّل لخطوات التحليل والتركيب.

تتمثل إحدى المساهمات الرئيسية لهذه الأطروحة في تطوير ثلاثة خوارزميات جديدة لتقدير المدخلات المجهولة لفئة من الأنظمة غير الخطية التي تجمع بين الأجزاء ذات المعاملات المتغيرة خطيًا (LPV) واللاخطية من نوع ليبشيتز بحتة. تم تصميم كل خوارزمية وفقًا لتوزيع المدخلات الجهولة داخل النظام، مما يسمح بتقدير العدد الأقصى الممكن من هذه المدخلات المجهولة، بخلاف الطرق الموجودة التي لا تأخذ بعين الاعتبار إلا بعض الحالات الخاصة. وقبل عرض هذه الخوارزميات، تم تطوير منهجية عامة لتصميم مراقب $\mathcal{H}_\infty$ تعتمد على المتراجحات المصفوفية الخطية (LMI) لفائدة الأنظمة الوصفية غير الخطية ذات المخرجات غير الخطية. تعتمد هذه المقاربة على استخدام دالة ليابونوف خاصة لتجنب اشتقاق الاضطرابات، مما يؤدي إلى شروط LMI أقل تحفظًا. ويَرجع تقليل التحفّظ إلى البنية الخاصة لدالة ليابونوف، وإلى التطبيق الذكي لمتراجعة يونغ، إضافةً إلى إعادة صياغة شرط ليبشيتز.

في نهاية هذه الأطروحة تم اقتراح استراتيجيتين متقدمتين للتحكم في تنظيم الأوكسجين المذاب في عمليات معالجة مياه الصرف الصحي بواسطة نظام الحمأة المنشطة.
الاستراتيجية الأولى هي التحكم التنبؤي القائم على الشبكات العصبية (NNMPC) والمُحسَّنة باستخدام خوارزميات ميتا-ابتكارية مثل خوارزمية سرب الجسيمات (PSO) والخوارزميات الجينية (GO).

أما الاستراتيجية الثانية فتتمثل في منظومة تحكم متسامحة مع الأعطال تعتمد على آلية الاسترجاع الديناميكي للمخرجات (DOFFTC).

ترتكز هذه المنظومة على خوارزمية التقدير المطوَّرة للمدخلات المجهولة ضمن فئة الأنظمة غير الخطية من نوع LPV/Lipschitz والمُبرمجة وفق قيود رياضية معبر عنها بمتراجحات مصفوفية خطية (LMI)، وذلك بغرض تحقيق تقدير دقيق وتعويض فعال للأعطال الديناميكية في المستشعرات، بما يضمن تعزيز المتانة والاعتمادية في الأداء العام لمنظومة التحكم. قد تم تنفيذ هذه الاستراتيجية بشكل مستقل والتحقق من صحتها على النموذج المرجعي ASM1 باستخدام MATLAB/Simulink حيث أظهرت تحسينات كبيرة من حيث المتانة، القدرة على التكيّف مع الأعطال والدقة العامة في التحكم.

تشكل الاستراتيجية المقترحة (DOFFTC) حلاً متقدمًا وموثوقًا من أجل إدارة مستدامة وفعّالة لعمليات معالجة مياه الصرف الصحي.

الكلمات المفتاحية: التحكم المتسامح مع الأعطال، الأنظمة المفردة (Singuliers)، المراصد ذات المدخلات المجهولة، النماذج ذات المعاملات المتغيرة خطيًا (LPV)، معالجة مياه الصرف الصحي، المتراجحات المصفوفية الخطية (LMI)، التحكم المتين ($\mathcal{H}_\infty$) الأنظمة الديناميكية غير الخطية، أنظمة الحمأة المنشطة، طرق ليابونوف، كشف الأعطال.

Dedication

I proudly dedicate this thesis :

*To **Allah**, the source of all knowledge and inspiration.*

*To my husband **Khaled** and cherished daughters **Ratil and Tasnim**,*
my sanctuary and reason for being.

To my parents, pillars of my life,
and to my brothers and sisters, fellow travelers.

To all who illuminated my path:
professors, mentors, and research companions,
whose guidance shaped this work.

Acknowledgments

First and foremost, I would like to thank Almighty God for granting me the strength, patience, and determination to carry out this work and for guiding me throughout my academic journey.

I would like to express my sincere gratitude to my thesis supervisor, **Professor Messaoud Ramdani**, for his unwavering support, valuable guidance, and encouragement throughout the preparation of this thesis. His expertise and trust were instrumental in helping me overcome challenges and move forward with confidence. I also acknowledge **Professor Lamine Mehenneoui**, my co-supervisor, whose presence in the supervision committee is appreciated.

I am deeply grateful to **Professor Ali Zemouche**, whose support has been both scientific and personal. His generosity, availability, and inspiring guidance have played a key role in my progress. I especially thank him for welcoming me for a long-term research internship at the CRAN laboratory, which constituted a pivotal experience in the development of this thesis.

I would also like to warmly thank **Dr. Khadidja Chaib Draa**, who provided significant assistance during a crucial phase of my research. Her involvement, especially during the preparation and production of my article, was extremely valuable, and I am deeply grateful for her dedication and constant support.

My special thanks go to **Professor Abderrazek Lachouri**, whose help was decisive during a particularly critical period. His timely and efficient intervention greatly facilitated the administrative process, enabling me to defend this thesis on time. I sincerely thank him for his availability and support.

I am also grateful to my colleagues and all those who, through their discussions, advice, and presence, contributed in various ways to the completion of this thesis.

Finally, I would like to express my deepest gratitude to **my family**, whose love, encouragement, and patience have supported me throughout every step of this journey. To **my friends**, thank you for being a source of comfort, motivation, and joy during both the difficult and the rewarding moments of this academic adventure.

Chaouche Alima

List of Notations and Acronyms

Acronyms

LTI	Linear Time Invariant
LPV	Linear Parameter Varying
UIO	Unknown Input Observer
LMI	Linear Matrix Inequality
BMI	Bilinear Matrix Inequality.
DMVT	Differential Mean Value Theorem
NNMPC	Neural Network Model Predictive Control
PSO	Particle Swarm Optimization.
GA	Genetic Algorithm
LM	Levenberg Marquardt
FTC	Fault Tolerant Control
DOFC	Dynamic Output Feedback Control
DOF_FTC	Dynamic Output Feedback FTC
ARE	Algebraic Riccati Equation
ARI	Algebraic Riccati Inequality
ASM	Activated Sludge Model
DAE	Differential-Algebraic Equations
DCO	Chemical Oxygen Demand
IAWQ	International Association on Water Quality
IWA	International Water Association
MPC	Model Predictive Control
ODE	Ordinary Differential Equations
ASM	Activated Sludge Model
BOD	Biological Oxygen Demand
DO	Dissolved Oxygen
SBR	Sequencing Batch Reactor
WWTP	Wastewater Treatment Plant

Mathematical Notations

Sets and Spaces

$\mathbb{R}, \mathbb{C}$	Real, Complex numbers
$\mathbb{N}, \mathbb{N}^*$	Natural numbers
$\mathbb{R}_+$	$[0, \infty)$
$\mathbb{R}^n$	n-dim real space
$\mathbb{R}^{n\times m}$	$n \times m$ matrices
C^k, C^∞	k-times differentiable function , Smooth (infinitely differentiable) function
l_2^s	$\|x\|_{l_2} = (\sum \|x(k)\|^2)^{1/2}$
$C^1(\mathbb{R}^n)$	Continuously differentiable functions
$\mathrm{Im}\, B$	Column space of B
$f(\cdot) > 0$	Positive definite
$f(\cdot) \geq 0$	Positive semi-definite

Linear Algebra

$P > 0$	Positive definite matrix
$P \geq 0$	Positive semi-definite
$A > B$	$A - B > 0$
$A \geq B$	$A - B \geq 0$
$\mathrm{He}(A)$	$A + A^T$
A^T, A^{-1}	Transpose, Inverse
I, I_r	Identity matrix
$0, 0_{(n,m)}$	Zero matrices
$\mathrm{tr}(A)$	Trace of A
$\mathrm{rk}(A)$	Rank of A
$\det(A)$	Determinant
$\mathrm{Im}(A)$	Image space
$\ker(A)$	Kernel
$\lambda(A)$	Eigenvalues
$\sigma(A)$	Singular values
$\|v\|$	Euclidean norm
diag	Block diagonal
$e_s(i)$	Basis vector

Contents

List of Tables

List of Figures

Chapter 1

General introduction

"The thesis of a thousand pages begins with a single equation."
(Adapted from Lao Tzu)

Wastewater treatment represents a major public health challenge worldwide, with several million deaths annually attributed to the consumption of contaminated water [7]. Originating from domestic, agricultural, and industrial activities, wastewater contains pollutants that can severely harm aquatic ecosystems when discharged without prior treatment. To address this, increasingly sophisticated treatment methods are being developed, among which the biological treatment phase, particularly the activated sludge process, plays a central role. However, ensuring the stability and optimal performance of such systems is a challenging task due to their large-scale nonlinear dynamics, frequent perturbations in influent flow rate and pollutant load, and uncertainties related to the composition of the incoming wastewater.

In the context of wastewater treatment, the development of accurate yet tractable models is a critical step toward achieving reliable operation, particularly in the presence of strong nonlinearities, unmeasured variables, and external disturbances. Traditional modeling approaches, such as the Activated Sludge Model No.1 (ASM1) [8], offer a detailed description of biological processes through a set of 13 nonlinear differential equations and more than 20 parameters. While accurate, the computational complexity of ASM1 renders it impractical for real-time control and estimation tasks.

To bridge the gap between model accuracy and computational tractability, the Takagi-Sugeno (TS) fuzzy framework [9] and its equivalent quasi-LPV representation [10] offer a powerful solution by expressing nonlinear dynamics through convex combinations of local linear models. These approaches provide universal approximation capabilities [11] while enabling LMI-based stability analysis [12]. The derived multi-model structure preserves nonlinear system properties through smooth interpolation between operating regions, yet remains computationally tractable via linear synthesis techniques. This is particularly evident in the LPV formalism [12, 13], where parameter variations are governed by measurable scheduling variables (e.g., influent flow rate Q_{in}, substrate concentration S_{in}), allowing conventional linear control methods to handle inherently nonlinear behaviors.

Reduced-order models, such as those proposed by Chachuat [14], preserve essential

process dynamics while simplifying their structure and reduce the number of variables. However, they remain challenging for estimation due to inherent nonlinearities and unknown inputs. A major issue in the real-time estimation of reduced-order model $ASM1$ variables is the unavailability of influent concentrations such as $X_{\text{in}}^{\text{DCO}}$, $S_{\text{in}}^{\text{NO}}$, $S_{\text{in}}^{\text{NH}}$, and $S_{\text{in}}^{\text{ND}}$. To handle these unmeasured states, the system is reformulated by isolating nonlinear terms under a Lipschitz condition, enabling the design of a robust unknown input observer based on Linear Matrix Inequalities (LMIs).

State estimation of nonlinear systems is essential for control design, fault diagnosis [15, 16], and health monitoring, as these applications typically require complete state information that is often unavailable through measurements alone. Numerous estimation methods have been developed, including moving horizon estimation [17], sliding mode observers [18], and LMIs-based observers [19, 20]. Hence, various observer design approaches have been elaborated under specific assumptions regarding the system's nonlinearities. Among these, one of the most widely used is the well-known high-gain observer, specifically designed for systems that can be expressed in triangular form [21], [22], [23]. Another effective method for nonlinear systems, particularly those with Lipschitz nonlinearities is addressed using sliding mode observers. The design of such estimators is based on the solution of an algebraic Riccati equation, which maybe difficult to solve [24]. Therefore, a simpler approach is the Extended Kalman Observer (EKO), which uses a first order linearizion technique. However, although the EKO is simple to design and is largely used in real applications [25], it is very sensitive to the initialization and its convergence is guaranteed only locally.

For linear systems, we can cite the observer design methods proposed by [26], [27], and [28]. Although, these observers are simple to design, unfortunately, there is no mention of the existence conditions. Later, new existence conditions have been established in [29] by considering a more complex issue, namely functional observers.

The above mentioned observers deal only with state estimation of nonlinear systems without unknown inputs. In the presence of unknown inputs, the problem becomes more

complicated and depends on the distribution of the unknown inputs in the system [29]. Usually, controlled real systems are subject to exogenous inputs, such sensor/actuator faults or disturbances affecting the system state variables and the output measurements. Within this context, unknown input estimation has owned a great interest in the areas of observer-based fault diagnosis [30], chaotic synchronization and secure communications [31], and observer-based fault tolerant control [32], [33]. For nonlinear systems, some recent observer design methods for simultaneous estimation of the system states and the unknown inputs have been proposed in the literature [34], where the nonlinearities are assumed to be Lipschitz. In [35], the authors used the Sobolev norms to investigate a new performance criterion for continuous nonlinear time-delay systems with uncertainties. Similarly, in [31], an observer in presence of disturbances in both of the system dynamics and outputs has been proposed. Despite all these techniques allow simultaneous estimation of the state variables and the unknown inputs, only few results have been tackling the issue of nonlinearity terms in the output measurements of the descriptor systems.

Therefore, in this thesis, we will present a novel and general estimation algorithm to cope with this problem. Indeed, we will design an observers able to estimate, simultaneously, the unknown inputs and the disturbed system dynamics. We use a Lyapunov function independing on the disturbances to avoid the presence of the disturbance's derivatives aimed at meeting a $\mathcal{H}_\infty$ performance criterion, which is based on the Lebesgue space $\mathcal{L}_2$ for obtaining local input-output stability. Since, nonlinearities in the system outputs lead to more complexity in the observer design, some assumptions on the system parameters such the number of unknown inputs, and nonlinear functions in the measurement equations will be discussed. To guarantee the observer convergence, tractable LMI conditions will be formulated. Their feasibility will be enhanced due to a convenient use of the Young's inequality. This will be possible through the introduction of additional decision variables, which lead to additional degrees of freedom and, consequently, better performances in the LMI feasibility.

The rising demographic and the mismanagement of water resources have negatively af-

fected the water quality. Naturally, in a water body, the organic matter is converted into inert mineral products by purely natural mechanisms. However the waste water treatment plant (WWTP), under some specific conditions, the purification phenomenon is activated by human control actions [36] in order to comply the effluent quality within the legislative limits [37], [38]. In ASM1-based bioreactors, dissolved oxygen (DO) is a key operational variable that directly influences active biomass activity and process efficiency. It supports both heterotrophic oxidation of organic matter and autotrophic nitrification. Maintaining DO around a setpoint of 2 $g{\cdot}m^{-3}$ (2 $mg{\cdot}L^{-1}$) is essential to balance these processes and prevent metabolic shifts or byproduct formation. Control is typically achieved by manipulating the aeration rate, which directly affects the oxygen transfer coefficient, k_La. Insufficient DO levels (hypoxia, DO $<$ 1 $mg{\cdot}L^{-1}$) can lead to ammonia accumulation, excessive sludge production, and poor effluent quality. Conversely, excessive oxygenation (hyperoxia, DO $>$ 4 $mg{\cdot}L^{-1}$) inhibits denitrification, increases oxidative stress, and results in unnecessary energy consumption. Thus, regulating DO through advanced control strategies such as NNMPC or observer-based feedback control ensures both biological performance and energy efficiency [39, 40].

The COST/IWA benchmark simulation model (BSM1) has been available to create a platform for the design and comparison of different control strategies [41] for a standard WWTP. The Proportional-Integral (PI) is the default control method for BSM1, however, owing to the complexity behavior of WWTP, a fixed parameter linear controller is not able to maintain a satisfactory performance of regulation under the full range of operating conditions. Therefore, the advanced control, nonlinear model predictive control (MPC), is a good candidate for a such demanding task [42]. MPC also known as moving horizon control (MHC) or receding horizon control (RHC), is a popular technique for the control of slow dynamical systems, such as those encountered in chemical process control [43].

The control performance of MPC mainly depends on the accuracy of the model describing the plant behavior. These plant models can be represented by conventional mathematical approaches like state-space [44], ARMA (Autoregressive-moving-average).

Machine learning technique based models like neural networks (NN) is also used to model the plants behavior [45, 46]. Generally, NNMPC algorithms are based on solving an online optimization problem which reflects the desired control performance, subject to the constraints on inputs, states and outputs.

Accurate minimizing of cost function with reliable controller performance is a challenging and ongoing research problem. In such case , This optimization problem is nonlinear, high-dimensional with complex constraints on the states and the control variables. In some case, the optimization with nonlinear programming methods provides eventually local optimum values and depend on the selection of the starting point. Fortunately, recent natural-inspired metaheuristic optimization methods are a good alternative, such as genetic algorithm (GA), particle swarm optimization (PSO).

To enhance the reliability and efficiency of dissolved oxygen (DO) regulation in biological reactor of wastewater treatment processes, this thesis develops a novel dynamic output feedback fault-tolerant control (DOF-FTC) strategy, specifically adapted to nonlinear dynamics modeled by reduced ASM1. The proposed control architecture leverages a LPV framework and reformulation Liptchiz equation to handle model nonlinearities and time-varying operating conditions through measurable scheduling variables (the influent flow rate $D^{in} = \rho$).

A key component of the strategy is our unknown input estimation algorithm for a class of nonlinear systems with mixed nonlinear terms, namely LPV parts and purely Lipschitz nonlinearities, which allows simultaneous estimation of unmeasured influent concentrations such as (Ammonia nitrogen, Soluble biodegradable organic nitrogen) and a fault-affected system (e.g., bias or drift), even under bounded disturbances. Based on the estimated states and faults sensor outputs, a dynamic output feedback fault-tolerant controller ensures accurate tracking of the DO reference setpoint (2 mg·L^{-1}), incorporating an integral action to eliminate steady-state errors. The controller explicitly compensates for sensor faults within the feedback loop, thereby preserving performance and avoiding unnecessary energy consumption.

Lyapunov based Linear Matrix Inequality (LMI) conditions are derived to ensure closed-loop stability and guarantee an $\mathcal{H}_\infty$ performance level under disturbances such as influent load variations. The observer and controller gains are co-designed via convex optimization techniques, enabling real-time feasibility and implementation using standard tools.

1.1 Main Contributions of the Thesis

To sum-up, the contributions of the thesis can be summarized as follows:

- A general LMI-based $\mathcal{H}_\infty-$ observer design method for a class of nonlinear descriptor systems with nonlinear outputs is proposed. The provided LMI conditions are less conservative than those proposed in the previous literature. This is due to:
  - the use of specific Lyapunov function candidate containing the disturbances in order to avoid their derivatives in the derivative of the Lyapunov function along the trajectories of the estimation error dynamics;
  - expressing the nonlinearities of the system in convenient way to exploit all their properties in the Lyapunov analysis;
  - the use of Young's inequality in a judicious manner, which provides additional decisions variables, and then leads to more general LMI conditions compared to those found in the literature.
- Three estimation algorithms are proposed to reconstruct unknown inputs of the system. Each estimation algorithm requires specific assumptions related to rank conditions expressing the distribution of the unknown inputs in the system dynamics and in the output measurements. To this end, mathematical artifacts and some convenient and judicious matrix decompositions are introduced to overcome obstacles encountered in the Lyapunov analysis.
- The proposed estimation algorithms are applied to a reduced model of activated sludge wastewater treatment plant (ASM1), which was developed in the European

program COST 624 for control purposes [47].

- An efficient control strategy, namely neural network model predictive NNMPC controller based on metaheurstics optimization has been designed and investigated for dissolved oxygen control in aerated Activated Sludge processes. Thereby a comparative study between the classical controller (PI) and the advanced one NNMPC indicates that the NNMPC is the most efficient to achieve a high control precision.
- Comparative analysis of optimization methods (Levenberg-Marquardt vs PSO vs GA) demonstrating metaheuristics superiority in handling nonlinearities with faster convergence and better solution quality
- Development of a precision control scheme achieving system stabilization through optimal metaheuristic-based tuning
- Developed a novel LPV/Lipschitz-based DOF-FTC strategy for dissolved oxygen regulation in wastewater treatment, handling nonlinearities through measurable scheduling variables ($D^{in} = \rho$) in reduced ASM1 dynamics
- Established LMI-based stability conditions with $\mathcal{H}_\infty$ performance guarantees, controller gains via convex optimization for real-time implementation

1.2 Outline of the Thesis

The present thesis is composed of five chapters organised as follows :

- In chapter.1, a foundational overview of biological wastewater treatment is presented,, starting with the main stages (pre-treatment, primary treatment, and secondary treatment), with a particular focus on the activated sludge process, which plays a central role in secondary treatment. The activated sludge process involves various biological mechanisms such as organic matter degradation, nitrification, denitrification, biomass decay, and sludge recycling. These processes are mathematically described by the ASM1, which includes 13 state variables and uses Monod-based kinetics to represent biomass growth. Due to the complexity of ASM1, a

reduced-order nonlinear model from [14] is adopted to facilitate observer and controller design. This reduced model maintains the essential dynamics while simplifying implementation.

- In chapter.2, an overview of singular systems is provided, which are used to model complex dynamics combining differential equations and algebraic constraints. After a brief comparison with classical state-space systems, the fundamental structural properties are introduced. The discussion then extends to singular LPV systems, which are more closely related to the practical applications addressed in the subsequent chapters. Finally, the main stability analysis approaches adapted to this class of systems are presented, laying the groundwork for the control and observation syntheses developed later in the thesis.

- In chapter.3, a theoretical study based on the state of the art regarding state observation in linear singular systems is introduced, particularly in the presence of unknown inputs. After recalling classical observer approaches under detectability conditions, more advanced methods are introduced, such as the proportional observer based on impulsive observability and the separation of dynamic and algebraic subspaces. The synthesis of an unknown input observer is then developed through a structured transformation of the original system, enabling the design of a reduced-order observer. The stability of the latter is ensured via an LMI condition derived from a Lyapunov function, guaranteeing the convergence of the estimation error despite the presence of unmeasured inputs.

- In chapter.4, the problem of unknown input estimation is developed for a class of nonlinear systems with mixed nonlinear terms, namely Linear Parameter Varying (LPV) parts and purely Lipschitz nonlinearities. Three new unknown input estimation algorithms are proposed, where each algorithm depends on the distribution of the unknown inputs in the system. These algorithms provide estimation of the maximum possible unknown inputs in a system, contrarily to the methods available in the literature, which consider only particular cases. Before introducing these

estimation algorithms, a general LMI-based $\mathcal{H}_\infty-$ observer design methodology is provided, as a preliminary result, for a class of nonlinear descriptor systems with nonlinear outputs. To this end, a specific Lyapunov function is exploited to avoid derivatives of the disturbances. The proposed LMI conditions are less conservative than those existing in the literature. This is due to the specific Lyapunov function, the use of Young inequality in a judicious way, and the reformulation of the Lipschitz inequality. The proposed algorithms are applied to a wastewater treatment model to show their effectiveness and performances.

- In chapter.5, introduces two distinct approaches for the regulation of dissolved oxygen (DO) in wastewater treatment plants (WWTP): neural network model predictive control (NNMPC) and a dynamic output feedback fault-tolerant controller. The NNMPC, based on a NNARX neural model and optimized using methods such as Levenberg-Marquardt, particle swarm optimization (PSO), and genetic algorithm (GA), achieves accurate control of the dissolved oxygen concentration at ($2mg \cdot L^{-1}$). while minimizing energy consumption. Meanwhile, the dynamic output feedback fault-tolerant control employs the unknown input estimation formulated with linear matrix inequality (LMI) constraints to actively estimate and compensate sensor faults and guarantees precise tracking of the dissolved oxygen (DO) reference value. Both strategies are applied independently and validated on the BSM1 benchmark using MATLAB/Simulink, demonstrating significant improvements in accuracy, robustness, and resilience to disturbances and faults. These results offer advanced solutions for the sustainable and efficient management of WWTP.

Chapter 2

Biological Wastewater Treatment Process

"Water treatment is civilization's immune system."
(Adapted from Edgeworth David)

2.1 Introduction

Water pollution control has become a critical challenge in environmental engineering, requiring increasingly sophisticated treatment methods to address diverse contaminants. This chapter presents a comprehensive examination of biological wastewater treatment systems, focusing on the activated sludge process as the most widely implemented secondary treatment technology worldwide. The discussion begins with fundamental concepts of wastewater treatment stages, from preliminary screening to advanced tertiary processes. Particular emphasis is placed on the activated sludge system, which utilizes activated sludge communities to biologically degrade organic matter and remove nutrients. In wastewater treatment, the adoption by the European Union of increasingly stringent discharge standards has led to the need for more reliable and better controlled treatment plants. Mathematical models then become highly valuable tools to assist in the development of effective control strategies, and potentially enable real-time operation of treatment units. Over the past two decades, numerous studies have focused on modeling the activated sludge process. This work culminated in the publication by the IAWQ[1] of the ASM models: ASM1 [1, 2], ASM2 [48], ASM2d [49], and ASM3 [50] .

Although these models have been widely applied across various fields and have proven predictive capabilities, their large number of parameters and state variables makes them unsuitable for online process control. After a brief overview of the main operational stages of an activated sludge wastewater treatment plant, we present a simplified (reference) model derived from the most widely used biological model, ASM1. Due to its complex structure, numerous reduced-order models have been proposed in the literature ([51], [52], [53], [54], [55], and [56]) in order to obtain a more practical and applicable model for real-world applications. Various model reduction techniques are therefore reviewed. The resulting reduced model is a nonlinear model introduced by [14]. Since the influent concentrations $X_{\text{in}}^{\text{DCO}}$, $S_{\text{in}}^{\text{NO}}$, $S_{\text{in}}^{\text{NH}}$, and $S_{\text{in}}^{\text{ND}}$ are typically not measured, they must be considered as unknown inputs.

2.2 Fundamentals of biological wastewater treatment

Water serves as the ideal medium for the transport and dispersion of a wide range of pollutants. Increasingly stringent sanitation regulations [57] require the removal of an expanding array of contaminants, including organic compounds, minerals, pathogens, and toxic substances. Given this diversity, wastewater purification typically involves multiple treatment stages [58], each specifically tailored to address the distinct characteristics of the targeted pollutants. In general, a wastewater treatment system consists of several modules through which raw influent passes, undergoing successive purification processes before final discharge [59]. Wastewater treatment methods are commonly categorized into three main stages: primary, secondary, and tertiary treatments [60]. Alternatively, these processes can be classified according to their physical or biological nature, with primary treatments typically based on physical separation methods, while secondary and tertiary treatments often involve biological and/or advanced chemical processes [61]. Another possible classification is based on physical and biological criteria, roughly distinguishing primary treatments on one side and secondary and tertiary treatments on the other.

2.2.1 pre-treatment:

The primary objective of pre-treatment [62] is to remove coarse materials (such as twigs, leaves, fabrics, etc.) and elements that could impede subsequent treatment stages. This phase comprises:

Screening: is performed by passing water through grids of varying coarseness [63] to capture solid elements larger than the grid spacings;

grit removal, grease and oil removal: The flow rate of the water is slowed down, [62] allowing smaller particles to sediment (primary sludge), while less dense fats rise to the surface. Sand is then removed by pumping, and the foam is skimmed off.

In the strict sense, the primary treatment involves a physico-chemical process where coagulants and flocculants can be introduced to the water [63]. This facilitates the removal

of a substantial quantity of suspended particles through sedimentation or flotation, resulting in the formation of physico-chemical sludge. This stage effectively eliminates 90% of suspended particles and objects, a standard procedure in most wastewater treatment plants. Nonetheless, dissolved elements such as nitrogen, phosphorus, active compounds, and fine particles persist in the water. Subsequent secondary and potentially tertiary treatments are then applied.

2.2.2 The secondary treatment

The fundamental principles [4] involved in the biological treatment of wastewater are common to all processes such as activated sludge, bacterial beds, lagooning, etc. Microorganisms, mainly bacteria, decompose organic and mineral substances present in wastewater for their own development (metabolism). These substances exist in the form of particles, colloids, or dissolved molecules, the stages of the degradation process are schematically represented in figure 2.1. Due to their significant size, particles and macromolecules must first be hydrolyzed into simpler compounds to be assimilated by bacteria, along with the dissolved substances. Each step, depending on substrate availability, hydraulic regime of reactors, or environmental conditions (temperature, etc.), can be limiting for the overall degradation process [63]. In biological treatment processes, metabolism always leads to the production of new cells. While this process maintains an adequate quantity of bacteria in the system, an excessive bacterial mass can cause serious malfunctions, necessitating the extraction of a portion of the produced sludge.

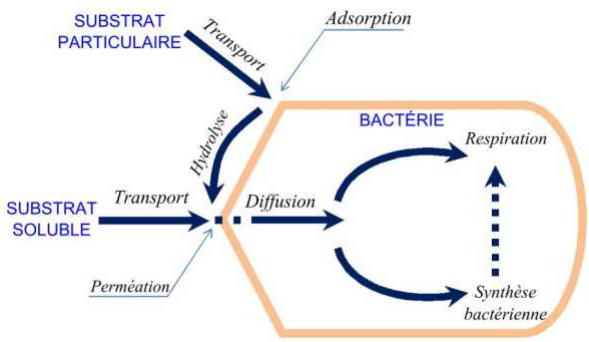

Figure 2.1: Stages of the biological degradation process [4]

2.2.2.1 The secondary treatment with activated sludge process

The activated sludge process is the most widely used biological wastewater treatment method [5] in developed countries. The treatment process is referred to as "activated sludge" because all the favorable conditions for maximum bacterial activity are implemented : an adequate supply of oxygen, nutrient input if the effluent lacks all the compounds necessary for bacterial growth, continuous agitation to enhance contact between bacteria and pollutants, and a high bacterial concentration to increase treatment efficiency. The treatment chain consists of a bioreactor, a clarifier, and a sludge recycling loop, as shown in figure 2.2 .

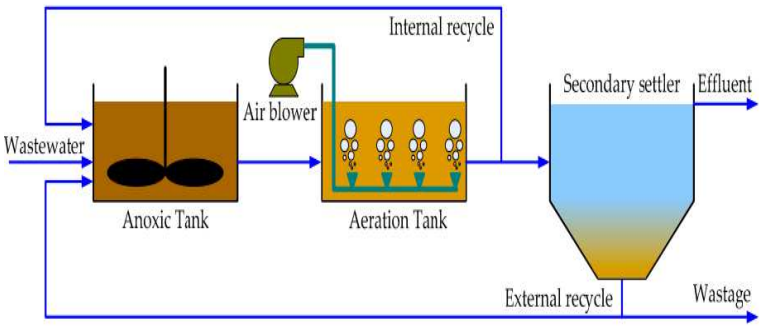

Figure 2.2: Typical biological Activated Sludge Process to treat wastewater [5].

The bioreactor The mixture, called "mixed liquor" [4] consists of a solid phase (microorganisms, organic debris, mineral matter) and a liquid phase containing dissolved substances. To remove nitrogenous matter, the biological reactor can be divided into two distinct aerobic and anoxic zones see figure 2.2. In most cases, the anoxic zone is placed upstream of the aerobic zone, just at the inlet of the effluent into the reactor, so that bacteria have enough biodegradable organic matter to carry out the denitrification reaction. Recycling the mixed liquor from the aerobic zone to the anoxic zone allows for the removal of oxidized nitrogenous pollutants.

The clarifier At the outlet of the reactor, we obtain a mixed liquor composed of flocculated sludge and purified water ready to be discharged into the natural environment. They are separated within the clarifier, which has a phase separation function and a thickening

function to bring back the most concentrated sludge possible into the biological reactor. Due to the absence of oxygen [63], the sludge retention time must be as short as possible to prevent them from becoming anaerobic. This would result in the appearance of odors as well as a deterioration in the mechanical quality of the sludge, disrupting both the biological treatment of water and the subsequent treatment of the sludge.

Sludge recycling The growth of biomass within the bioreactor is not sufficient to compensate for the loss generated by the flow rate of the mixed liquor outlet. To maintain a constant biomass concentration in the reactor, a portion of the sludge from the clarifier is recycled back to the reactor. Purges also occur to extract the excess amount of sludge in the process. The recycling and purging rates also help control the sludge age, θ_C, which is the time at which the biomass is entirely renewed [4].. This time characterizes the physiological form of the biomass in the reactor as well as its composition. Taking the example of nitrogenous matter treatment: autotrophic bacteria responsible for the nitrification reaction will only be present if the sludge age exceeds 6 days (for a mixed liquor at 20C), with their duplication time being 4 days.

2.2.3 The tertiary treatments

As regulations regarding discharge limits into natural ecosystems become increasingly stringent, numerous investigations are underway to propose tertiary treatment methods designed to eliminate remaining compounds post-secondary treatment [64]. The treatment can adopt various approaches:

- Biological methods for eliminating nitrogen (nitrification-denitrification) and phosphorus (dephosphatation) [63].
- Physico-chemical techniques involving phosphorus precipitation (coagulation-settling) or the removal of lingering suspended matter (filtration through sand beds or activated carbon) [64].
- Chemical processes addressing desinfection disinfection [62] and the elimination of

bacteriological contamination risks (using chlorine or ozone).

2.2.4 The sludge treatment

A significant sludge production is typically characterized by a composition containing 95% to 98% water. The treatment of sludge is conventionally carried out in various stages, including thickening, anaerobic digestion, dewatering, drying, and utilization. This utilization can either be in the form of agricultural practices (direct spreading or composting) or energy related processes (incineration, anaerobic digestion).

2.3 The ASM1 model

The Activated Sludge Model No.1 [1] is a comprehensive model capable of accurately representing the behavior of the process during the treatment of wastewater loaded with nitrogenous and carbonaceous substances. ASM1, was developed and published in 1987 by the International Association Water Quality (IAWQ),(Henze et al. 1987) has been extensively applied in both academic and practical applications. This model provides a detailed description of biological mechanisms, process kinetics, as well as the degradation rates of organic matter, nitrification, and denitrification within activated sludge wastewater treatment plants. Between 1998 and 2004, European working groups affiliated with COST Actions 682 and 624 dedicated efforts to develop benchmark tools for the simulation-based assessment of control strategies in activated sludge plants. It also underwent significant modifications that gave rise to models such as ASM2 [48], ASM2d [49] and ASM3 [50].

2.3.1 State variables

The ASM1 model comprises thirteen state variables (related to biological phenomena), eight processes, and nineteen different kinetic and stoichiometric parameters. The letter **X** is suggested for particulate compounds, and the letter **S** for soluble compounds. We can classify these state variables into five groups:

1. **The substrates :** Consist of the rapidly biodegradable substrate S_s ($mg_{O2}.l^{-1}$) and the slowly biodegradable substrate X_s ($mg_{O2}.l^{-1}$).

2. **The biomasses :** The heterotrophic biomass X_{BH} ($mg_{O2}.l^{-1}$), responsible for the oxidation of organic matter and denitrification, and the autotrophic biomass X_{BA} ($mg_{O2}.l^{-1}$), responsible for nitrification. The growth of biomasses is described by the Monod equation. A third state variable, denoted X_P ($mg_{O2}.l^{-1}$), represents products resulting from the death of the biomass.

3. **The nitrogen compounds :** Are distinguished based on their oxidation state and are divided into 3 categories:

   - Organic forms (soluble $S_{ND}(mg_N.l^{-1})$ and particulate $X_{ND}(mg_N.l^{-1})$),
   - Ammoniacal forms (S_{NH} ($mg_N.l^{-1}$)),
   - Oxidized forms (S_{NO} ($mg_N.l^{-1}$)- nitrates-nitrites).

4. **The dissolved oxygen :** Represented as S_O ($mg_{O2}.l^{-1}$)

5. **Biologically inert states :** Soluble inert organic compounds $S_I(mg_{O2}.l^{-1})$, particulate inert compounds X_I ($mg_{O2}.l^{-1}$), and S_{alk} alkalinity ($mol.l^{-1}$).

Consequently, the model comprises a total of thirteen state variables gathered in the vector X:

$$X = \left[\; S_O \quad S_{NO} \quad S_{NH} \quad S_S \quad X_{BH} \quad X_{BA} \quad Q_{eff} \quad COD \quad BOD \quad TSS \quad TKN \quad TP \quad PH \; \right] \tag{2.1}$$

Where:

- **COD** (Chemical Oxygen Demand): the amount of oxygen required to chemically oxidize all organic matter in the water, both biodegradable and non-biodegradable (mg O_2/L).
- **BOD** (Biochemical Oxygen Demand): the amount of oxygen consumed by microorganisms to biologically degrade biodegradable organic matter over 5 days (mg O_2/L).

- **TSS** (Total Suspended Solids): the concentration of undissolved solid particles in the water (mg/L).
- **TKN** (Total Kjeldahl Nitrogen): the total concentration of organic nitrogen and ammonia nitrogen in the water (mg N/L).
- **TP** (Total Phosphorus): the total amount of phosphorus, including orthophosphates, organic phosphates, and particulate phosphorus (mg P/L).
- **pH**: a dimensionless measure indicating the acidity or alkalinity of the water (range from 0 to 14, with 7 being neutral).

2.3.1.1 Input variables

The concentrations of soluble $S_{*,in}$ and particulate components $X_{*,in}$ in the polluted water entering the bio-reactor are considered as input variables of the model. The inlet flow rates Q_{in}, recycling Q_R, and extraction Q_W are also part of this set of variables, with the elements forming the input vector defined by u;

$$\begin{aligned} u = \big[& S_{I,in}, \quad S_{S,in}, \quad X_{I,in}, \quad X_{S,in}, \quad X_{BH,in}, \quad X_{BA,in}, \quad X_{P,in}, \\ & S_{NO,in}, \quad S_{NH,in}, \quad S_{ND,in}, \quad X_{ND,in}, \quad S_{O,in}, \quad S_{alk,in}, \quad q_{in}, \quad q_R, \quad q_W \big] \end{aligned} \tag{2.2}$$

2.3.1.2 Output Variables

The concentrations of soluble, represented by $S_{*,out}$ and particulate components, represented by $X_{*,out}$ in the water leaving the bio-reactor are considered output variables of the model. The output flow rate q_{out} is also part of this set of measurable variables; the vector gathers the output variables is mentioned by y :

$$y = \begin{bmatrix} S_{I,out} & S_{S,out} & X_{I,out} & X_{S,out} & X_{BH,out} & X_{BA,out} & X_{P,out} & ; \\ & S_{NO,out} & S_{NH,out} & S_{ND,out} & X_{ND,out} & S_{O,out} & S_{alk,out} & q_{out} \end{bmatrix} \tag{2.3}$$

2.3.2 List of processes

The various processes integrated into the IWA model are briefly described below. These have been detailed by [65], [66]

2.3.2.1 Aerobic growth of heterotrophs ρ_1

A fraction of the easily biodegradable substrate is utilized for the growth of heterotrophic biomass, leading to an associated oxygen demand. Growth is modeled using Monod kinetics [67], [68]. Ammonia is used as a nitrogen source for synthesis and is incorporated into the cell mass. Both the concentration of S_S and S_O can limit the rate of the growth process. This process is generally the primary contributor to the production of new biomass and the removal of COD. It is also associated with a change in alkalinity.

$$\rho_1 = \mu_h \left(\frac{S_S(t)}{K_S + S_S(t)} \right) \left(\frac{S_O(t)}{K_{O,H} + S_O(t)} \right) X_{B,H}(t) \tag{2.4}$$

2.3.2.2 Anoxic growth of heterotrophs ρ_2

In the absence of oxygen, heterotrophic organisms can use nitrate as the terminal electron acceptor with S_s as a substrate. The process leads to the production of heterotrophic biomass and nitrogen gas (denitrification). Nitrogen gas is the result of nitrate reduction with an associated change in alkalinity. The same Monod kinetics used for aerobic growth are applied, except that the kinetic expression is multiplied by a factor $\eta_g \prec 1$. This reduced rate could either be caused by a lower maximum growth rate under anoxic conditions or because only a fraction of the heterotrophic biomass is capable of functioning with nitrate as the electron acceptor. Ammonia is used as a nitrogen source for cell synthesis, which in turn alters alkalinity [1], [69].

$$\rho_2 = \mu_h \left(\frac{S_S(t)}{K_S + S_S(t)} \right) \left(\frac{K_{O,H}(t)}{K_{O,H} + S_O(t)} \right) \left(\frac{S_{NO}(t)}{K_{NO} + S_{NO}(t)} \right) \eta_g X_{B,H}(t) \tag{2.5}$$

2.3.2.3 Aerobic growth of autotrophs ρ_3

Ammonia is oxidized to nitrate through a single-step process (nitrification), resulting in the production of autotrophic biomass and leading to an associated oxygen demand. Ammonia is also used as a nitrogen source for synthesis and incorporated into the cell mass. The process has a significant effect on alkalinity (both from biomass conversion to ammonia and from the oxidation of ammonia to nitrate) and total oxygen demand. The

impact on the amount of biomass formed is low because the yield of autotrophic nitrifiers is low. Once again, the growth rate is modeled using Monod kinetics.

$$\rho_3 = \mu_A \left(\frac{S_{NH}(t)}{K_{NH} + S_{NH}(t)} \right) \left(\frac{S_O(t)}{K_{O,A} + S_O(t)} \right) X_{B,A}(t) \tag{2.6}$$

2.3.2.4 Decay of heterotrophs ρ_4 and autotrophs ρ_5

Both processes are modeled in the same way using the assumption of death-regeneration. Organisms die at a certain rate, and a portion of the material is considered non-biodegradable and adds to the X_p fraction. The rest adds to the slowly biodegradable substrates. The associated organic nitrogen X_s becomes available as particulate organic nitrogen. No COD loss or electron acceptors are involved. The process is assumed to continue at the same rate as under aerobic, anoxic, and anaerobic conditions [70].

$$\rho_4 = b_H X_{B,H}(t) \tag{2.7}$$

$$\rho_5 = b_A X_{B,A}(t) \tag{2.8}$$

2.3.2.5 Ammonification of soluble organic nitrogen ρ_6

The biodegradable organic nitrogen is converted into free ammonia and a saline solution in a first-order process through active heterotrophs. The hydrogen ions consumed in the conversion process result in a change in alkalinity.

$$\rho_6 = k_a S_{ND}(t) X_{B,H}(t) \tag{2.9}$$

2.3.2.6 Hydrolysis of absorbed organic compounds ρ_7

The slowly biodegradable substrate trapped in the sludge mass decomposes extracellularly, producing an easily biodegradable substrate available for organism growth. The process is modeled based on surface reaction kinetics and occurs only under aerobic and anoxic conditions. The hydrolysis rate is reduced under anoxic conditions compared to aerobic conditions by a factor $\eta_h \leq 1$. The rate is also first-order with respect to the present heterotrophic biomass but saturates as the amount of absorbed substrate becomes

large in proportion to the biomass [71].

$$\rho_7(t) = k_h \frac{X_S(t)/X_{\{BH\}}(t)}{K_X + X_S(t)/X_{\{BH\}}(t)} \left(\frac{S_O(t)}{K_{O,H} + S_O(t)} + \eta_h \frac{K_{O,H}}{K_{O,H} + S_O(t)} \frac{S_{NO}(t)}{K_{NO} + S_{NO}(t)} \right) X_{B,H}(t) \tag{2.10}$$

2.3.2.7 Hydrolysis of entrapped (absorbed) organic nitrogen ρ_8

The biodegradable particulate organic nitrogen is decomposed into soluble organic nitrogen at a rate defined by the hydrolysis reaction for the absorbed organic matter described earlier [72].

$$\begin{aligned} \rho_8(t) = k_h & \frac{X_S(t)/X_{B,H}(t)}{K_X + X_S(t)/X_{B,H}(t)} \\ & \left(\frac{S_O(t)}{K_{O,H} + S_O(t)} + \eta_h \frac{K_{O,H}}{K_{O,H} + S_O(t)} \frac{S_{NO}(t)}{K_{NO} + S_{NO}(t)} \right) X_{B,H} \frac{X_{ND}(t)}{X_S(t)} \end{aligned} \tag{2.11}$$

2.3.3 Conversion rates

From the expression of kinetics and stoichiometric coefficients, the conversion rates (r_i), of each compound is given by the following relationship:

$$r_i = \sum_j v_{ij} \rho_j, \quad i = 1 \dots 13 \tag{2.12}$$

- $S_I (i = 1)$;

$$r_1 = 0 \tag{2.13}$$

- $S_S (i = 2)$;

$$r_2 = -\frac{1}{Y_H}.\rho_1 - \frac{1}{Y_H}.\rho_2 + \rho_7 \tag{2.14}$$

- $X_I (i = 3)$;

$$r_3 = 0 \tag{2.15}$$

- $X_S (i = 4)$;

$$r_4 = (1 - f_p).\rho_4 + (1 - f_p).\rho_5 - \rho_7 \tag{2.16}$$

- $X_{B,H}(i = 5)$;

$$r_5 = \rho_1 + \rho_2 - \rho_4 \tag{2.17}$$

- $X_{B,A}(i = 6)$;

$$r_6 = \rho_3 - \rho_5 \tag{2.18}$$

- $X_P(i = 7)$;

$$r_7 = f_p.\rho_4 + f_p.\rho_5 \tag{2.19}$$

- $S_O(i = 8)$;

$$r_8 = \frac{1 - Y_H}{Y_H}\rho_1 - \frac{4.57 - Y_A}{Y_A}\rho_3 \tag{2.20}$$

- $S_{NO}(i = 9)$;

$$r_9 = -\frac{1 - Y_H}{2.86.Y_H}.\rho_2 - \frac{1}{Y_A}.\rho_3 \tag{2.21}$$

- $S_{NH}(i = 10)$;

$$r_{10} = -i_{XB}.\rho_1 - i_{XB}.\rho_2 - (i_{XB} + \frac{1}{Y_A}).\rho_3 + \rho_6 \tag{2.22}$$

- $S_{NH}(i = 11)$;

$$r_{11} = -\rho_6 + \rho_8 \tag{2.23}$$

- $X_{ND}(i = 12)$;

$$r_{12} = (i_{XB} - f_p.i_{XB}).\rho_4 + (i_{XB} - f_p.i_{XB}).\rho_5 - \rho_8 \tag{2.24}$$

- $S_{ALK}(i = 13)$;

$$r_{13} = \frac{i_{XB}}{14}.\rho_1 + (\frac{1 - Y_H}{14 \bullet 2.86Y_H} - \frac{i_{XB}}{14}).\rho_2 + (\frac{i_{XB}}{14} + \frac{1}{7Y_A}).\rho_3 + \frac{1}{14}.\rho_6 \tag{2.25}$$

2.3.4 Biological parameter values

The biological parameter values employed in the the Benchmark Simulation Model no. 1 (BSM1) are approximately defined with a temperature of 15°C . The stoichiometric parameters can be found in table(2.1), while the kinetic parameters are detailed in table(2.2).

Parameter	Significance	Unit	Value [1, 73]
Y_A	Autotrophic yield	g COD.(g N)$^{-1}$	0.24
Y_H	Heterotrophic yield	g COD.(g COD)$^{-1}$	0.67
f_P	Inert fraction from decay	-	0.08
i_{XB}	N in biomass	g N.(g COD)$^{-1}$	0.08
i_{XP}	N in products	g N.(g COD)$^{-1}$	0.06

Table 2.1: Stoichiometric parameters of ASM1 [1]

Parameter	**Significance**	**Unit**	**Value**[1, 2]
μ_H	Maximum growth rate of heterotrophs	d^{-1}	4
μ_A	Maximum growth rate of autotrophs	d^{-1}	0.5
b_H	Decay coefficient of heterotrophs	d^{-1}	0.30
b_A	Decay coefficient of autotrophs	d^{-1}	0.05
K_{OH}	O_2 half-saturation (heterotrophs)	mgO_2·L^{-1}	0.20
K_{NO}	NO_3 half-saturation (denitrification)	mgN·L^{-1}	0.50
K_S	Substrate half-saturation	mgCOD·L^{-1}	10
K_{NH}	NH_3-N half-saturation (nitrifiers)	mgN·L^{-1}	1.0
K_{OA}	O_2 half-saturation (autotrophs)	mgO_2·L^{-1}	0.4
η_g	Anoxic growth correction factor	–	0.8
k_a	Ammonification rate	L·(gCOD·d)$^{-1}$	0.05
k_h	Maximum hydrolysis rate	gCOD·(gCOD·d)$^{-1}$	3.0
K_X	Hydrolysis half-saturation	gCOD·(gCOD)$^{-1}$	0.1
η_h	Anoxic hydrolysis correction factor	–	0.8

Table 2.2: Kinetic parameters of ASM1 [1–3]

2.4 Mass balances in the reactor

The model of the biological reactor is obtained by performing simple mass balances for each component. The mass balance equations are as follows [74], [75], [76], [77] , [78] :

$$\frac{dx_i}{dt} = \frac{Q_{rec}}{V^r} x_i^{rec} + \frac{Q_{in}}{V^r} x_i^{in} - \frac{Q_{in} + Q_{rec}}{V^r} x_i + r_i \tag{2.26}$$

where:

- V^r: represents the reaction volume
- Q_{rec}: recycle flow rate
- Q_{in}: reactor inlet flow rate

and x_i, x_i^{rec}, and x_i^{in} represent the concentrations of compound i in the aeration tank, in the recycle, and in the influent, respectively, that is:

$$x_i = [S_I, S_S, X_I, X_S, X_{BH}, X_{BA}, X_P, S_{NO}, S_{NH}, S_{ND}, X_{ND}, S_O, S_{alk}] \tag{2.27}$$

The balance related to the dissolved oxygen concentration includes an additional term A_O for the oxygen supply by the turbines:

$$\frac{dS_O}{dt} = \frac{Q_{rec}}{V^r} S_O^{rec} + \frac{Q_{in}}{V^r} S_O^{in} - \frac{Q_{in} + Q_{rec}}{V^r} S_O + r_O + A_O \tag{2.28}$$

In its general form, the oxygen supply term is written as:

$$A_O = k_L a(x) \left(S_O^{sat} - S_O \right)$$

where:

- $k_L a(x)$: is the oxygen transfer coefficient from the gas phase to the liquid phase, dependent on volume, agitation speed, injected air flow rate, viscosity, and density of the solution
- S_O^{sat}: The oxygen saturation concentration in water in the presence of biomass

In general, the model for the biological reactor is expressed in the form of an affine differential system in terms of the control variable:

$$\frac{dx_i}{dt} = f(x_i, x^{rec}, x^{in}) + u^{aer} g(x_i) \tag{2.29}$$

2.5 Mass balance in Secondary settler

The secondary clarifier is considered as a non-reactive and one-dimensional system divided into 10 horizontal layers, according to the double exponential settling velocity

model proposed by [79]. The solid flux due to gravity is given by:

$$J_s = v_s(X)X \tag{2.30}$$

where X is the total sludge concentration. A double-exponential settling velocity function has been selected, as in [79]:

$$V_s(X) = \max\left[0, \min\left\{v'_0, v_0\left(e^{-r_h(X-X_{\min})} - e^{-r_p(X-X_{\min})}\right)\right\}\right] \tag{2.31}$$

with

$$X_{\min} = f_{ns}X_f$$

X_f : is the total solid concentration from the biological reactor.

The parameter values for the settling velocity function are given in table(2.3). The

Parameter	significance	Unit	Value
v'_0	Maximum settling velocity	$m.d^{-1}$	250
v_0	Maximum Vesilind settling velocity	$m.d^{-1}$	474
r_h	Hindered zone settling parameter	$m^{-3}.(gSS)^{-1}$	0.000576
r_p	Flocculant zone settling parameter	$m^{-3}.(gSS)^{-1}$	0.00286
f_{ns}	Non-settleable fraction	dimensionless	0.00228

Table 2.3: Settling parameters

upward (v_{up}) and downward (v_{dn}) velocities are calculated as:

$$v_{dn} = \frac{Q_u}{A} = \frac{Q_r + Q_w}{A} \tag{2.32}$$

$$v_{up} = \frac{Q_e}{A} \tag{2.33}$$

According to these notations, the mass balances for the sludge are written as: For the feed layer (m = 6):

$$\frac{dX_{sc,m}}{dt} = \frac{\frac{Q_f X_f}{A} + J_{sc,m+1} - (v_{up} + v_{dn})X_{sc,m} - \min(J_{s,m}, J_{s,m-1})}{Z} \tag{2.34}$$

For the intermediate layers below the feed layer (m = 2 to m = 5):

$$\frac{dX_{sc,m}}{dt} = \frac{v_{dn}(X_{sc,m+1} - X_{sc,m}) + \min(J_{s,m}, J_{s,m+1}) - \min(J_{s,m}, J_{s,m-1})}{Z_m} \tag{2.35}$$

For the bottom layer (m = 1):

$$\frac{dX_{sc,1}}{dt} = \frac{v_{dn}(X_{sc,2} - X_{sc,m}) + \min(J_{s,2}, J_{s,1})}{Z_1} \tag{2.36}$$

For the intermediate clarification layers above the feed layer (m = 7 to m = 9)

$$\frac{dX_{sc,m}}{dt} = \frac{v_{up}(X_{sc,m-1} - X_{sc,m}) + J_{s,m+1} - J_{s,m}}{Z_m} \tag{2.37}$$

$$J_{sc,j} = \begin{cases} \min(v_{s,j}X_{sc,j}, v_{s,j-1}X_{sc,j-1}) & \text{if } X_{sc,j-1} \geq X_t \\ v_{s,j}X_{sc,j} & \text{if } X_{sc,j-1} \leq X_t \end{cases} \tag{2.38}$$

For the top layer (m = 10)

$$\frac{dX_{sc,10}}{dt} = \frac{v_{up}(X_{sc,9} - X_{sc,10}) + J_{s,10}}{Z_{10}} \tag{2.39}$$

$$\frac{dZ_{sc,m}}{dt} = \frac{\frac{Q_f Z_f}{A} - (v_{up} + v_{dn})Z_{sc,m}}{Z_m} \tag{2.40}$$

$$\frac{dZ_{sc,m}}{dt} = \frac{v_{dn}(Z_{sc,m+1} - Z_{sc,m})}{Z_m} \tag{2.41}$$

$$\frac{dZ_{sc,m}}{dt} = \frac{v_{up}(Z_{sc,m-1} - Z_{sc,m})}{Z_m} \tag{2.42}$$

reformulation for the soluble components including dissolved oxygen, each layer represents a completely mixed volume and the concentrations of soluble components are calculated accordingly. For the feed layer (m=6)

$$\frac{dZ_{sc,m}}{dt} = \frac{\frac{Q_f Z_f}{A} - (v_{up} + v_{dn})Z_{sc,m}}{Z_m} \tag{2.43}$$

For the layers m = 1 to 5

$$\frac{dZ_{sc,m}}{dt} = \frac{v_{dn}(Z_{sc,m+1} - Z_{sc,m})}{Z_m} \tag{2.44}$$

For the layers m = 7 to 10

$$\frac{dZ_{sc,m}}{dt} = \frac{v_{up}(Z_{sc,m-1} - Z_{sc,m})}{Z_m} \tag{2.45}$$

The concentrations in the recycle and wastage flow are equal to those of the first (bottom) layer. In process engineering, dynamic simulation based on rigorous physical models is widely employed to analyze system behavior, particularly under extreme operating conditions [80]. Although these models offer high accuracy and reliability, their complexity - arising from the large number of state variables and parameters - poses significant challenges for tasks such as *state estimation* and *control*, where simplified or reduced-order models are often more appropriate [81]. This limitation is especially pronounced in activated sludge processes, where the intrinsic complexity severely restricts practical control implementation. For example, the ASM1 model (see Section 2.3 for an overview of the underlying principles) developed by the IAWQ consists of thirteen nonlinear state equations and more than twenty parameters [1]. Even in its simplified form (reduced to eleven state equations), the parameter count remains unchanged, preserving much of the original model's complexity. Consequently, it remains largely unsuitable for real-time estimation and control [52]. This underscores the need for further model reduction to enable effective application in such contexts.

2.6 Development of a reduced-order model

In this thesis, we use the reduced model proposed in [14], derived from ASM1 and adapted for sequencing batch activated sludge processes to enable optimal aeration control. The model applies two simplification steps: removal of slow dynamics using a homotopy method, and heuristic reductions including a single organic compound and the neglect of nitrogenous organics, resulting in a five-state model. It is shown to be observable and identifiable from online measurements of dissolved oxygen, ammonia, and nitrate. This model is selected for its suitability in future closed-loop predictive control applications.

2.6.1 Simplification of the reference model

The simplification assumptions used are inspired by the thesis of [14]. It should be noted that the purpose of this section is to recall the various simplification steps carried out to obtain the reduced-order model.

2.6.1.1 Simplification of slow dynamics

This step is based on the separation of slow and fast dynamics using singular perturbation theory. It can be readily observed that the dynamics of inert organic compounds (S_I), heterotrophic biomass (X_{BH}), and autotrophic biomass (X_{BA}) are significantly slower than those of the other components in the system, throughout the entire operational cycle. Given that these components exhibit time constants on the order of several days, it is thus reasonable to consider their concentrations (S_I, X_{BH}, and X_{BA}) as constant over the course of a few hours. By applying this assumption and additionally removing the concentration of soluble inert organic matter S_I whose dynamics are decoupled from those of the other compounds the number of state variables is reduced from 11 to 7.

2.6.1.2 Simplification of organic compounds

The ASM1 model distinguishes between biodegradable soluble compounds S_S, assumed to be directly assimilable by microorganisms, and particulate compounds X_S, which must first be hydrolyzed into soluble compounds before assimilation. These compounds play a significant role in the nitrogen degradation process, particularly in denitrification, and therefore require careful consideration. In this work, the description of these compounds is simplified by introducing a single state variable $X_{\text{DCO}} = S_S + X_S$, whose dynamics are expressed as:

$$\dot{X}_{DCO} = D^{in}\left(X^{in}_{DCO} - \frac{K_S}{K_{DCO}}X_{DCO}\right) - \frac{1}{Y_H}\left(\rho_1 + \rho_2\right) + \theta_2 \tag{2.46}$$

where $D^{in} = \frac{Q_{in}}{V_0}$ and X^{in}_{DCO} represent the dilution rate and the concentration of organic compounds in the influent, respectively. The aerobic growth kinetics ρ_1 and anoxic growth

kinetics ρ_2 of the heterotrophic biomass are then written as functions of state variables:

$$\rho_1 = \theta_1 \frac{X_{\mathrm{DCO}}}{X_{\mathrm{DCO}} + K_{\mathrm{DCO}}} \frac{S_O}{S_O + K_{O,H}} \tag{2.47}$$

$$\rho_2 = \theta_1 \eta_{NO,g} \frac{X_{\mathrm{DCO}}}{X_{\mathrm{DCO}} + K_{\mathrm{DCO}}} \frac{K_{O,H}}{K_{O,H} + S_O} \frac{S_{NO}}{S_{NO} + K_{NO}} \tag{2.48}$$

where the specific parameters θ_1 and K_{DCO} are defined as:

$$\theta_1 = \mu_H X_{B,H} \tag{2.49}$$

$$K_{DCO} = K_s \frac{X_{DCO}}{s_s} = \frac{K_S}{f_{ss}} \tag{2.50}$$

The parameter θ_1 depends only on the slow variables of the ASM1 model and thus evolves slowly, while variations in K_{DCO} maintain a relatively stable average value. The consideration of a single organic compound thus allows for the elimination of an additional state variable and also offers the advantage of avoiding the description of the hydrolysis mechanism of particulate compounds into soluble compounds.

2.6.1.3 Simplification of nitrogen compounds

The ASM1 model distinguishes four nitrogen fractions: S_{NO}, S_{NH}, S_{ND}, and X_{ND}. Since the concentrations of ammoniacal nitrogen S_{NH} and nitrate/nitrite S_{NO} account for the majority of total nitrogen discharges and can be measured online, it is hardly conceivable that these compounds would not appear in the expression of the reduced model. In contrast, the two organic nitrogen fractions soluble S_{ND} and particulate X_{ND} whose role is to describe the internal formation of S_{NH} through hydrolysis and ammonification processes, represent only a small part of nitrogen discharges. The simplification consists in decoupling the dynamics of the two organic nitrogen compounds by simplifying the description of the hydrolysis mechanism. Noting that $i_{\mathrm{NBM}} \ll \frac{1}{Y_A}$ and $Y_A \ll 4.57$, the ammonification rate ρ_6 and the nitrification rate $\frac{1}{Y_A}\rho_3$ can be expressed as follows:

2.7 Reduced model formulation

The nitrification and ammonification kinetics are presented in Table 2.4, as described in [12]. The additional parameters involved in these expressions are defined in Table 2.5. Based on these expressions and the previously discussed simplifications, the reduced model is formulated by equations 2.51.

Table 2.4: Kinetic expressions of the simplified model

Variable	*Expression*
ρ_1	$\theta_1 \frac{X_{DCO}}{X_{DCO}+K_{DCO}} \cdot \frac{S_O}{S_O+K_{O,H}}$
ρ_2	$\theta_1 \eta_{NO,g} \cdot \frac{X_{DCO}}{X_{DCO}+K_{DCO}} \cdot \frac{K_{O,H}}{K_{O,H}+S_O} \cdot \frac{S_{NO}}{S_{NO}+K_{NO}}$
$\frac{1}{Y_A}\rho_3$	$\theta_3 \frac{S_{NH}}{S_{NH}+K_{NH,A}} \cdot \frac{S_O}{S_O+K_{O,A}}$
ρ_4	$b_H X_{B,H}$
ρ_5	$b_A X_{B,A}$
ρ_6	$\theta_4 S_{ND}$
ρ_8	$\theta_5 \frac{X_{DCO}}{X_{DCO}+K_{ND}} \cdot \frac{S_O}{S_O+K_{O,H}} + \eta_{NO,h} \cdot \frac{K_{O,H}}{K_{O,H}+S_O} \cdot \frac{S_{NO}}{S_{NO}+K_{NO}}$

Table 2.5: Definition of the additional parameters used in the simplified model

Parameter	**Expression**
θ_1	$\mu_H X_{B,H}$
θ_2	$(1-f_{rXI})(\rho_4+\rho_5)$
θ_3	$\frac{\mu_A}{Y_A} X_{B,A}$
θ_4	$\kappa_a X_{B,H}$
θ_5	$\kappa_h \frac{X_{ND}}{X_S} X_{B,H}$
K_{DCO}	$K_S \cdot \frac{X_{DCO}}{S_S} = \frac{K_S}{f_S S}$
K_{ND}	$K_X \cdot \frac{X_{DCO}}{X_S} X_{B,H}$
D_{in}	$\frac{Q_{in}}{V_O}$

$$\dot{X}_{DCO} = D_{in}X_{DCO,in} - \frac{K_S}{K_{DCO}}X_{DCO} - Y_{1H}(\rho_1 + \rho_2) + \theta_2 \tag{2.51}$$

$$\dot{S}_{NO} = D_{in}S_{NO}^{in} - S_{NO} - (1 - Y_H) \cdot \frac{1}{2.86Y_H}\rho_2 + \frac{1}{Y_A}\rho_3 \tag{2.52}$$

$$\dot{S}_{NH} = D_{in}S_{NH}^{in} - S_{NH} - i_{NBM}(\rho_1 + \rho_2) - \frac{1}{Y_A}\rho_3 + \rho_6 \tag{2.53}$$

$$\dot{S}_{ND} = D_{in}S_{ND}^{in} - S_{ND} - \rho_6 + \rho_8 \tag{2.54}$$

$$\dot{S}_O = D_{in}S_O - (1 - Y_H) \cdot \frac{1}{Y_H}\rho_1 - 4.57 \cdot \frac{1}{Y_A}\rho_3 + k_La(S_{O,sat} - S_O) \tag{2.55}$$

This reduced model includes five state variables (X_{DCO}, S_{NO}, S_{NH}, S_{ND}, and S_O), 16 parameters, as well as the flow rate Q_{in} and the influent concentrations $X_{DCO,in}$, S_{NO}^{in}, S_{NH}^{in}, and S_{ND}^{in}. The stoichiometric and kinetic parameters are the same as those defined in the ASM1 model (see Tables 2.1 2.2). However, the additional parameters θ_i ($i = 1, \ldots, 5$), K_{DCO}, and K_{ND} result from simplifications. Their specific values are provided in Table 2.5.

It is worth noting that the parameters θ_1 and θ_2 can be interpreted as the maximum degradation rates of organic compounds and ammoniacal nitrogen [14]. In the reduced model (Equations 2.51), the influent concentration S_{NO}^{in} is assumed to be no-zero, contrary to what was proposed in [14].

2.8 Conclusion

This chapter presented the fundamentals of biological wastewater treatment, with a focus on the activated sludge process, widely used for its ability to remove organic and nitrogenous pollutants. Following a brief overview of the treatment stages, emphasis was placed on the importance of mathematical modeling for analyzing and controlling these complex processes. We introduced the ASM1 model, known for its detailed representation of biological reactions, while highlighting its complexity that limits real-time applications. To address this, a reduced-order model adapted to sequencing batch reactors was presented. This simplified model, developed using reduction techniques such as singular perturbations and variable aggregation, retains the essential dynamics while

remaining suitable for control purposes. This reduced-order model thus provides an effective foundation for the design of observers and advanced control strategies, which will be addressed in the following chapters.

Chapter 3

Structural analysis and stability of descriptor-LPV systems

The holy quran "Verily, with hardship comes ease"
(Quran 94:6 - Al-Inshirah)

3.1 Introduction

This chapter presents a comprehensive study of the structural properties of singular (descriptor) systems and Linear Parameter Varying (LPV) systems, along with their stability analysis and performance characteristics. Descriptor systems, represented by Differential-Algebraic Equations (DAEs), provide a more general modeling framework than standard state-space systems by incorporating algebraic constraints and hybrid dynamics [82, 83]. LPV systems extend Linear Time-Invariant (LTI) models by introducing time-varying parameter dependencies, enabling the capture of nonlinear behaviors while maintaining linear analysis tools [13, 84].

The first part examines the **structural properties of singular systems**. We present fundamental concepts including system equivalence, Kronecker-Weierstrass decomposition (separating differential and algebraic subsystems), and canonical forms (such as SVD form). Key definitions of regularity, non-impulsiveness, and admissibility are introduced with their algebraic characterizations via rank conditions [82]. Controllability and observability notions (C-, R-, and impulse variants) are detailed with corresponding matrix-based criteria.

The second part focuses on **LPV systems**, which generalize LTI models through parameter-dependent dynamics. We distinguish three main classes: affine LPV (linear parameter dependence), polytopic LPV (convex hull of vertex systems), and quasi-LPV (state/input-dependent scheduling) [13, 85]. Each class is illustrated with application examples highlighting their respective advantages. Descriptor-LPV (D-LPV) systems, combining both frameworks, are then introduced with a concrete bioreactor case study [86, 87].

The third part develops **stability analysis** for dynamical systems, beginning with Lyapunov stability definitions adapted for DAEs. Stability theorems using Lyapunov functions, including both linear and nonlinear cases, are presented [88, 89]. For LPV systems, we discuss quadratic stability and Parameter-Dependent Quadratic (PDQ) Lya-

punov methods that account for parameter variation rates [84, 90].

Finally, the last part explores **performance criteria**, particularly the $\mathcal{H}_\infty$ norm and its LPV generalization through induced $\mathcal{L}_2$-gain. The Bounded Real Lemma is formulated as Linear Matrix Inequalities (LMIs), providing a powerful tool for robust control analysis and synthesis [91, 92].

3.2 Structural properties of singular systems

Two descriptor linear systems are *equivalent* if there exist nonsingular matrices M and N such that their system matrices can be transformed into each other [82]. This equivalence preserves fundamental system properties while allowing different state-space representations.

Lemma 3.2.1 (Kronecker-Weierstrass Decomposition)**.** *A regular descriptor system* (E, A) *admits the decomposition:*

$$M_1 E N_1 = \begin{bmatrix} I_{n_1} & 0 \\ 0 & N \end{bmatrix} \tag{3.1}$$

$$M_1 A N_1 = \begin{bmatrix} A_s & 0 \\ 0 & I_{n_2} \end{bmatrix} \tag{3.2}$$

where N *is nilpotent* ($N^h = 0,\ N^{h-1} \neq 0$) *and* $n_1 + n_2 = n$ *[93].*

The system decomposes into:

- Slow subsystem (differential):

$$\begin{cases} \dot{x}_1 = A_s x_1 + B_1 u \\ y_1 = C_1 x_1 \end{cases} \tag{3.3}$$

- Fast subsystem (algebraic):

$$\begin{cases} N\dot{x}_2 = x_2 + B_2 u \\ y_2 = C_2 x_2 \end{cases} \tag{3.4}$$

Theorem 3.2.2 (Complete Response)**.** *For $u(t) \in C^{h-1}$, the output is:*

$$y(t) = C_1 e^{A_s t} x_{10} + C_1 \int_0^t e^{A_s(t-\tau)} B_1 u(\tau) d\tau - \sum_{k=0}^{h-1} C_2 N^k B_2 u^{(k)}(t) \tag{3.5}$$

Definition 3.2.3 (SVD Form)**.** The singular value decomposition yields [94]:

$$M_2 E N_2 = \begin{bmatrix} I_r & 0 \\ 0 & 0 \end{bmatrix}, \quad M_2 A N_2 = \begin{bmatrix} A_{11} & A_{12} \\ A_{21} & A_{22} \end{bmatrix} \tag{3.6}$$

where $r = \text{rank}(E)$

Definition 3.2.4 (Regularity)**.** A descriptor system is *regular* if $\det(sE - A) \not\equiv 0$ for $s \in \mathbb{C}$, ensuring existence and uniqueness of solutions.

Definition 3.2.5 (Non-Impulsiveness)**.** A system is *non-impulsive* if its state trajectory $x(t)$ remains continuous for all continuous inputs and initial conditions.

Definition 3.2.6 (Admissibility)**.** A descriptor system is *admissible* if it satisfies:

- Regularity ($\det(sE - A) \not\equiv 0$)
- Non-impulsiveness (finite energy jumps)
- Stability (all finite poles in $\mathbb{C}^-$)

Definition 3.2.7 (Controllability Types)**.** For descriptor systems:

- *C-controllability*: Complete state-to-state controllability
- *R-controllability*: Reachability within the reachable subspace
- *Impulse-controllability*: Control of impulsive modes

Definition 3.2.8 (Observability Types)**.** For descriptor systems:

- *C-observability*: Complete initial state reconstruction

- *R-observability*: Observability within the reachable subspace
- *Impulse-observability*: Detection of impulsive modes

Theorem 3.2.9 (Characterization)**.** *The following rank conditions characterize these properties:*

- *Regularity:* $\text{rank}[sE - A] = n$ *for some* $s \in \mathbb{C}$
- *Non-impulsiveness:* $\text{rank}\begin{bmatrix} E & 0 \\ A & E \end{bmatrix} = n + \text{rank}(E)$
- *C-controllability:* $\text{rank}[sE - A \ B] = n \ \forall s \in \mathbb{C}$
- *C-observability:* $\text{rank}[sE^T - A^T \ C^T] = n \ \forall s \in \mathbb{C}$

3.3 Linear Parameter-Varying (LPV) Systems

LPV systems extend Linear Time-Invariant (LTI) models by incorporating time-varying parameters (scheduling variables) that depend on measurable or estimable external signals [13]. Unlike LTI systems, which are limited to local approximations, LPV systems preserve nonlinear dynamics while leveraging linear analysis tools [84]. The general state-space representation is:

$$\begin{cases} \dot{x}(t) = A(\rho(t))x(t) + B(\rho(t))u(t), \\ y(t) = C(\rho(t))x(t) + D(\rho(t))u(t), \end{cases} \tag{3.7}$$

where $\rho(t) \in \mathbb{R}^{n_\rho}$ is the bounded scheduling vector, and $A(\rho)$, $B(\rho)$, $C(\rho)$, $D(\rho)$ are parameter dependent matrices.

3.3.1 Affine LPV systems

The system matrices depend affinely on $\rho(t)$, confined to a polytope $\mathcal{P}\rho(t) \in \mathcal{P} = \{\rho_j(t) \mid \underline{\rho}_j \leq \rho_j(t) \leq \overline{\rho}_j\}$ The matrices decompose as:

$$A(\rho) = A_0 + \sum_{j=1}^{n_\rho} \rho_j A_j,$$

$$B(\rho) = B_0 + \sum_{j=1}^{n_\rho} \rho_j B_j,$$

(similarly for C, D)

3.3.2 Polytopic LPV Systems

A Linear Parameter-Varying (LPV) system is termed *polytopic* when its state-space matrices depend affinely on a *scheduling parameter vector* $\rho(t) \in \mathbb{R}^m$ evolving within a bounded polytope Λ. The system admits a vertex-based representation as a **convex combination** of matrices $S_i = [A_i, B_i, C_i, D_i]$ corresponding to the polytope vertices [95]:

$$\begin{cases} \dot{x}(t) = \sum_{i=1}^{\tau} \mu_i(\rho(t))(A_i x(t) + B_i u(t)) \\ y(t) = \sum_{i=1}^{\tau} \mu_i(\rho(t))(C_i x(t) + D_i u(t)) \end{cases} \tag{3.8}$$

where the *barycentric coordinates* $\mu_i(\rho(t))$ satisfy for all $\rho \in \Lambda$:

$$\mu_i(\rho(t)) \geq 0, \quad \sum_{i=1}^{\tau} \mu_i(\rho(t)) = 1$$

and form a convex decomposition over the parameter domain [91]. This representation generalizes affine LPV models by capturing complex parametric dependencies while enabling vertex-based analysis via convexity principles [85]. The equivalent matrix formulation expresses the parameter-dependent state-space matrices as:

$$\begin{bmatrix} A(\rho) & B(\rho) \\ C(\rho) & D(\rho) \end{bmatrix} = \sum_{i=1}^{\tau} \mu_i(\rho(t)) \begin{bmatrix} A_i & B_i \\ C_i & D_i \end{bmatrix}. \tag{3.9}$$

3.3.3 Quasi-LPV Systems

For nonlinear systems, quasi-LPV models introduce state-/input-dependent scheduling variables ξ [96]:

$$\begin{cases} \dot{x}(t) = A(\xi)x(t) + B(\xi)u(t), \\ y(t) = C(\xi)x(t) + D(\xi)u(t). \end{cases} \tag{3.10}$$

This enables exact nonlinear embedding via state transformations, broadening applicability beyond purely exogenous parameter variations [97].

Affine LPV: Direct dependence on $\rho(t)$; suitable for bounded parameter rates [84].

Polytopic LPV: Vertex-based representation; handles complex parameter spaces [92].

Quasi-LPV: Captures nonlinearities via state/input-dependent scheduling [98].

3.4 Descriptor-Linear Parameter Varying systems

Descriptor-Linear Parameter Varying (D-LPV) systems, also known as singular LPV systems, represent a class of dynamic models that combine features of Linear Parameter Varying (LPV) systems and singular (descriptor) systems. Unlike standard LPV systems, which are described solely by differential equations depending on measurable time-varying parameters, D-LPV systems introduce a descriptor matrix $E(\rho(t))$ that can be singular, leading to differential-algebraic equations (DAEs) parameter-dependent. This structure allows for a more accurate representation of complex physical phenomena involving structural constraints or fast/slow dynamics coupling [82, 99].

A practical example of a Descriptor-LPV system can be found in the modeling of certain biochemical reactors, such as anaerobic digesters used for wastewater treatment [86]. These systems exhibit both fast and slow dynamics: for instance, the acidogenesis stage (fast dynamics) and the methanogenesis stage (slow dynamics) are tightly coupled. The dynamics of the process can be described by differential-algebraic equations, where some variables (e.g., substrate or intermediate metabolite concentrations) are subject to algebraic constraints due to quasi-steady-state assumptions or mass conservation laws. More-

over, key parameters such as temperature, pH, and influent composition vary over time and significantly influence reaction rates and microbial activity. By modeling these parameters as scheduling variables, the system becomes a Descriptor-LPV model [13, 87]. This approach provides a flexible and structured framework for analysis and control design of such complex and nonlinear biochemical processes.

Example: Continuous Stirred Tank Bioreactor (CSTR) A Continuous Stirred Tank Bioreactor (CSTR) is a common process unit where a microbial species consumes a substrate (e.g., glucose) and produces a product (e.g., ethanol). The dynamics of this system are strongly influenced by the temperature $T(t)$, which acts as a time-varying scheduling parameter [78, 100]. The state vector is:

$$x(t) = \begin{bmatrix} S(t) \\ X(t) \\ P(t) \end{bmatrix},$$

where $S(t)$ is the substrate concentration, $X(t)$ the biomass, and $P(t)$ the product. The model adopts a Differential-Algebraic Equation (DAE) structure:

$$E\dot{x}(t) = A(T(t))x(t) + Bu(t),$$

with:

$$E = \begin{bmatrix} 1 & 0 & 0 \\ 0 & 1 & 0 \\ 0 & 0 & 0 \end{bmatrix}, \quad A(T) = \begin{bmatrix} -\mu(T) & 0 & 0 \\ \mu(T) & -k_d & 0 \\ 0 & \alpha\mu(T) & -k_p \end{bmatrix}.$$

The specific growth rate $\mu(T)$ is temperature-dependent and follows an Arrhenius law:

$$\mu(T) = \mu_{\max} \exp\left(-\frac{E_a}{RT}\right),$$

where $\mu_{\max}$ is the maximum growth rate, E_a is the activation energy, and R is the universal gas constant.

The matrix E introduces algebraic constraints reflecting fast dynamics or conservation laws.

The time-varying temperature $T(t)$ makes the system Linear Parameter Varying (LPV). The resulting Descriptor-LPV model is suitable for advanced control strategies, such as gain-scheduling or robust control via LMIs [100].

3.5 Stability of Dynamical Systems

In this part, we recall some fundamental concepts regarding the stability of dynamical systems. The notion of stability of a dynamical system characterizes the behavior of its trajectories in the neighborhood of equilibrium points. Stability analysis thus allows us to study how the system's state trajectory evolves when the initial state is close to an equilibrium point [101, 102].

Consider the differential-algebraic equations described by

$$E\dot{x}(t) = f(x(t), t), \quad x(t_0) = x_0, \quad E = \begin{bmatrix} I_r & 0 \\ 0 & 0 \end{bmatrix} \tag{3.11}$$

Let $x \in \mathcal{X}$, $x(t) \in \mathbb{R}^n$ and $f : \mathbb{R}^n \times \mathbb{R}^+ \to \mathbb{R}^n$ be a continuous function. We denote by x_e an equilibrium point of system (3.11), such that $f(x_e, t) = 0, \quad \forall t \geq t_0$, Without loss of generality, we shall always assume that $f(x)$ satisfies $f(0) = 0$ [103].

Definition 3.5.1 (**Equilibrium points**). A state $x_e, \in \Re^n$ is called equilibrium state (or equilibrium point) of descriptor system (3.11) if once the solution $x(t, t_0, E(x_0))$ of (3.11) is equal to x_e, it remains equal to x_e, for all future time. For the constrained system (3.11), define the set EQ of all equilibrium points, as : $\text{EQ} = \{x \in \mathcal{X} \,|\, F(x) = 0\}$.

This motivates the introduction of the following definitions related to the stability of Differential-Algebraic Equations (DAEs) [104]. Let $\mathbb{B}_\delta$ denote the open ball of radius δ, i.e., $\mathbb{B}_\delta = \{x \in \mathbb{R}^n \,|\, \|x\| < \delta\}$, and let $x = x(t; t_0, Ex(0))$ be the solution trajectory of the system. We also denote $\mathbb{R}_+ = [0, \infty)$.

Definition 3.5.2 (**Stability**). The origin is a Lyapunov stable equilibrium point of system (3.11) if, for all $\varepsilon > 0$, for all $t_0 \geq 0$, there exists a positive scalar $\delta(\varepsilon, t_0)$ such

that:

$$\|x_0\| < \delta(\varepsilon, t_0) \quad \Rightarrow \quad \|x(t; t_0, Ex(0))\| < \varepsilon, \quad \forall t \geq t_0.$$

Otherwise, the origin is said to be unstable.

Note. The initial condition is given in the form $Ex(0) \in Im\, E$, i.e., it is a consistent initial condition.

Definition 3.5.3 (**Uniform Stability**)**.** The origin is said to be a uniformly stable equilibrium point of system (3.11) if, for all $\varepsilon > 0$, there exists a positive scalar $\delta(\varepsilon)$ such that:

$$\|x_0\| < \delta(\varepsilon) \quad \Rightarrow \quad \|x(t, t_0, E(x_0))\| < \varepsilon, \quad \forall t \geq t_0.$$

Definition 3.5.4 (**Attractivity**)**.** The origin is said to be an attractive equilibrium point of system (3.11) if, for all $\varepsilon > 0$, there exists a positive scalar $\delta(t_0)$ such that:

$$\|x_0\| < \delta(t_0) \quad \Rightarrow \quad \lim_{t \to \infty} x(t, t_0, E(x_0)) = 0, \quad \forall t \geq t_0.$$

When $\delta(t_0) = +\infty$, the origin is said to be globally attractive.

Definition 3.5.5 (**Asymptotic Stability**)**.** The origin is said to be an asymptotically (resp. globally asymptotically) stable equilibrium point of system (3.11) if it is stable and attractive (resp. globally attractive).

Definition 3.5.6 (**Exponential Stability**)**.** The origin is said to be locally exponentially stable for system (3.11) if there exist two strictly positive constants α and β such that:

$$\|x(t, t_0, E(x_0))\| \leq \alpha \exp\left(-\beta(t - t_0)\right), \quad \forall t \geq t_0, \forall x_0 \in B_r.$$

When $B_r = \mathbb{R}^n$, the origin is said to be globally exponentially stable.

3.5.1 Example :

This example illustrates the definitions and concepts discussed earlier by demonstrating a singular descriptor system that combines differential and algebraic equations. It provides a concrete application of the theoretical framework, showcasing how these components

interact in practice.

$$E\dot{\mathbf{x}} = A\mathbf{x} + f(\mathbf{x}) \tag{3.12}$$

where:

- $\mathbf{x} = [x_1, x_2, x_3, x_4]^\top \in \mathbb{R}^4$ is the state vector
- Singular matrix with rank 2,

$$E = \begin{bmatrix} 1 & 0 & 0 & 0 \\ 0 & 1 & 0 & 0 \\ 0 & 0 & 0 & 0 \\ 0 & 0 & 0 & 0 \end{bmatrix}$$

- The linear dynamics matrix,

$$A = \begin{bmatrix} -1 & 1 & 0 & 0 \\ 0 & -1 & -1 & 0 \\ 1 & 0 & -1 & 0 \\ 1 & 1 & 0 & 1 \end{bmatrix}$$

- $f(\mathbf{x})$ represents nonlinear terms (if present)

Differential Equations (Dynamic states):

$$\dot{x}_1 = -x_1 + x_2 + f_1(\mathbf{x}) \tag{3.13}$$

$$\dot{x}_2 = -x_2 - x_3 + f_2(\mathbf{x}) \tag{3.14}$$

Algebraic Constraints (Manifold conditions):

$$0 = x_1 + x_2 + x_4 \tag{3.15}$$

$$0 = x_2 + x_3 + x_4 \tag{3.16}$$

Solving (3.15)-(3.16) yields:

$$x_3 = x_1 \quad \text{and} \quad x_4 = -x_1 - x_2 \tag{3.17}$$

Substituting (3.17) into (3.13)-(3.14) gives the constrained flow:

$$\begin{aligned} \dot{x}_1 &= -x_1 + x_2 \\ \dot{x}_2 &= -2x_2 - x_1 \end{aligned} \tag{3.18}$$

The equilibrium point $\mathbf{x}_e$ satisfies:

$$A\mathbf{x}_e + f(\mathbf{x}_e) = \mathbf{0} \quad \text{with} \quad \mathbf{x}_e = [0, 0, 0, 0]^\top \tag{3.19}$$

The Jacobian of (3.18) at equilibrium:

$$J = \begin{bmatrix} -1 & 1 \\ -1 & -2 \end{bmatrix}, \quad \text{eigenvalues: } \lambda = -1.5 \pm 0.87i \tag{3.20}$$

The phase portrait in figure 3.1 illustrates the system's dynamic behavior:

The vector field shows spiral convergence toward equilibrium

All trajectories remain confined to the constraint manifold

Global asymptotic stability is confirmed by the eigenvalues $\lambda = -1.5 \pm 0.87i$

The constraint $x_2 = -x_1$ is maintained throughout convergence

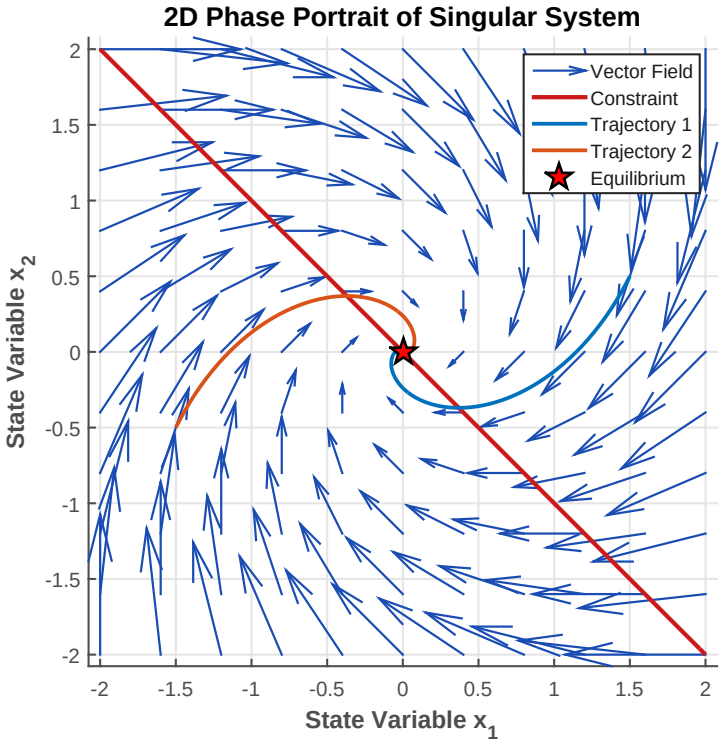

Figure 3.1: Two-dimensional phase portrait of the singular descriptor system

3.6 Lyapunov Stability Theorems

The application of the aforementioned definitions to prove the stability of system about its equilibrium point necessitates obtaining closed-form solutions of the differential equation. Since analytical solutions are generally unavailable for most nonlinear systems, Lyapunov's direct method offers a powerful alternative. The method relies on finding an appropriate energy-like function whose existence directly establishes stability properties [88, 105, 106].

Theorem 3.6.1 (**Theorem**). *Consider the DAE* (3.11) *with* $F(0) = 0$. *Let* $x(0) \in \Im\mathrm{m}E$ *be given. Suppose that there exists a* C^3 *function* $V : \mathcal{X} \to \mathbb{R}$ *vanishing at* $Ex = 0$ *and positive elsewhere which satisfies the following properties [89, 107, 108]:*

(i) $\dfrac{\partial V}{\partial x}(x) = V^T(x)E$ *for some* C^2 *function* $V : \mathcal{X} \to \mathbb{R}^n$, *and*

(ii) $V^T(x)F(x) < 0$, *and*

(iii) $E^T V_x = V_x^T E \geq 0$, *where* V_x *denotes the Jacobian of* $V(x)$, *i.e.,* $V_x = \frac{\partial V(x)}{\partial x}$.

Then the equilibrium point $x = 0$ *is locally asymptotically stable with index one [82, 109, 110].*

Example : (Linear Case) This example shows how Lyapunov theory generalizes to descriptor systems (DAEs) under structural assumptions [107, 111] : Consider a linear index-1 DAE :

$$E\dot{x} = Ax$$

where E is singular and A is stable, if we take $V(x) = x^T E^T P x$ (where $P > 0$), then:

- $\frac{\partial V}{\partial x} = 2x^T E^T P$, so $V^T(x) = 2Px$.
- Condition (ii) becomes $x^T(A^T P + PA)x < 0$, which is a standard Lyapunov condition [88, 112].
- Condition (iii) is satisfied if $E^T P \geq 0$.

Key Points:

- **Structure:** The Lyapunov function $V(x) = x^T E^T P x$ respects the DAE's algebraic constraints via E [107, 111].
- **Stability:** The condition $A^T P + PA < 0$ ensures exponential stability of the ODE part [88, 106].
- **Positivity:** $E^T P \geq 0$ guarantees compatibility between E and the Lyapunov matrix P.

3.6.1 Stability analysis of LPV systems

Theorem 4.4.2 demonstrated how the stability of DAE systems relies on Lyapunov functions constrained by their algebraic structure (via matrix E). For Linear Parameter-Varying (LPV) systems, the use of parameter-dependent Lyapunov functions $V(x, \rho)$ plays a crucial role in the stability analysis of systems whose dynamics are influenced by time-varying or uncertain parameters [84, 90, 113]. These functions extend classical Lyapunov theory by explicitly integrating the dependence on parameters (ρ) into the Lyapunov function framework.

To address this limitation, the concept of robust stability is introduced, aiming to ensure stability despite uncertainties or extreme parameter variations. Quadratic stability fits into this approach by providing a systematic method to analyze the global stability of the system [90, 91, 112].

Definition 3.6.2 (**Quadratic Stability**). Given the compact set $\mathcal{P}$, the autonomous LPV System is said to be *quadratically stable* on $\mathcal{P}$ if there exists a positive definite matrix $P \in \mathbb{S}^n$ satisfying:

$$A^T(p)P + PA(p) \prec 0 \quad \text{for all } p \in \mathcal{P} \tag{3.21}$$

where $\mathbb{S}^n$ denotes the set of symmetric $n \times n$ matrices [91, 113].

An alternative approach, which enables the formulation of less restrictive results compared to those using quadratic stability and can exploit knowledge of bounds on parameter

variation rates, is the *parameter-dependent Lyapunov function* method [90, 114].

3.6.1.1 Parameter-Dependent Lyapunov Functions

We introduce the concept of *Parameter-Dependent Quadratic (PDQ) stability* for LPV systems as a generalization of classical quadratic stability theory, that guarantees the stability of the LPV system dynamics over the entire parameter domain [84, 114].

Definition 3.6.3 (**PDQ Stability**)**.** Consider the following LPV system:

$$\dot{x}(t) = A(p)x(t) \tag{3.22}$$

The system (3.22) is PDQ stable if there exists a differentiable matrix function $P(\rho) \succ 0$ such that:

$$A^T(\rho)P(\rho) + P(\rho)A(\rho) + \sum_{i=1}^{n_\rho} \frac{\partial P}{\partial \rho_i}\dot{\rho}_i \prec 0 \tag{3.23}$$

for all admissible parameter trajectories $\rho(t) \in P$ and rates $\dot{\rho}(t) \in V$ [84, 90, 113].

The quadratic Lyapunov function guaranteeing stability for system (3.22) is given by:

$$V(x, \rho) = x^T P(\rho)x \tag{3.24}$$

For all admissible parameter trajectories $p \in \mathcal{P}$, definition 3.6.2 requires verifying that:

- The function is positive definite: $V(x, \rho) > 0 \quad \forall x \neq 0$
- Its time derivative is negative definite: $\frac{d(V(x,\rho))}{dt} < 0 \quad \forall (x, \rho) \neq (0, 0)$

3.7 Performance and Analysis of LPV Systems

System performance analysis reveals that any control law must satisfy both closed-loop stability requirements and specific performance criteria. These include energy-related performance metrics, disturbance rejection capabilities, and time-domain specifications such as response time and rise time [112, 113].

In the case of LTI systems, in order to mathematically formulate performance indices associated with certain requirements, the concept of performance is often linked, for ex-

ample, to the existence of a bound on the $\mathcal{H}_\infty$ or $\mathcal{H}_2$ norm of the transfer function or to the location of its poles [106, 114]. In general, a controller synthesis problem with a performance constraint can be formulated by specifying a performance criterion to optimize. Such a criterion can be, for example, the norm of the closed-loop system's transfer matrix. The most commonly used norms are the $\mathcal{H}_\infty$ and $\mathcal{H}_2$ norms [115]. A norm serves as both an analysis and synthesis tool, allowing us to characterize not only stability a necessary requirement but also a certain level of performance [116]. We recall here the definition of the $\mathcal{H}_\infty$ norm.

3.7.1 $\mathcal{H}_\infty$ Criterion (Norm)

Consider the LTI system G described by the following state-space representation:

$$G : \begin{cases} \dot{x}(t) = Ax(t) + Bu(t) \\ \\ y(t) = Cx(t) + Du(t) \end{cases} \tag{3.25}$$

The $\mathcal{H}_\infty$ norm of the LTI system (3.25) is the smallest value $\gamma > 0$ satisfying the inequality:

$$\|G\|_{\mathcal{H}_\infty} = \sup_{\omega \in \mathbb{R}} \bar{\sigma}\big(G(j\omega)\big) \leq \gamma \tag{3.26}$$

When the $\mathcal{H}_\infty$ norm of a linear system is finite and bounded by γ, this implies that:

1. The system is stable, and
2. The output energy remains less than or equal to γ times the input energy,

where $\bar{\sigma}$ denotes the maximum singular value [117].

3.7.1.1 Extension of the $\mathcal{H}_\infty$ Norm

In the LPV case, we more precisely refer to the induced $\mathcal{L}_2$ norm and performance in the induced $\mathcal{L}_2$ norm [118]. Indeed, the induced $\mathcal{L}_2$ norm is the extension of the $\mathcal{H}_\infty$ norm to the LPV system case in the sense that it measures the largest possible amplification of the input signal energy over all admissible parameter trajectories [119]. The induced $\mathcal{L}_2$

norm of an LPV system is bounded by γ if:

$$\forall u \in \mathcal{L}_2[0,\infty),\ \forall T \geq 0, \quad \int_0^T y^T(t)y(t)dt \leq \gamma^2 \int_0^T u^T(t)u(t)dt \tag{3.27}$$

for all admissible parameter trajectories $\rho \in \mathcal{P}$ [120].

We note that this definition coincides with the classical $\mathcal{H}_\infty$ norm for LTI systems. Since the notion of poles cannot be defined for LPV systems, there is no frequency-domain interpretation for this norm [119]. Note that, for a QDP stable LPV system, there always exists a finite upper bound on the induced $\mathcal{L}_2$ norm according to the following lemma.

Lemma 3.7.1. *Given a **QDP** stable LPV system, there exists a scalar $\gamma > 0$ such that for zero initial conditions $x(t_0) \equiv 0$,*

$$\sup_{\rho \in \mathcal{F}_p} \sup_{u \in \mathcal{L}_2[0,\infty)} \frac{\|y\|_2}{\|u\|_2} \leq \gamma^2 < \infty. \tag{3.28}$$

The LPV version of the bounded real lemma provides a result that allows us to compute an upper bound of the induced norm using $LMIs$ [118].

Theorem 3.7.2 (**Bounded Real Lemma**). *The LPV system*

$$\begin{cases} \dot{x}(t) = A(\rho)x(t) + B(\rho)u(t) \\ y(t) = C(\rho)x(t) + D(\rho)u(t) \end{cases} \tag{1.8}$$

is quadratically stable over $\mathcal{P}_\rho$ and its induced $\mathcal{L}_2$ norm is bounded by γ, a positive real number, if there exists a symmetric positive definite matrix P such that

$$\begin{bmatrix} A(\rho)^T P + PA(\rho) & PB(\rho) & C(\rho)^T \\ B(\rho)^T P & -\gamma I & D(\rho)^T \\ C(\rho) & D(\rho) & -\gamma I \end{bmatrix} < 0 \tag{3.29}$$

for all admissible parameter trajectories $\rho \in \mathcal{P}_\rho$. ■

Using a unique quadratic Lyapunov function, this theorem provides a sufficient condition to verify whether the induced $\mathcal{L}_2$ norm of an LPV system is smaller than a given value γ [120]. This means that even if condition (4.1) is not satisfied for a given γ, the

actual $\mathcal{L}_2$ norm may be less than γ. This condition can also be used to compute an upper bound of the induced $\mathcal{L}_2$ norm by minimizing γ subject to LMIs (4.1) [112, 113].

3.8 Conclusion

This chapter has laid the theoretical foundations necessary for the robust control synthesis of descriptor-LPV systems. We began with a detailed exploration of the structural properties of singular systems, introducing fundamental notions such as system equivalence, Kronecker-Weierstrass decomposition, and canonical forms including SVD. We also defined regularity, non-impulsiveness, and admissibility, supported by algebraic characterizations through rank conditions. The controllability and observability properties, including C-, R-, and impulsive types, were addressed based on system matrices. Next, we investigated LPV systems, which generalize LTI models by incorporating time-varying parameters. The three main classes affine, polytopic, and quasi-LPV systems were concisely described and illustrated with examples, emphasizing their respective modeling capabilities. A descriptor-LPV system modeling a bioreactor with thermal parameters served as a concrete example of the combined framework. We then focused on the stability analysis of dynamic systems. Classical definitions such as Lyapunov stability, attractivity, and exponential stability were adapted to descriptor systems. Lyapunov-based theorems were presented for both singular and LPV systems, including the use of parameter-dependent Lyapunov functions (PDLFs) to account for parametric variations. Finally, we examined performance analysis criteria, especially the $\mathcal{H}_\infty$ norm and its extension to LPV systems using the induced $\mathcal{L}_2$ norm. The Bounded Real Lemma was introduced in the context of Linear Matrix Inequalities (LMIs), providing a powerful tool for robust control design.

The tools, methods, and concepts presented in this chapter serve as a foundation for the robust control strategies that will be developed and applied in the upcoming chapters. The theoretical contributions are illustrated through examples and practical applications, highlighting their relevance to the modeling and analysis of complex dynamical systems.

Chapter 4

Unknown Input Observer Synthesis for Nonlinear Singular Systems

"A scholar's work is never completed, only abandoned to meet deadlines."
(Paul Val)

4.1 Introduction

State estimation for singular systems subject to unknown inputs represents a critical challenge in modern control theory, with significant applications in robust control, fault diagnosis, and secure system monitoring. This chapter presents a structured observer design framework for such systems, drawing upon foundational works by [121], [122], [123], and [124].

The first part of the chapter focuses on the synthesis of an observer for linear singular systems, In such systems, the state space representation inherently includes algebraic constraints due to the singularity of the matrix E. To decouple the dynamic and algebraic components of the system, a projection matrix $E^{\perp}$ is typically employed [125]. Moreover, the Sylvester equation ensures structural observer-system compatibility by simultaneously addressing differential dynamics and algebraic constraints [93], while output/input matching conditions guarantee convergence of the estimated state [126]. Building on this framework, the chapter addresses the design of an Unknown Input Observer (UIO) for linear time-invariant singular systems subject to both known control inputs and unknown disturbances. The aim is to estimate the system states while completely decoupling the influence of the unknown input . To achieve this, a suitable transformation of the original system allows for the separation of the measurable output components affected and unaffected by the unknown input. Based on this reformulation, a reduced-order observer is constructed using a projection-based framework and a stability condition expressed as a Linear Matrix Inequality (LMI). This approach ensures that the estimation error converges exponentially to zero [127].

The framework is then extended to nonlinear singular systems incorporating Lipschitz-type nonlinearitie in the dynamic system and the disturbance channels. This extension maintains the core robustness and estimation properties of the linear case, while enabling applicability to a specific class of systems. A numerical case study is presented to demonstrate the effectiveness of the studied design, particularly in accurate state estimation,

disturbance attenuation, and robustness against nonlinearitie. While the present chapter lays the theoretical groundwork, two critical aspects namely the handling of structural uncertainties in descriptor LPV system framework subject to Lipschitz nonlinear in both state evolution and output generation, and the integration of sensor fault estimation are not addressed here. These extensions will be developed in the next chapter. This chapter thus provides a rigorous and foundational overview of observer design for singular systems with unknown inputs, serving as a basis for more advanced developments in robust and fault-tolerant control.

4.2 Observers for systems

A state observer is designed to estimate the system's state variables in an asymptotic manner. For this purpose, it is required to fulfill the following conditions [128]:

1. The observer should utilize both the systems control input and its measured output as inputs.
2. The estimation error, defined as $e(t) = \hat{x}(t) - x(t)$, must asymptotically converge to zero, i.e., $\lim_{t\to\infty} e(t) = 0$.

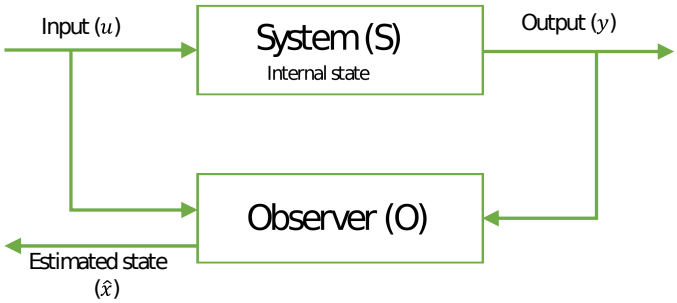

Figure 4.1: State observer principle.

The general scheme of an observer is shown in Figure 4.1. State estimation techniques exhibit significant variation based on system characteristics, measurement availability, and modeling assumptions. The following presents a concise review of observer designs for basic linear systems across various system classes, providing an introduction for the subsequent chapter [129, 130].

4.2.1 Observability of a dynamical system

Before designing an observer, the system's observability must be verifiedthe ability to reconstruct states from input-output data. For nonlinear systems of the form :

$$\begin{cases} \dot{x}(t) = f(x(t), u(t)) \\ y(t) = h(x(t), u(t)) \end{cases} \tag{4.1}$$

where $f : \mathbb{R}^n \times \mathbb{R}^m \to \mathbb{R}^n$ and $h : \mathbb{R}^n \times \mathbb{R}^m \to \mathbb{R}^p$, the observability depends on both input signals and initial conditions, unlike linear systems where algebraic criteria (e.g., Kalman rank condition) apply [131].

Definition 4.2.1 (**Indistinguishability**)**.** A pair of states $(x_0, x_0') \in \mathbb{R}^n \times \mathbb{R}^n$ is said to be indistinguishable for the system (4.1) if, for any input $u \in U$ and for all times $t \geq 0$, their outputs are identical:

$$h(\chi_u(t; x_0)) = h(\chi_u(t; x_0'))$$

where $\chi_u(t; x_0)$ denotes the solution of the state equation under input u, with initial condition $\chi_u(t_0; x_0) = x_0$. In the case of an autonomous system (without control input), the dependence on u is omitted. A state x is indistinguishable from x_0 if the pair (x, x_0) is indistinguishable. This concept directly leads to the notion of observability [132].

Definition 4.2.2 (**Observability**)**.** The system (4.1) is said to be *observable at* x_0 if x_0 can be distinguished from any other state $x \in \mathbb{R}^n$. Moreover, the system (4.1) is *observable* if, for every $x_0 \in \mathbb{R}^n$, the system is observable at x_0 [133].

4.3 State Observers for Linear Singular Systems

Singular systems have attracted considerable interest in the control theory community [134]. Several methods for controller and observer synthesis have been proposed for linear singular systems, generally extending standard results while addressing their

specific characteristics [135]. Consider the linear singular system:

$$\begin{cases} E\dot{x}(t) = Ax(t) + Bu(t) \\ y(t) = Cx(t) \end{cases} \tag{4.2}$$

where $x(t) \in \mathbb{R}^n$ is the state vector, $y(t) \in \mathbb{R}^p$ is the output, and $u(t) \in \mathbb{R}^m$ is the input. E is singular with $\text{rank}(E) = r < n$, while A, B, and C are properly dimensioned matrices [136]. For standard systems ($E = I$), detectability reduces to:

$$\text{rank} \begin{bmatrix} sI - A \\ C \end{bmatrix} = n, \quad \forall s \in \overline{\mathbb{C}^+}. \tag{4.3}$$

For singular systems ($\text{rank}(E) = r < n$):

- Ensures all **unstable modes** ($s \in \overline{\mathbb{C}^+}$) are **observable** [137]
- Admits a singular observer of the form:

$$E\dot{\hat{x}}(t) = A\hat{x}(t) + Bu(t) + L(y(t) - C\hat{x}(t)) \tag{4.4}$$

where $\hat{x}(t)$ is the estimated state and $L \in \mathbb{R}^{n \times p}$ is the observer gain. The error dynamics $e(t) = x(t) - \hat{x}(t)$ satisfy:

$$E\dot{e}(t) = (A - LC)e(t) \tag{4.5}$$

Under detectability, the pair $(E, A - LC)$ has stable finite eigenvalues [138]:

$$\lim_{t \to \infty} e(t) = 0, \quad \forall x_0, \hat{x}_0$$

System (4.4) is therefore an asymptotic generalized Luenberger observer [139].

4.3.1 Proportional observers for singular systems

The estimation of unmeasured variables in singular systems (also known as descriptor systems) can be achieved using a Proportional Observer (PO), whose design was developed by [140]. This type of observer is based on the concept of partial impulse

observability [130]. Consider the following singular system:

$$\begin{cases} E\dot{x}(t) = Ax(t) + Bu(t) \\ y(t) = C_1 x(t) \\ z(t) = Lx(t) \end{cases} \tag{4.6}$$

where $x(t) \in \mathbb{R}^n$ is the descriptor state vector, $u(t) \in \mathbb{R}^m$ is the input, $y(t) \in \mathbb{R}^q$ is the measured output, and $z(t) \in \mathbb{R}^p$ is the quantity to be estimated. The matrices E, A, B, C_1 and L are constant and known [135].

Separation of dynamics and algebraic constraints : In singular systems, the state-space representation involves algebraic constraints (due to the singularity of E). To decouple the dynamic and algebraic components, a projection matrix $E^{\perp}$ is introduced [137]. The output matrix C_1 ensures algebraic constraints are properly considered in the estimation process [138].

Structure of the proportional observer (PO) The observer proposed by [140] is defined by:

$$\dot{\zeta}(t) = N\zeta(t) + F \begin{bmatrix} -E^{\perp}Bu(t) \\ y(t) \end{bmatrix} + Hu(t) \tag{4.7}$$

$$\hat{z}(t) = P\zeta(t) + Q \begin{bmatrix} -E^{\perp}Bu(t) \\ y(t) \end{bmatrix} \tag{4.8}$$

where $\zeta(t) \in \mathbb{R}^q$ is the observer state, and $\hat{z}(t)$ is the estimation of $z(t)$. The matrices N, F, H, P, and Q are to be determined [141].

Estimation error dynamics : The estimation error is defined as:

$$\varepsilon(t) = \zeta(t) - TEx(t)$$

where T is a matrix to be determined. The error dynamics are given by:

$$\dot{\varepsilon}(t) = N\varepsilon(t) + \left(NTE - TA + F \begin{bmatrix} E^{\perp}A \\ C_1 \end{bmatrix} \right) x(t) + (H - TB)u(t)$$

Observer design conditions : To ensure asymptotic convergence of the estimation error to zero, the following conditions must be satisfied:

1. **Sylvester equation (dynamic coupling condition)**

$$NTE - TA + F \begin{bmatrix} E^{\perp}A \\ C_1 \end{bmatrix} = 0 \tag{4.9}$$

This condition ensures that all terms involving $x(t)$ vanish from the error dynamics [142].

Remark 4.3.1. The Sylvester equation guarantees that the dynamics imposed by the observer are compatible with the singular system's structure, by coupling both the differential dynamics and algebraic constraints [143].

2. **Output matching condition**

$$[P \quad Q] \begin{bmatrix} TE \\ E^{\perp}A \\ C_1 \end{bmatrix} = L \tag{4.10}$$

This condition ensures accurate estimation of $z(t)$ [144].

3. **Input matching condition**

$$H = TB$$

This guarantees correct consideration of input effects [145].

Error convergence : Under these conditions, the error dynamics reduce to:

$$\dot{\varepsilon}(t) = N\varepsilon(t)$$

The estimation error asymptotically converges to zero if N is Hurwitz [146].

Design procedure : The method provides a systematic procedure to design reduced-order proportional observers for singular systems [147]. The matrices can be obtained by solving the Sylvester equation and associated algebraic conditions.

4.3.2 Full-Order Observer Design for Singular System

Consider the linear time-invariant singular system (4.2). The following rank condition is assumed:

$$\operatorname{rank}\begin{bmatrix} E & A \\ 0 & E \\ 0 & C \end{bmatrix} = n + \operatorname{rank}(E) \tag{4.11}$$

This condition guarantees that the algebraic constraints, the system dynamics, and the output measurements are consistent. It ensures the existence of a unique, impulse-free solution and provides a well-posed framework for observer design [82, 140, 148]. Physically, it means that the number of independent dynamic and algebraic equations, together with the output constraints, is sufficient to fully describe the system's behavior without ambiguity or inconsistency. Since $\operatorname{rank}(E) = r$, there exists a nonsingular matrix $P \in \mathbb{R}^{m\times m}$ such that:

$$PE = \begin{bmatrix} E^* \\ 0 \end{bmatrix}, \quad PA = \begin{bmatrix} A^* \\ A_1 \end{bmatrix}, \quad PB = \begin{bmatrix} B^* \\ B_1 \end{bmatrix} \tag{4.12}$$

with $E^* \in \mathbb{R}^{r\times n}$, $\operatorname{rank}(E^*) = r$, $A^* \in \mathbb{R}^{r\times n}$, $A_1 \in \mathbb{R}^{(m-r)\times n}$, $B^* \in \mathbb{R}^{r\times q}$, and $B_1 \in \mathbb{R}^{(m-r)\times q}$. This decomposition separates the dynamic and algebraic parts of the system. By this transformation, we obtain an equivalent system:

$$\begin{aligned} E^*\dot{x} &= A^*x + B^*u \\ y^* &= C^*x \end{aligned} \tag{4.13}$$

where

$$y^* = \begin{bmatrix} -B_1u \end{bmatrix} \in \mathbb{R}^{q_1}, \quad C^* = \begin{bmatrix} A_1 \\ C \end{bmatrix} \in \mathbb{R}^{q_1\times n}, \quad q_1 = m + p - r. \tag{4.14}$$

Using these transformations, we can verify that:

$$\operatorname{rank}\begin{bmatrix} E^* & A^* \\ 0 & E^* \\ 0 & C^* \end{bmatrix} = n + \operatorname{rank}(E^*) \tag{4.15}$$

Analogously, since E^* has full row rank, we have:

$$\operatorname{rank}\begin{bmatrix} E^* \\ C^* \end{bmatrix} = n \tag{4.16}$$

To proceed with observer design, it is necessary to eliminate algebraic dependencies. Therefore, there exists an invertible matrix $\begin{bmatrix} a & b \\ c & d \end{bmatrix}$ is constructed such that :

$$\begin{aligned} aE^* + bC^* &= I_n \\ cE^* + dC^* &= 0. \end{aligned} \tag{4.17}$$

These relations help to decouple the algebraic parts and ensure the system is in a form suitable for observer design.

Remark 4.3.2 (SVD decomposition). The nonsingular matrix $\begin{bmatrix} a & b \\ c & d \end{bmatrix}$ can be obtained from the singular value decomposition (SVD) of $\begin{bmatrix} E^* \\ C^* \end{bmatrix}$. Since this matrix has full column rank [149], there exist unitary matrices U and V of appropriate dimensions such that:

$$U^\top \begin{bmatrix} E^* \\ C^* \end{bmatrix} V = \begin{bmatrix} \Sigma_1 \\ 0 \end{bmatrix} \tag{4.18}$$

where $\Sigma_1 = \operatorname{diag}(\sigma_1, \ldots, \sigma_n)$ with $\sigma_i > 0$ for all $i = 1, \ldots, n$.

The objective is to synthesize a full-order observer (order n) satisfying the following form [148, 150]:

$$\begin{cases} \dot{z} = Nz + L_1 y^* + L_2 y^* + Gu \\ \hat{x} = z + by^* + Kdy^* \end{cases} \tag{4.19}$$

where N, L_1, L_2, G, and K are matrices of appropriate dimensions to be determined so that $\hat{x}$ converges asymptotically to x.

Theorem 4.3.3. *Sufficient conditions for the existence of the observer* (4.19) *are:*

1. $rank \begin{bmatrix} E & A \\ 0 & E \\ 0 & C \end{bmatrix} = n + rank\, E,$

2. $rank \begin{bmatrix} sE - A \\ C \end{bmatrix} = n, \ \forall s \in \mathbb{C}, \ Re(s) \geq 0.$

4.3.3 Reduced-order Observer Design for Singular System

Without loss of generality, we assume that the rank of C^* is q_1 see (4.14). Our goal is to design an observer for the singular system under consideration (4.13) of the form :

$$\dot{z} = \pi z + Ly^* + Hu \tag{4.20}$$

$$\hat{x} = Mz + Fy^* \tag{4.21}$$

where $z \in \mathbb{R}^{n-q_1}$ represents the dynamics of the reduced-order observer. The task is to determine matrices π, L, H, M, and F to ensure that $\hat{x}$ converges asymptotically to x.

Theorem 4.3.4. *Let* $T \in \mathbb{R}^{(n-q_1)\times r}$ *satisfy*

$$TA^* - \pi TE^* = LC^* \tag{4.22}$$

and

$$\det \begin{bmatrix} TE^* \\ C^* \end{bmatrix} \neq 0 \tag{4.23}$$

Then, defining

$$H = TB^* \tag{4.24}$$

and

$$\begin{bmatrix} TE^* \\ C^* \end{bmatrix} \begin{bmatrix} M & F \end{bmatrix} = \begin{bmatrix} I_{n-q_1} & 0 \\ 0 & I_{q_1} \end{bmatrix} \tag{4.25}$$

we obtain

$$\hat{x}(t) - x(t) = Me^{\pi t}[w(0) - TE^*x(0)] \tag{4.26}$$

The observer converges if and only if π is stable.

We now outline a method to compute T based on Sylvester's equation (4.22) [140, 151]. We introduce the following nonsingular matrices:

$$\begin{bmatrix} R^* \\ C \end{bmatrix} = \begin{bmatrix} I_{n-q_1} & K \\ 0 & I_{q_1} \end{bmatrix} \begin{bmatrix} TE^* \\ C^* \end{bmatrix} \tag{4.27}$$

where $K \in \mathbb{R}^{(n-q_1)\times q_1}$ is arbitrary, and $R \in \mathbb{R}^{(n-q_1)\times n}$ is full-row rank. This leads to

$$\begin{bmatrix} T & K \end{bmatrix} \begin{bmatrix} E^* \\ C^* \end{bmatrix} = R \tag{4.28}$$

Since $\begin{bmatrix} E^* \\ C^* \end{bmatrix}$ is full column rank, the general solution is:

$$\begin{bmatrix} T & K \end{bmatrix} = R \begin{bmatrix} E^* \\ C^* \end{bmatrix}^+ + Z \left(I_{r+q_1} - \begin{bmatrix} E^* \\ C^* \end{bmatrix} \begin{bmatrix} E^* \\ C^* \end{bmatrix}^+ \right) \tag{4.29}$$

where $\begin{bmatrix} E^* \\ C^* \end{bmatrix}^+$ denotes the Moore-Penrose pseudo-inverse and Z is an arbitrary matrix. Explicitly:

$$T = R\Delta E^{*\mathrm{T}} + Z \begin{bmatrix} I_r - E^*\Delta E^{*\mathrm{T}} \\ -C^*\Delta E^{*\mathrm{T}} \end{bmatrix} \tag{4.30}$$

$$K = R\Delta C^{\mathrm{T}} + Z \begin{bmatrix} -E^*\Delta C^{*\mathrm{T}} \\ I_{q_1} - C^*\Delta C^{*\mathrm{T}} \end{bmatrix} \tag{4.31}$$

with $\Delta = \left(E^{*\mathrm{T}}E^* + C^{*\mathrm{T}}C^*\right)^{-1}$. From (4.22), we deduce:

$$\pi = TA^*M \tag{4.32}$$

$$L = TA^*F \tag{4.33}$$

Thus:

$$\pi = \Gamma + Z\Omega \tag{4.34}$$

where

$$\Gamma = R\Delta E^{*\mathrm{T}}A^*M \tag{4.35}$$

$$\Omega = \begin{bmatrix} I_r - E^*\Delta(E^*)^{\mathrm{T}} \\ -C^*\Delta(E^*)^{\mathrm{T}} \end{bmatrix} A^*M \tag{4.36}$$

We conclude that if the pair (Γ, Ω) is detectable, π is stable and a stable observer can be designed [130].

Theorem 4.3.5. *For system (4.13), a reduced-order observer of type (4.20)–(4.21) exists if conditions (a) and (b) of Theorem 4.3.3 are satisfied [152].*

The synthesis algorithm can be summarized as follows:

1. Select $R \in \mathbb{R}^{(n-q_1)\times q_1}$ such that $\begin{bmatrix} R^* \\ C \end{bmatrix}$ is nonsingular.
2. Compute M from (4.25) and (4.28):

$$M = \begin{bmatrix} R^* \\ C \end{bmatrix}^{-1} \begin{bmatrix} I_{n-q_1} \\ 0 \end{bmatrix} \tag{4.37}$$

3. If (Γ, Ω) is detectable, determine Z and deduce T via (4.30).
4. Compute F from (4.25):

$$F = \begin{bmatrix} TE^* \\ C^* \end{bmatrix}^{-1} \begin{bmatrix} 0 \\ I_{q_1} \end{bmatrix} \tag{4.38}$$

5. Compute H and L using (4.24) and (4.33). □

4.4 Unknown input observer for linear singular systems

Consider the following singular linear time-invariant (LTI) system:

$$\begin{aligned} E\dot{x}(t) &= Ax(t) + Bu(t) + E_2 d(t) \\ y(t) &= Cx(t) + E_3 d(t) \end{aligned} \tag{4.39}$$

where $x(t) \in \mathbb{R}^n$ is the state vector, $u(t) \in \mathbb{R}^q$ the known control input, $y(t) \in \mathbb{R}^p$ the measured output, and $d(t) \in \mathbb{R}^m$ an unknown input. The matrices E, A, B, E_2, C, and E_3 are known with appropriate dimensions, and E is singular. The objective is to design an Unknown Input Observer (UIO) that estimates the state $x(t)$ without being affected by the unknown input $d(t)$ [130, 140].

Assumption 4.4.1. The following assumptions are considered:

A1. $\operatorname{rank}\begin{bmatrix} E & E_2 \end{bmatrix} = m \leq p$, The effect of $d(t)$ is observable in the outputs..

A2. The effect of $d(t)$ is observable in the outputs, which ensures the consistency of the differential-algebraic equations with the output measurements.

$$\operatorname{rank}\begin{bmatrix} E & A & E_2 & 0 \\ 0 & E & 0 & E_2 \\ 0 & C & E_3 & 0 \\ 0 & 0 & 0 & E_3 \end{bmatrix} - \operatorname{rank}\begin{bmatrix} E & E_2 \\ 0 & E_3 \end{bmatrix} = n + m$$

A3. $\operatorname{rank}(E) = r < n$

A4. $\operatorname{rank}\begin{bmatrix} C & E_3 \end{bmatrix} = p$, all components of $d(t)$ appear in the outputs.

Before proceeding with the synthesis, we need to apply the necessary transformations to the initial model (4.39) to ensure the existence and synthesis of this observer. These transformations allow us to separate the part of the measurements unaffected by the unknown inputs from the part affected by these inputs [151].

4.4.1 Transformation of the initial model

This decomposition separates the differential equations (associated with E^*) from the algebraic constraints (associated with the zero block). Since $\text{rank}(E) = r$, there exists an invertible matrix P such that:

$$PE = \begin{bmatrix} E^* \\ 0_{(n_1-r)\times n} \end{bmatrix}, \quad PA = \begin{bmatrix} A^* \\ A_1 \end{bmatrix}, \quad PB = \begin{bmatrix} B^* \\ B_1 \end{bmatrix}, \quad PE_2 = \begin{bmatrix} F \\ F_1 \end{bmatrix} \tag{4.40}$$

where

$$P \in \mathbb{R}^{n_1\times n_1}, \quad E^* \in \mathbb{R}^{r\times n}\ (\text{rank}(E^*) = r), \quad A^* \in \mathbb{R}^{r\times n}, \quad B^* \in \mathbb{R}^{r\times q}, \quad F \in \mathbb{R}^{r\times m},$$

$$A_1 \in \mathbb{R}^{(n_1-r)\times n}, \quad B_1 \in \mathbb{R}^{(n_1-r)\times q}, \quad F_1 \in \mathbb{R}^{(n_1-r)\times m}.$$

Thus, the system (4.39) can be equivalently written as follows:

$$\begin{aligned} E^*\dot{x}(t) &= A^*x(t) + B^*u(t) + Fd(t) \\ y^*(t) &= C^*x(t) + D^*d(t) \end{aligned} \tag{4.41}$$

where

$$y^* = \begin{bmatrix} -Bu \\ y_1 \end{bmatrix} \in \mathbb{R}^{p_1}, \quad C^* = \begin{bmatrix} A_1 \\ C \end{bmatrix} \in \mathbb{R}^{p_1\times n}, \quad D^* = \begin{bmatrix} F_1 \\ E_3 \end{bmatrix} \in \mathbb{R}^{p_1\times m}. \tag{4.42}$$

with $p_1 = n_1 + p - r$. If $\text{rank}(D^*) = q_1 \leq m$, then there exist two invertible matrices U and V such that:

$$UD^*V = \begin{bmatrix} I_{q_1} & 0 \\ 0 & 0 \end{bmatrix} \tag{4.43}$$

By setting

$$d = V \begin{bmatrix} d_1 \\ d_2 \end{bmatrix} \quad \text{and} \quad F_V = \begin{bmatrix} F_{11} & F_{12} \end{bmatrix}$$

equation (4.41) becomes

$$E^*\dot{x}(t) = A^*x(t) + B^*u(t) + F_{11}d_1(t) + F_{12}d_2(t) \tag{4.44}$$

and using (4.42), with

$$Uy^* = \begin{bmatrix} y_1 \\ y_2 \end{bmatrix} \quad UC^* = \begin{bmatrix} C_{11} \\ C_{12} \end{bmatrix}$$

(4.41) becomes

$$\begin{aligned} y_1 &= C_{11}x + d_1 \\ y_2 &= C_{12}x \end{aligned} \tag{4.45}$$

Therefore from (4.4.1), (4.4.1), the system (4.41) becomes

$$\begin{aligned} E^*\dot{x}(t) &= \Phi x(t) + B^*u(t) + F_{11}y_1(t) + F_{12}d_2(t) \\ y_1(t) &= C_{11}x(t) + d_1(t) \\ y_2(t) &= C_{12}x(t) \end{aligned} \tag{4.46}$$

with $\Phi = A^* - F_{11}C_{11}$, $y_2 \in \mathbb{R}^{p_1-q_1} = \mathbb{R}^{p_2}$, $y_1 \in \mathbb{R}^{q_1}$, and $\text{rank}(C_{12}) = p_2 = p_1 - q_1$, $\text{rank}\begin{bmatrix} C \\ E \end{bmatrix} = p$. According to [153, 154], a reduced-order observer for the singular system (4.39) is given by:

$$\begin{aligned} \dot{z}(t) &= \Pi z(t) + L_1 y_1(t) + L_2 y_2(t) + Hu(t) \\ \hat{x}(t) &= Mz(t) + Ny_2(t) \end{aligned} \tag{4.47}$$

where $z \in \mathbb{R}^{n-p_2}$, $\hat{x} \in \mathbb{R}^n$ is the estimate of x, and the matrices Π, L_1, L_2, H, M, and N are designed such that $\hat{x} \to x$.

4.4.2 Reduced-order unknown-input observer synthesis procedure

The following theorem presents a systematic design procedure for the reduced-order unknown-input observer, building upon recent advances in descriptor system observation [130, 140].

Theorem 4.4.2. *Consider matrices $T \in \mathbb{R}^{(n-p_2)\times r}$ satisfying the following conditions:*

$$T\Phi - \Pi T E^* = L_2 C_{12} \tag{4.48}$$

$$TF_{12} = 0, \tag{4.49}$$

with the full-rank condition $\det \begin{bmatrix} TE^* \\ C_{12} \end{bmatrix} \neq 0$. *Then, defining:*

$$H = TB^* \tag{4.50}$$

$$L_1 = TF_{11}, \tag{4.51}$$

and solving the matrix equation:

$$\begin{bmatrix} TE^* \\ C_{12} \end{bmatrix} \begin{bmatrix} M & N \end{bmatrix} = \begin{bmatrix} I_{n-p_2} & 0 \\ 0 & I_{p_2} \end{bmatrix}, \tag{4.52}$$

the estimation error dynamics satisfy:

$$\hat{x}(t) - x(t) = Me^{\Pi t}\big(z(0) - TE^* x(0)\big). \tag{4.53}$$

The exponential convergence of the reduced-order observer is guaranteed when Π *is Hurwitz stable [155].*

The observer matrix Π admits the following parameterization:

$$\Pi = \Omega + Z\Gamma, \tag{4.54}$$

where Ω and Γ are derived matrices and Z represents the observer gain. Following modern robust design approaches [153, 156], we employ an LMI-based synthesis method to ensure observer stability while accommodating additional performance criteria.

Lemma 4.4.3. *The reduced-order observation problem for the descriptor system* (4.39) *with observer* (4.46) *admits a solution if there exist matrices* $X = X^\top \succ 0 \in \mathbb{R}^{(n-p_2)\times(n-p_2)}$ *and* $Y \in \mathbb{R}^{(n-p_2)\times(r+p_2)}$ *satisfying the LMI:*

$$X\Omega + \Omega^\top X + Y\Gamma + \Gamma^\top Y^\top \prec 0. \tag{4.55}$$

The observer gain matrix is then given by $Z = X^{-1}Y$ *[157].*

Proof. Considering the relations (4.48)–(4.51) and parameterization (4.54), the estimation

error dynamics:

$$e(t) = z(t) - TE^{*}x(t) \tag{4.56}$$

evolve according to:

$$\dot{e}(t) = (\Omega + Z\Gamma)e(t). \tag{4.57}$$

Employing the quadratic Lyapunov function from [158]:

$$V(e,t) = e^{\top}(t)Xe(t), \tag{4.58}$$

with $X = X^{\top} \succ 0$, we derive the stability condition:

$$(\Omega + Z\Gamma)^{\top}X + X(\Omega + Z\Gamma) \prec 0. \tag{4.59}$$

The result follows by substituting $Y = XZ$ [159]. □

The complete synthesis procedure, extending the framework of [160], is summarized as follows:

1. Select matrix R ensuring the invertibility condition:

$$\det \begin{bmatrix} R \\ C_{12} \end{bmatrix} \neq 0 \text{ [161]}$$

2. Compute M via the explicit formula:

$$M = \begin{bmatrix} R \\ C_{12} \end{bmatrix}^{-1} \begin{bmatrix} I_{n-p_1} \\ 0 \end{bmatrix}.$$

3. Determine observer matrices following [135]:

$$\Delta = \left(\begin{bmatrix} E^{*} \\ C_{12} \end{bmatrix}^{\top} \begin{bmatrix} E^{*} \\ C_{12} \end{bmatrix} \right)^{-1}$$

$$\varphi = \begin{bmatrix} I_r - E^{*}\Delta(E^{*})^{\top} \\ -C_{12}\Delta(E^{*})^{\top} \end{bmatrix}$$

$$\alpha = I_r - F_{12}(\varphi F_{12})^{+}\varphi$$

$$\Omega = R\Delta(E^*)^{\top}\alpha\Phi M$$

$$\Gamma = \varphi\alpha\Phi M.$$

4. Solve the LMI (4.55) using convex optimization techniques from [**?**] to obtain Z.

5. Compute N via the partitioned inverse:

$$N = \begin{bmatrix} TE^* \\ C_{12} \end{bmatrix}^{-1} \begin{bmatrix} 0 \\ I_{p_2} \end{bmatrix}. \tag{4.60}$$

6. Finally, determine the remaining observer matrices H, L_1, and L_2 following [**?**].

4.5 Observer design for a class of nonlinear singular systems with unknown inputs

Building on the foundational work of [82] and extending recent developments in [162], we consider the class of nonlinear systems described by:

$$\begin{cases} \dot{x}(t) = Ax(t) + B_d d(t) + B_u u(t) + f\big(x(t), d(t), y(t)\big) \\ y(t) = Cx(t) + Dd(t) \end{cases} \tag{4.61}$$

where the system matrices follow standard definitions as in [121], with the nonlinear function f satisfying:

Assumption 4.5.1. The Lipschitz condition from [163] holds:

$$\big\|f(x_1, d_1, y) - f(x_2, d_2, y)\big\| \leq \gamma \Big\| \begin{bmatrix} x_1 - x_2 \\ d_1 - d_2 \end{bmatrix} \Big\| \tag{4.62}$$

Assumption 4.5.2. Following [122], the matrix D has full column rank:

$$\operatorname{rank}(D) = m \tag{4.63}$$

The transformation to singular system form uses the approach of [164]:

$$\begin{cases} E\dot{\xi}(t) = M\xi(t) + B_u u(t) + f\big(\xi(t), y(t)\big) \\ y(t) = H\xi(t) \end{cases} \tag{4.64}$$

Lemma 4.5.3. *Extending results from [91], we have:*

$$ZY^T + YZ^T \leq \beta\, YY^T + \frac{1}{\beta}\, ZZ^T \tag{4.65}$$

Theorem 4.5.4. *Combining techniques from [124] and [165], the observer exists if:*

$$\begin{bmatrix} (RM)^T P + P(RM) - H^T X^T - XH + \beta\gamma^2 I & PR \\ R^T P & -\beta I \end{bmatrix} < 0 \tag{4.66}$$

Proof. The Lyapunov stability proof follows [88] with adaptations from [166]. □

4.5.1 Numerical example

We consider state estimation for a chaotic Lorenz system [167] in the form (4.61) with matrices:

$$A = \begin{bmatrix} -10 & 10 & 0 \\ 28 & -1 & 0 \\ 0 & 0 & -8/3 \end{bmatrix}, \quad B_u = \begin{bmatrix} 30 \\ 28 \\ 0 \end{bmatrix}, \quad f(x) = \begin{bmatrix} 0 \\ -x_2 x_3 \\ x_2^2 \end{bmatrix}$$

Output matrices:

$$C = \begin{bmatrix} 1 & 0 & 0 \\ 0 & 1 & 0 \end{bmatrix}, \quad D = \begin{bmatrix} 1 & 0 \end{bmatrix}$$

The system is subject to:

- Unknown inputs $d(t) = 0.05\sin(1.6\pi t)$

Observer design results The LMI constraints from Equation (4.66) were successfully solved in 32 iterations with the following characteristics:

- Best objective value: 1.000002×10^{-6}
- Absolute accuracy: 3.64×10^{-11}

- Full rank condition for Φ satisfied

Optimized matrices:

$$P = 10^8 \times \begin{bmatrix} 3.2717 & -0.8639 & -0.0665 & 1.5848 \\ -0.8639 & 0.9569 & 0.1790 & 0.3631 \\ -0.0665 & 0.1790 & 2.8104 & 0.0175 \\ 1.5848 & 0.3631 & 0.0175 & 2.5705 \end{bmatrix}, \quad F = \begin{bmatrix} -2.2732 & 9.6587 \\ -3.1774 & 16.6086 \\ 0.1043 & -0.8562 \\ 3.3054 & -9.1744 \end{bmatrix}$$

Observer characteristics:

- Eigenvalues of N: $\{-17.1732, -1.7497, -7.6435, -8.1058\}$ (stable)
- Gain matrix L:

$$\begin{bmatrix} -0.0315 & 10.2657 \\ -0.7188 & 7.6807 \\ 0.0773 & -0.7242 \\ 0.0055 & -9.9566 \end{bmatrix}$$

4.5.2 Simulation results

Initial conditions:

- Real states: $x(0) = [2\ 5\ 8]^\top$
- Estimated states: $\hat{x}(0) = [0\ 0\ 0]^\top$

The results demonstrate:

- Rapid convergence of estimated states (Fig. 4.2)
- Stable error dynamics (Fig. 4.3)
- Robustness against unknown inputs $d(t)$
- Finite-time convergence of estimation errors

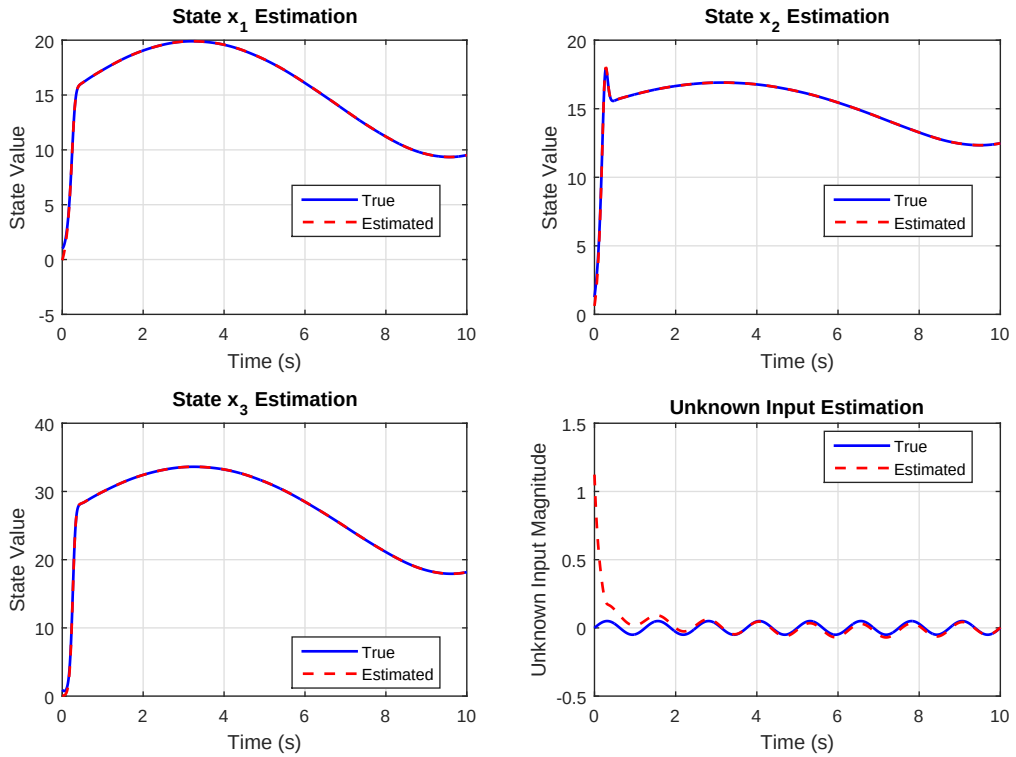

Figure 4.2: State and Unknown Input Estimation Performance for states x_1, x_2, x_3.

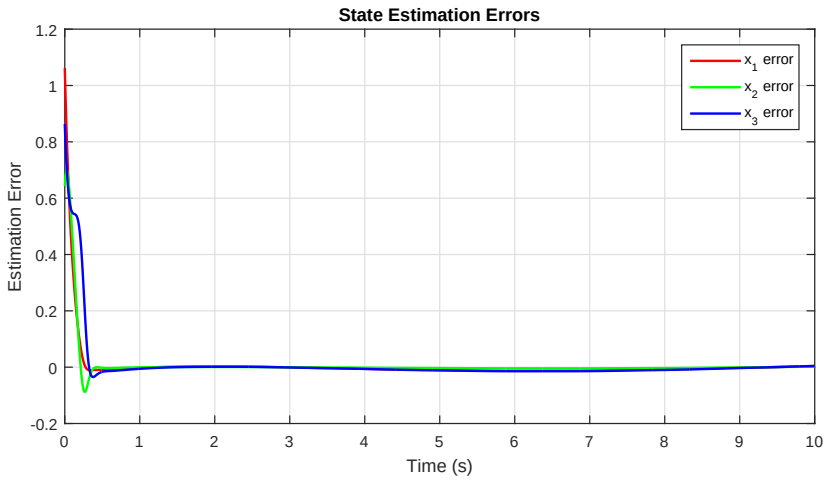

Figure 4.3: Estimation errors ($e_i = x_i - \hat{x}_i$, $i = 1, 2, 3$) demonstrating observer convergence.

4.6 Extension to $\mathcal{H}_\infty$ filtering: robust observer design

Building on the foundational work of [82] and recent advances in [162], we consider the class of nonlinear systems:

$$\begin{cases} \dot{x}(t) = Ax(t) + B_d d(t) + B_u u(t) + f(x(t), d(t), y(t)) + D_x w(t) \\ y(t) = Cx(t) + Dd(t) + D_y w(t) \end{cases} \tag{4.67}$$

where the system matrices follow standard definitions from [121], with the nonlinear function f satisfying :

Assumption 4.6.1. The disturbance properties follow [168]: $w \in \mathbb{L}_2([0, +\infty))$

Assumption 4.6.2. The structural condition aligns with [122]:

$$\operatorname{rank}\left(\begin{bmatrix} D & D_y \end{bmatrix}\right) = m + r$$

Following the descriptor system approach of [164], we transform the system:

$$\begin{cases} E\dot{\xi}(t) = M\xi(t) + B_u u(t) + f(\xi(t), y(t)) + D_x w \\ y(t) = H\xi(t) + D_y w \end{cases} \tag{4.68}$$

The matrix decomposition builds on results from [121]:

$$\begin{bmatrix} R_1 & Q_1 \\ R_2 & Q_2 \end{bmatrix} = \mathcal{M}^{-1} \begin{bmatrix} E & 0 \\ H & D_y \end{bmatrix}^\top \tag{4.69}$$

where $R_1 \in \mathbb{R}^{(n+m)\times n}$, $R_2 \in \mathbb{R}^{r\times n}$, $Q_1 \in \mathbb{R}^{(n+m)\times p}$, $Q_2 \in \mathbb{R}^{r\times p}$.

$$\begin{bmatrix} R_1 & Q_1 \\ R_2 & Q_2 \end{bmatrix}$$

$$\begin{bmatrix} E & 0 \\ H & D_y \end{bmatrix} = \begin{bmatrix} I_{n+m} & 0 \\ 0 & I_q \end{bmatrix}$$

4.6.1 Observer structure

Following the observer design methodology of [121] and extending the approach in [124], we propose the following observer structure for system (4.68):

$$\begin{cases} \dot{z}(t) = Nz(t) + Ly(t) + R_1 f(\hat{\zeta}(t), y(t)) + R_1 B_u u(t) \\ \hat{\zeta}(t) = z(t) + Q_1 y(t) \end{cases} \tag{4.70}$$

where:

- $z(t) \in \mathbb{R}^{n+m}$ is the observer state vector
- $\hat{\zeta}(t) \in \mathbb{R}^{n+m}$ represents the estimated augmented state
- Matrices N and L are designed to ensure robust estimation

The estimation error dynamics are given by:

$$e(t) = \hat{\zeta}(t) - \zeta(t) \tag{4.71}$$

4.6.2 Observer design problem

The observer design problem requires finding matrices N and L that satisfy the following $\mathcal{H}_\infty$ performance criteria:

1. **Asymptotic convergence**:

$$\lim_{t\to\infty} e(t) = 0 \quad \text{when} \quad w(t) = 0 \tag{4.72}$$

2. **Disturbance attenuation**:

$$\|e\|_{L_2} \leq \gamma \|w\|_{L_2}, \quad e(0) = 0 \tag{4.73}$$

4.6.2.1 Lyapunov stability condition

Building on the results of [91], we establish the following stability condition:

$$\mathcal{V} \triangleq \dot{V}(e) + e^\top e - \gamma^2 w^\top w < 0 \tag{4.74}$$

where $V(e) = e^\top P e$ is the Lyapunov function candidate.

Theorem 4.6.3. *Under Assumptions 4.6.1 and 4.6.2, the observer error dynamics are asymptotically stable with $\mathcal{H}_\infty$ performance γ if there exist matrices $P = P^\top > 0$, X, and scalar $\beta > 0$ satisfying:*

$$\begin{bmatrix} \Gamma(P,X) & PR_1 & X^\top D_y - PR_1 D_x \\ * & -\beta I & 0 \\ * & 0 & -\gamma^2 I \end{bmatrix} < 0 \tag{4.75}$$

where $\Gamma(P,X) = (R_1 M)^\top P + P(R_1 M) - H^\top X - X^\top H + (1+\beta\gamma^2)I$.

Proof. Following the approach in [169], the proof involves:

1. Deriving the error dynamics using (4.6)
2. Applying the Lipschitz condition from Assumption 4.5.1
3. Using the bounding lemma from [91]
4. Applying the Schur complement

Remark 4.6.4. The observer gains are obtained through:

$$\begin{cases} F = P^{-1}X \\ N = R_1 M - FH \\ L = F + NQ_1 \end{cases} \tag{4.76}$$

Using the system dynamics in equation (4.68) and the observer in equation (4.70), the estimation error dynamics (**??**) is written as:

$$\dot{e} = Ne + (LH + NR_1E - R_1M)\zeta + R_1\Delta f + (LD_y - NQ_1D_y - R_1D_x)w \tag{4.77}$$

with

$$\Delta f = f(\zeta, \hat{y}) - f(\zeta, y)$$

Assuming that matrices N and L are chosen to satisfy

$$\begin{cases} LH + NR_1E - R_1M = 0, \\ F = L - NQ_1, \\ N = R_1M - FH \end{cases} \tag{4.78}$$

The error dynamics simplifies to:

$$\dot{e} = (R_1M - FH)e + (FD_y - R_1D_x)w + R_1\Delta f \tag{4.79}$$

Following the approach of [91], we aim to determine matrix F to minimize the noise effect on $e(t)$. Consider the Lyapunov function $V = e^\top Pe$, where $P = P^\top > 0$, the derivative along trajectories is:

$$\dot{V} = e^\top[(R_1M-FH)^\top P+P(R_1M-FH)]e+2e^\top PR_1\Delta f+2e^\top P(FD_y-R_1D_x)w \tag{4.80}$$

As shown in [169], condition (4.74) can be reformulated as:

$$\begin{aligned} \mathcal{V} \triangleq & e^\top\Big[\big(R_1M - FH\big)^\top P + P\big(R_1M - FH\big)\Big]e \\ & + 2e^\top PR_1\Delta f \\ & + 2e^\top P\big(FD_y - R_1D_x\big)w \\ & + e^\top e - \lambda^2\omega^\top\omega < 0 \end{aligned} \tag{4.81}$$

By Lemma (4.5.3) and Assumption 4.5.1, following [88]:

$$2e^\top PR_1\Delta f \leq \tfrac{1}{\beta}e^\top PR_1R_1^\top Pe + \beta\gamma^2e^\top e \tag{4.82}$$

Thus, we obtain:

$$\begin{aligned} \mathcal{V} \leq & e^\top\Big[\big(R_1M - FH\big)^\top P + P\big(R_1M - FH\big) \\ & + \tfrac{1}{\beta}PR_1R_1^\top P + (1+\beta\gamma^2)I\Big]e \\ & + 2e^\top P\big(FD_y - R_1D_x\big)w \\ & - \lambda^2\omega^\top\omega \end{aligned} \tag{4.83}$$

The matrix inequality can be expressed as:

$$\mathcal{V} \leq \begin{bmatrix} e \\ w \end{bmatrix}^{\top} \mathbb{M} \begin{bmatrix} e \\ w \end{bmatrix} \tag{4.84}$$

where

$$\mathbb{M} = \begin{bmatrix} \Gamma(P,F) + \frac{1}{\beta} P R_1 R_1^{\top} P & P(FD_y - R_1 D_x) \\ \star & -\lambda^2 I \end{bmatrix} \tag{4.85}$$

with $\Gamma(P,F) = (R_1 M)^{\top} P + P(R_1 M) - H^{\top} F^{\top} P - PFH + (1+\beta\gamma^2) I$. Applying the Schur complement [170]:

$$\begin{bmatrix} \Gamma(P,F) & PR_1 & P(FD_y - R_1 D_x) \\ * & -\beta I & 0 \\ * & 0 & -\lambda^2 I \end{bmatrix} < 0 \tag{4.86}$$

The substitution $X = PF$ yields the LMI (4.75), completing the proof following [91]. □

4.6.3 Study of a particular case

Building on [171] solution for discrete-time systems, we extend the approach to continuous-time. Consider the block-diagonal structure:

$$D = \begin{bmatrix} \Sigma & 0 \\ 0 & 0 \end{bmatrix}, \tag{4.87}$$

where Σ is nonsingular, obtained via SVD [172]. The measurement transformation [121]:

$$y = \begin{bmatrix} y_1 \\ y_2 \end{bmatrix} = \begin{bmatrix} C_1 \\ C_2 \end{bmatrix} x + \begin{bmatrix} \Sigma & 0 \\ 0 & 0 \end{bmatrix} \begin{bmatrix} d_1 \\ d_2 \end{bmatrix} \tag{4.88}$$

yields:

$$d_1 = \Sigma^{-1}(y_1 - C_1 x) \tag{4.89}$$

Assumption 4.6.5. rank $\left(\begin{bmatrix} D_x & B_{d_2} \end{bmatrix} \right)$ is full column rank [122]

Assumption 4.6.6. rank$(C_2 B_{d_2})$ is full column rank [124]

The state transformation [164]:

$$\zeta = T^{-1}x, \quad T = [S \; D_x \; B_{d_2}] \tag{4.90}$$

yields:

$$\begin{cases} \dot{\zeta} = M\zeta + T^{-1}B_{d_2}d_2 + T^{-1}f(T\zeta, y) + \cdots \\ y_2 = [C_2S \; C_2D_x \; C_2B_{d_2}]\zeta \end{cases} \tag{4.91}$$

The observer design follows [169]:

$$\begin{cases} \dot{z} = Nz + Ly_{u_2} + RT_1 f(Tz + TQy_{u_2}, y) + \cdots \\ \hat{\xi} = z + Qy_{u_2} \end{cases} \tag{4.92}$$

Theorem 4.6.7. *The $\mathcal{H}_\infty$ observer exists if [91]:*

$$\begin{bmatrix} \Gamma(P,X) & PRT_1 & -PRT_1D_x \\ * & -\beta_2 I & 0 \\ * & * & -\gamma^2 I \end{bmatrix} < 0 \tag{4.93}$$

where $\Gamma(P,X) = (RM_1)^\top P + P(RM_1) - H^\top X - X^\top H + \beta_2\gamma^2 T^\top T + I_n$.

Proof. Following [88], the error dynamics:

$$\dot{\epsilon} = (RM_1 - FH)\epsilon - RT_1D_x w + RT_1\Delta f \tag{4.94}$$

are analyzed via Lyapunov function $V = \epsilon^\top P\epsilon$ [166]. □

4.6.4 Numerical example

We consider a nonlinear singular system of order $n = 3$, with $m = 2$ control inputs, $p = 2$ measured outputs, $n_d = 2$ unknown inputs, and $r = 1$ disturbance affecting both the process and the measurements. The system is described by the following matrices:

System matrices:

$$A = \begin{bmatrix} -0.1 & 0 & 0.05 \\ 0 & -0.15 & 0 \\ 0.05 & 0 & -0.1 \end{bmatrix}, \quad B_u = \begin{bmatrix} 0 & 0 \\ 0.1 & 0 \\ 0 & 0.1 \end{bmatrix}, \quad B_d = \begin{bmatrix} 0.1 & 0 \\ 0 & 0.1 \\ 0 & 0 \end{bmatrix}$$

$$C = \begin{bmatrix} 0.3 & 0 & 0 \\ 0 & 0.3 & 0 \end{bmatrix}, \quad D = \begin{bmatrix} 0.1 & 0 \\ 0 & 0 \end{bmatrix}$$

Noise matrices:

$$D_x = 0.01 \cdot \mathbf{1}_{3\times 1} = \begin{bmatrix} 0.01 \\ 0.01 \\ 0.01 \end{bmatrix}, \quad D_y = 0.01 \cdot \mathbf{1}_{2\times 1} = \begin{bmatrix} 0.01 \\ 0.01 \end{bmatrix}$$

The nonlinear perturbation term is defined as:

$$f(x,d,y) = \begin{bmatrix} 0.01\sin(0.7x_1) + \dfrac{0.004\, d_1\, x_2}{1 + 0.05\|x\|} \\ 0.006\tanh(x_2 x_3) + 0.003\, d_2\, y_1 \\ \dfrac{0.009\, x_3}{1 + 0.1|x_3|} + 0.002\, d_1\, x_1 \end{bmatrix}$$

In this example, the Lipschitz constant $\beta = 0.044$ is derived from a numerical approximation over the system's typical input and state ranges.

Input signals :

$$u(t) = \begin{bmatrix} 0.5\sin(0.5t) \\ 0.3\cos(0.8t) \end{bmatrix} \quad \text{(known control inputs)}$$

$$d(t) = \begin{bmatrix} 0.2\sin(0.3t) \\ 0.1\cos(0.4t) \end{bmatrix} \quad \text{(unknown external disturbances)}$$

$$w(t) = 0.1 \cdot \mathcal{N}(0,1) \quad \text{(zero-mean Gaussian noise)}$$

System Properties : Since the assumptions stated in Table 4.1 are satisfied, it is therefore possible to perform a system transformation into the singular form given in

(4.68) Consequently, the matrices M_1, T_1, B_{d1}, H, and E take the following form :

Table 4.1: Key system characteristics

Property	Value
Stability	Hurwitz ($\lambda_{max}(A) = -0.05$)
Assumption4.5.2	$\text{rank}([D\ D_y]) = 2 \neq m + r/m + r = 3$
Assumption4.6.5	$\text{rank}([D_x\ B_{d_2}]) = \text{size}([D_x\ B_{d_2}], 2) = 2$
Assumption4.6.6	$\text{rank}(C_2 B_{d_2}) = \text{size}(C_2 B_{d_2}, 2) = 1$

$$M_1 = \begin{bmatrix} -0.3000 & 0.0021 & 0 \\ 10.6066 & -0.2000 & 0 \end{bmatrix}, \quad T_1 = \begin{bmatrix} -0.7071 & 0 & 0.7071 \\ 50.0000 & 0 & 50.0000 \end{bmatrix},$$

$$B_{d1} = \begin{bmatrix} 0.1000 \\ 0 \\ 0 \end{bmatrix}, \quad H = \begin{bmatrix} 0 & 0.0030 & 1.0000 \end{bmatrix}, \quad E = \begin{bmatrix} 1 & 0 & 0 \\ 0 & 1 & 0 \end{bmatrix}$$

Observer Design We now design a robust observer (4.92) to estimate the state variables with unknown inputs. The observer matrices are obtained by solving the LMI constraints defined in Theorem 4.6.7. The solution yields P and gain matrix X with an optimal attenuation level $\gamma = 0.5223$.

$$P = \begin{bmatrix} 0.2728 & -0.0020 & 0.0000 \\ -0.0020 & 0.0000 & 0.0011 \\ 0.0000 & 0.0011 & 0.3815 \end{bmatrix} \quad X = \begin{bmatrix} 0.0000 \\ 0.0021 \\ 0.6910 \end{bmatrix}$$

The observer gains are given by:

$$N = \begin{bmatrix} -0.3000 & 0.0021 & -0.0130 \\ 10.6066 & -0.2053 & -1.7615 \\ -0.0318 & -0.0048 & -1.8160 \end{bmatrix} \quad L = \begin{bmatrix} 0.0017 \times 10^{-15} \\ 0.2220 \times 10^{-15} \\ 0.2220 \times 10^{-15} \end{bmatrix} \quad F = \begin{bmatrix} 0.0130 \\ 1.7615 \\ 1.8160 \end{bmatrix}$$

The eigenvalues of the observer matrix N are:

$$\text{eig}(N) = \{-0.4081,\ -0.0919,\ -1.8213\}$$

The simulation was carried out with an initial condition of the model given by : $x_0 = \begin{bmatrix} 0.5 & 5 & 0.2 \end{bmatrix}$, and an initial value of the vector z_0 defined as $z_0 = \begin{bmatrix} 0.5 & -0.03 & 0.02 \end{bmatrix}$. The simulation results are presented in figures 4.4,4.5,4.6.

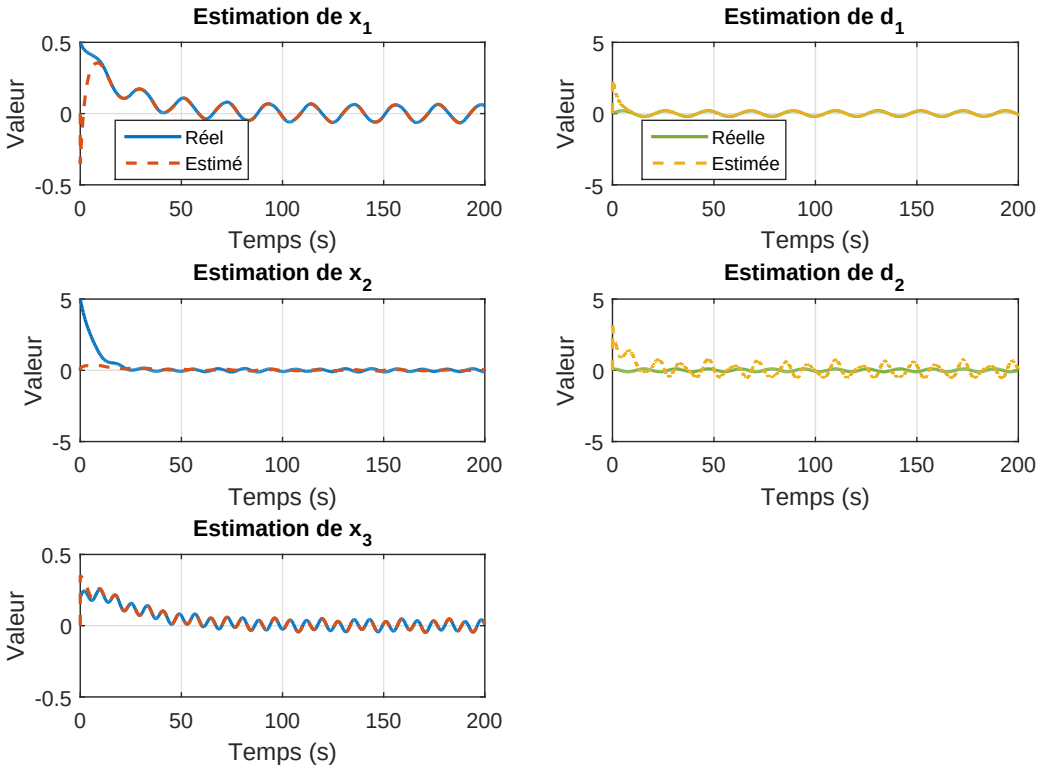

Figure 4.4: Reconstruction of State Variables and Unknown Inputs

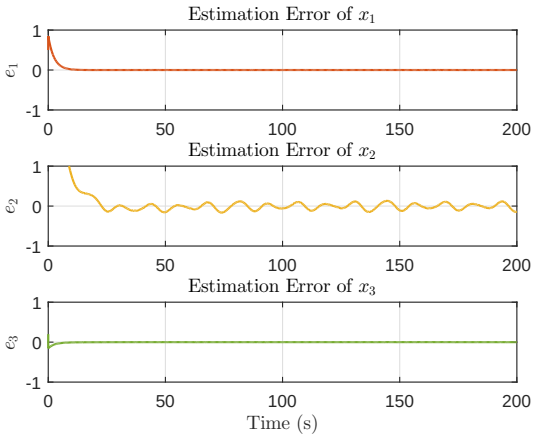

Figure 4.5: Estimation Errors of States

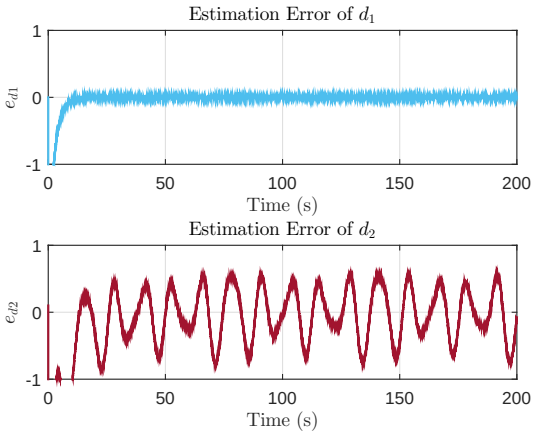

Figure 4.6: Estimation Errors of Unknown Inputs d_1 and d_2

As demonstrated in Figures 4.4–4.6, the observer exhibits excellent estimation performance: The estimated states $\hat{x}(t)$ converge exponentially to the true states $x(t)$, and estimation errors asymptotically approach zero. These results validate the effectiveness of the robust observer design, with essential advantages of **robustness**: Maintains accuracy despite unknown inputs $d(t)$

4.7 Conclusion

This chapter has presented a comprehensive and rigorous methodology for the design of observers applied to singular systems, both linear and nonlinear, in the presence of unknown inputs. The developed approach is based on a unified theoretical framework, which notably includes the systematic transformation of regular systems into descriptor form, the analytical decoupling of unknown inputs through appropriate matrix transformations, and the formulation of stability conditions in the form of linear matrix inequalities (LMIs), thus ensuring the feasibility of the solutions. Practical extensions have also been explored, allowing the methodology to be generalized to nonlinear systems satisfying a Lipschitz condition, while guaranteeing robust performance in the H_∞ sense. Experimental validation on representative test cases confirmed the relevance of the approach, notably by achieving convergence specifications with an error asymptotically approach zero, as well as robustness against disturbances. Despite these methodological contributions, important limitations remain. In particular, the nonlinearities and unmeasured disturbances

do not explicitly appear in the system output, which significantly complicates stability analysis using Lyapunov method. To overcome these challenges, the following chapter introduces a novel unknown input estimation approach specifically designed for nonlinear parameter-varying (LPV) systems. This new method explicitly incorporates nonlinearities and disturbances into the stability criteria expressions, thus addressing the identified limitations. Thus, this chapter serves as an essential theoretical foundation, while the structural uncertainties and sensor faults not fully addressed here will be the focus of the next chapter. That chapter will develop three original algorithms for unknown input estimation, tailored to LPV/nonlinear systems, and applied to the biological wastewater treatment process.

Chapter 5

Unknown input estimation for LPV/Nonlinear systems algorithms with application to waste water treatment process (WWTP)

"The ink of scholars is more sacred than the blood of martyrs."
(Prophet Muhammad)

5.1 Introduction

Nonlinear descriptor systems with unknown inputs represent an important class of models for many industrial applications, ranging from wastewater treatment to energy systems [173]. Although several techniques enable the simultaneous estimation of states and unknown inputs [174], very few studies have addressed the critical issue of nonlinearities in the measurement equations of such systems, particularly when the system has a singular structure. This limitation significantly restricts the applicability of existing observers, especially in cases where the system outputs exhibit complex structural nonlinearities [175]. In this chapter, we propose a new methodology for designing robust observers capable of simultaneously estimating the states and unknown inputs of nonlinear descriptor systems, even in the presence of nonlinearities in the measured outputs. Our approach relies on three main contributions [176]:

- A reformulation of the Lipschitz conditions that enables a more refined analysis of the nonlinearities, by exploiting precise bounds on their variations [177].
- A two-stage observer structure that incorporates correction terms to compensate for output nonlinearities while ensuring optimal disturbance attenuation in the H_∞ sense.
- The three proposed estimation algorithms are specifically designed to handle different configurations of unknown inputs, characterized by the rank of the distribution matrix C_μ. In the context of water treatment processes, this matrix C_μ represents the systems unknown inputs, which typically correspond to concentrations that are not accessible online, such as $S_{NO_{in}}$ and $S_{NH_{in}}$.

  These concentrations, critical for process control, are generally not measured in real time and therefore must be estimated.

To tackle challenges related to the descriptor system structure and nonlinearities, we employ innovative matrix decompositions and a reformulated Youngs inequality, enabling less conservative LMI conditions with enhanced feasibility through additional decision vari-

ables. A specialized Lyapunov analysis further ensures robust stability without requiring derivatives of disturbances. The proposed methodology is validated on a wastewater treatment plant model (COST 624 benchmark), demonstrating accurate estimation of both system states (organic substrate, nitrogen, dissolved oxygen) and unknown inputs (unmeasured influent concentrations and sensor faults), even in the presence of disturbances. The sensor fault specifically affects the dissolved oxygen measurement, yet the observer maintains reliable performance. Beyond water treatment, the approach holds potential for fault diagnosis in complex industrial systems [**?**], cyberattack detection in cyber-physical systems [**?**], and robust online parameter estimation in machine learning applications [**?**]. The chapter begins with a presentation of the mathematical preliminaries and key reformulations that lay the foundation for the proposed approach. It then proceeds with the development of the observer design and the associated stability analysis. Building on this, three algorithms for unknown input estimation are introduced and analyzed. Finally, the chapter concludes with a practical validation through a detailed case study based on a wastewater treatment plant model.

5.2 Notations and mathematical preliminaries

This section establishes fundamental notations and preliminary concepts that will serve as the foundation for ensuring asymptotic convergence of the estimation error to zero. To facilitate the development of observers with well-defined structural properties in subsequent sections, we adopt a generalized mathematical framework with the following objectives [172] [178]:

- The set $\mathrm{Co}(x, y) = \{\lambda x + (1-\lambda)y \mid 0 \leq \lambda \leq 1\}$ is the convex hull of $\{x, y\}$.
- $e_s(i) = \big(0, \ldots, 0, \underbrace{1}_{i\text{th}}, 0, \ldots, 0\big)^\top \in \mathbb{R}^s$, $s \geq 1$ is a vector of the canonical basis of $\mathbb{R}^s$.

Before introducing the class of nonlinear systems under consideration, we present two key theorems. These theorems notably allow the transformation of the state estimation

problem for an arbitrary nonlinear system into a stability analysis problem for an LPV system.

Theorem 5.2.1 (Mean Value Theorem for Vector-Valued Functions)**.** *Let $\phi : \mathbb{R}^n \to \mathbb{R}^q$. Let $a, b \in \mathbb{R}^n$. Suppose ϕ is differentiable on $Co(a, b)$. Then, there exist constants $z_1, \ldots, z_q \in Co(a, b)$, $z_i \neq a$, $z_i \neq b$ for $i = 1, \ldots, q$, such that:*

$$\phi(a) - \phi(b) = \left(\sum_{i=1}^{q} \sum_{j=1}^{n} e_q(i) e_n^\top(j) \frac{\partial \phi_i}{\partial x_j}(z_i) \right) (a - b) \tag{5.1}$$

5.2.1 Reformulated Lipschitz property

This subsection presents the reformulated Lipschitz property essential for our LPV approach, contrasting it with the classical DMVT framework [179]. While the DMVT (requiring differentiability) decomposes $\phi(a) - \phi(b)$ via Jacobians at intermediate points, the Lipschitz reformulation employs bounded component-wise functions ψ_{ij} to handle non-smooth systems. Two key lemmas will formalize this approach.

Lemma 5.2.2 (Scalar Function Decomposition)**.** *Consider a function $\psi : \mathbb{R}^n \to \mathbb{R}$. For any vectors*

$$X = \begin{pmatrix} x_1 \\ \vdots \\ x_n \end{pmatrix} \in \mathbb{R}^n \quad \text{and} \quad Y = \begin{pmatrix} y_1 \\ \vdots \\ y_n \end{pmatrix} \in \mathbb{R}^n,$$

there exist scalar functions $\psi_j : \mathbb{R}^n \times \mathbb{R}^n \to \mathbb{R}$, $j = 1, \ldots, n$ such that

$$\psi(X) - \psi(Y) = \sum_{j=1}^{n} \psi_j \left(X^{\mathcal{Y}_{j-1}}, X^{\mathcal{Y}_j} \right) e_n^\top(j)(X - Y)$$

where $X^{\mathcal{Y}_k}$ denotes the vector X with its first k components replaced by those of Y.

Lemma 5.2.3 (Vector Lipschitz Equivalence)**.** *Considering the function $\psi : \mathbb{R}^n \longrightarrow \mathbb{R}^n$, the two following items are equivalent:*

- ***Lipschitz property**: ψ is γ_ψ-Lipschitz with respect to its argument, i.e.:*

$$\|\psi(X) - \psi(Y)\| \leq \gamma_\psi \|X - Y\|, \quad \forall X, Y \in \mathbb{R}^n.$$

- ***Reformulated Lipschitz property***: *For all* $i, j = 1, \ldots, n$, *there exist functions*

$$\psi_{ij} : \mathbb{R}^n \times \mathbb{R}^n \longrightarrow \mathbb{R}$$

and constants $\underline{\gamma}_{\psi_{ij}}$ *and* $\overline{\gamma}_{\psi_{ij}}$, *so that* $\forall\, X, Y \in \mathbb{R}^n$,

$$\psi(X) - \psi(Y) = \sum_{i=1}^{n} \sum_{j=1}^{n} \psi_{ij} H_{ij} (X - Y)$$

and $\underline{\gamma}_{\psi_{ij}} \leq \psi_{ij} \leq \overline{\gamma}_{\psi_{ij}}$ *where* $\psi_{ij} \triangleq \psi_{ij}\left(X^{\mathcal{Y}_{j-1}}, X^{\mathcal{Y}_j}\right)$ *and* $H_{ij} = e_n(i) e_n^T(j)$.

In particular Lemma 5.2.3 provides a less conservative Lipschitz condition [91]. The reformulation allows precise treatment of nonlinearities by exploiting their specific properties.

For example, while the standard Lipschitz 4.5.1 condition doesn't distinguish between $\psi(\chi) = \sin(\chi_2)$ and $\psi(\chi) = \tanh(\chi_2)$, our reformulation shows the difference: for $\sin(\chi_2)$ we have $\overline{\gamma}_{\psi_{11}} = 1$ and for $\tanh(\chi_2)$ we have $\overline{\gamma}_{\psi_{11}} = 1$, but their actual bounds differ in practice.

Lemma 5.2.4 (Zemouche et al. (2016))**.** *Let* X *and* Y *be two matrices of appropriate dimensions. Then, for any symmetric positive definite matrix* S *of appropriate dimension, the following inequality holds:*

$$X^\top Y + Y^\top X \leq \frac{1}{2}(X + SY)^\top S^{-1}(X + SY). \tag{5}$$

Remark 5.2.5. The significance of Lemma 5.2.4 lies not in its trivial proof, but in its novel formulation of Young's inequality that bounds only half the quantity $X^\top Y + Y^\top X$. This refined version:

- Represents the first use of Young's inequality in this particular form [180]
- Plays a crucial role in deriving less conservative LMI synthesis conditions
- Provides tighter bounds in stability analysis

Lemma 5.2.6 (Young's inequality)**.** *Let* X *and* Y *be two given matrices of appropriate dimensions. Then, for any symmetric positive definite matrix* S, *the following inequality*

holds:

$$X^\top Y + Y^\top X \leq \underbrace{X^\top S^{-1} X + Y^\top S Y}_{U_1(X,Y)}. \tag{2.1}$$

Remark 5.2.7. Inequality (2.1) represents the classical Young's inequality, frequently employed in control theory to address parametric uncertainties [88]. However, the present work utilizes not only (2.1) but rather its refined reformulation.

Lemma 5.2.8 (Improved Young's inequality [181])**.** *Let X and Y be two given matrices of appropriate dimensions. Then, for any symmetric positive definite matrix S of appropriate dimension, the following inequality holds:*

$$X^\top Y + Y^\top X \leq \frac{1}{2}(X + SY)^\top S^{-1}(X + SY). \tag{2.2}$$

5.3 Problem formulation and preliminary results

This section is devoted to some preliminary results that we will exploit in the next section to develop new unknown input estimation algorithms. We will provide general LMI conditions ensuring the design of H_∞ observer for a class of nonlinear descriptor systems described by the following equations:

$$\begin{cases} \dot{E_\xi \xi(t)} &= A_\xi\big(\rho(t)\big)\xi(t) + B_f\big(\rho(t)\big) f\big(\xi(t), u(t)\big) + G_g\big(\rho(t)\big) g\big(y(t), u(t)\big) + D_\xi \omega(t) \\ y(t) &= C_\xi \xi(t) + B_h h\big(\xi(t), u(t)\big) + D_y \omega(t), \end{cases} \tag{5.2}$$

where $\xi \in \mathbb{R}^{n_\xi}$, $u \in \mathbb{R}^{n_u}$, and $y \in \mathbb{R}^{n_y}$ are respectively the state vector of the system, the known control input vector, the output measurements vector. The vector $\omega \in \mathbb{R}^{n_\omega}$ represents the unknown disturbances affecting the system dynamics and the measured variables. The matrices $E_\xi \in \mathbb{R}^{n_d \times n_\xi}$, $D_\xi \in \mathbb{R}^{n_d \times n_\omega}$, $C_\xi \in \mathbb{R}^{n_y \times n_\xi}$, and $D_y \in \mathbb{R}^{n_y \times n_\omega}$ are known and constant. As for the affine matrix $A_\xi\big(\rho(t)\big)$, $B_f\big(\rho(t)\big)$ and $G_g\big(\rho(t)\big)$ any matrix of appropriate dimension depending on the parameter $\rho(t)$, and are expressed under the form :

$$A_\xi(\rho) = A_0 + \sum_{j=1}^{s} \rho_j A_j,\ B_f(\rho) = B_0 + \sum_{j=1}^{s} \rho_j B_j,\ G_g(\rho) = G_0 + \sum_{j=1}^{s} \rho_j G_j \tag{5.3}$$

where $\rho(t) = \left[\rho_j(t), \ldots, \rho_s(t)\right]^\top \in \mathbb{R}^s$, is a parameter which is known and available in real-time, with

$$\rho_{j,\min}(t) \leq \rho_j(t) \leq \rho_{j,\max}(t) \tag{5.4}$$

which means that the parameter $\rho(t)$ belongs to a bounded convex set for which the set of 2^s vertices can be defined by:

$$\mathbb{V}_\rho = \left\{\rho(t) \in \mathbb{R}^s : \rho_j(t) \in \left\{\rho_{j,\min}(t), \rho_{j,\max}(t)\right\}\right\}$$

The functions

$$f : \mathbb{R}^{n_\xi} \times \mathbb{R}^{n_u} \longrightarrow \mathbb{R}^{n_f}$$

and

$$h : \mathbb{R}^{n_\xi} \times \mathbb{R}^{n_u} \longrightarrow \mathbb{R}^{n_h}$$

are globally Lipschitz [1] with respect to ξ, uniformly on u, with Lipschitz constants γ_f and γ_h, respectively. Assume also that the couple $\left(E_\xi, C_\xi\right)$ satisfies the following condition:

$$\operatorname{rank}\left(\begin{bmatrix} E_\xi \\ C_\xi \end{bmatrix}\right) = n_\xi. \tag{5.5}$$

The aim consists in finding an observer to estimate asymptotically or exponentially the state ξ. Contrarily to regular systems for which a simple Luenberger observer with one constant gain can be used to investigate the H_∞ criterion, the problem of state observer for descriptor systems 5.2 turns out to be difficult in some cases. In this dissertation, we will first consider a well known two-stage structure of the observer. The results we will propose can then be extended to more complicated structures. Although the structure of the state observer is simple, the synthesis of the observer parameters may lead to complicated obstacles that we need to overcome in order to have tractable sufficient LMI conditions.

[1] If f and h are only locally Lipschitz, we may consider their saturated versions f^s and h^s, respectively, on an invariant compact set $\mathcal{X}$ in which f^s and h^s satisfy the global Lipschitz property [182].

5.3.1 The two-stage observer structure

We consider the two-stage state observer described by the following equations:

$$\begin{cases} \dot{z}(t) &= A_z\big(\rho(t)\big)z(t) + A_y\big(\rho(t)\big)y_{\eta_1}(t) + B_z\big(\rho(t)\big)f\big(\hat{\xi}(t),u(t)\big) + G_z\big(\rho(t)\big)g\big(y(t),u(t)\big) \\ \hat{\xi}(t) &= z(t) + Q_z y_{\eta_2}(t) \\ y_{\eta_i}(t) &= y(t) - \eta_i(t),\ i=1,2 \end{cases} \tag{5.6}$$

where $\hat{\xi}(t)$ denotes the estimate of the state vector $\xi(t)$. The auxiliary variables $\eta_1(t)$ and $\eta_2(t)$, along with the matrices A_z, A_y, B_z, G_z, and Q_z, represent observer design parameters that must be determined to satisfy a predefined performance criterion, such as the $\mathcal{H}_\infty$. The estimation error is defined as :

$$\tilde{\xi}(t) = \hat{\xi}(t) - \xi(t). \tag{5.7}$$

Using equations (5.2) and (5.6), the error $\tilde{\xi}(t)$ can be expressed as:

$$\begin{aligned} \tilde{\xi}(t) = z(t) &+ \big(Q_z C_\xi - \mathbb{I}_{n_\xi}\big)\,\xi(t) \\ &+ Q_z B_h\big(\rho(t)\big)\,\big[h\big(\xi(t),u(t)\big) - \eta_2(t)\big] + Q_z D_y \omega(t). \end{aligned}$$

Remark 5.3.1. In the case $y(t) = C_\xi \xi(t)$, the problem becomes easy and the results are well known in the literature, because with $\eta_2(.) \equiv 0$, equation (5.8) is reduced to

$$\tilde{\xi}(t) = z(t) + \Big(Q_z C_\xi - \mathbb{I}_{n_\xi}\Big)\xi(t). \tag{5.8}$$

Given that $B_h = 0$ and $D_y = 0$, the output measurement simplifies to $y_{\eta_2} = y$.

Hence, from the condition (5.5), there exist two matrices P_z and Q_z such that

$$P_z E_\xi + Q_z C_\xi = \mathbb{I}_{n_\xi}. \tag{5.9}$$

Therefore, we can write the dynamics of the estimation error as:

$$\dot{\tilde{\xi}}(t) = \dot{z}(t) - P_z\overbrace{E_\xi \xi(t)}^{\dot{}} \tag{5.10}$$

and then we can exploit the singular equation in (5.2) and the dynamics of $z(t)$ in (5.6)

to lead to an appropriate and standard estimation error dynamics after some matrix manipulations [183], [184], [185].

However, the presence of $h\big(\xi(t), u(t)\big)$ and $\omega(t)$ in the output measurements renders the problem more complicated. Indeed, the computation of the parameters $A_z\big(\rho(t)\big)$, $A_y\big(\rho(t)\big)$, $B_z\big(\rho(t)\big)$, $G_z\big(\rho(t)\big)$, Q_z, and the choice of the performance criterion depends on additional assumptions on the matrices B_h, D_y, on the nonlinear function $h\big(\xi, u\big)$ and the disturbance $\omega(t)$ respectively.

In particular, the presence of nonlinearities in the output measurements renders the problem difficult and original from LMI point of view. Depending on the distribution of the nonlinearity $h(.,.)$ in $y(t)$ (this is related to the structure of the matrix B_h) and its time derivative, we will provide an LMI technique.

In addition to these standard conditions, we introduce the following assumption related to the presence of nonlinearities in the output measurements.

Assumption 5.3.2. Assume that the following condition is fulfilled:

$$\operatorname{rank} \begin{pmatrix} E_\xi & 0 \\ C_\xi & B_h \end{pmatrix} = n_\xi + n_h. \tag{5.11}$$

Condition (5.11) implies

$$n_d + n_y \geq n_\xi + n_h.$$

It is worth noticing that equations like (5.5) and (5.11) are usual in descriptor systems theory. For more details, we refer the reader to [186], [121], [187], [188], and the references therein.

Under Assumption 5.3.2 we can build an observer for the system (5.2). Indeed, if (5.11) holds then there exist matrices $P_z \in \mathbb{R}^{n_\xi \times n_d}, Q_z \in \mathbb{R}^{n_\xi \times n_y}, R_z \in \mathbb{R}^{n_h \times n_d}$, and $S_z \in \mathbb{R}^{n_h \times n_y}$

such that

$$\begin{bmatrix} P_z & Q_z \\ \\ R_z & S_z \end{bmatrix} \begin{bmatrix} E_\xi & 0 \\ \\ C_\xi & B_h \end{bmatrix} = \begin{bmatrix} \mathbb{I}_{n_\xi} & 0_{n_\xi \times n_h} \\ \\ 0_{n_h \times n_\xi} & \mathbb{I}_{n_h} \end{bmatrix}. \tag{5.12}$$

Equation (5.12) means that

$$\begin{cases} P_z E_\xi + Q_z C_\xi = \mathbb{I}_{n_\xi} \\ R_z E_\xi + S_z C_\xi = 0_{n_k \times n_\xi} \\ Q_z B_h = 0_{n_\xi \times n_h} \\ S_z B_h = \mathbb{I}_{n_h} \end{cases} \tag{5.13}$$

The matrices P_z, Q_z, R_z, S_z are computed by

$$\begin{bmatrix} P_z & Q_z \\ R_z & S_z \end{bmatrix} = \left(\begin{bmatrix} E_\xi & 0 \\ C_\xi & B_h \end{bmatrix}^\top \begin{bmatrix} E_\xi & 0 \\ C_\xi & B_h \end{bmatrix} \right)^{-1} \begin{bmatrix} E_\xi & 0 \\ C_\xi & B_h \end{bmatrix}^\top. \tag{5.14}$$

In other word, $\begin{bmatrix} P_z & Q_z \\ \\ R_z & S_z \end{bmatrix}$ is the Moore-Penrose pseudo-inverse of the full column rank matrix $\begin{bmatrix} E_\xi & 0 \\ \\ C_\xi & B_h \end{bmatrix}$.

The nonlinear filter exactly implements (5.6) through optimized correction terms $\eta_i(t)$:

$$\begin{cases} \dot{z}(t) &= A_z\big(\rho(t)\big)z(t) + A_y\big(\rho(t)\big)y_{\eta_1}(t) + B_z f\big(\hat{\xi}(t), u(t)\big) + G_z\big(\rho(t)\big)g\big(y(t), u(t)\big) \\ \hat{\xi}(t) &= z(t) + Q_z y_{\eta_2}(t) \\ y_{\eta_i}(t) &= y(t) - \eta_i(t),\ i = 1, 2 \\ \eta_1(t) &= B_h h\big(\hat{\xi}(t), u(t)\big) \\ \eta_2(t) &= 0_{\mathbb{R}^{n_y}}, \end{cases} \tag{5.15}$$

With the following design advantages and functional benefits of the η_i configuration :

- η_1 Compensates measurement nonlinearities via $h(\cdot)$ (inactive if $B_h = 0$)
- $\eta_2 = 0$ **simplifies the architecture** by:
  - Avoiding duplicate $y(t)$ processing

  - Direct injection $\hat{\xi} = z + Q_z y(t)$
  - Eliminates null terms when $D_y = 0$
- Preserves exact structure of (5.8)
- Enables efficient LMI design
- Optimal disturbance/complexity trade-off

where $A_z(.), A_y(.), B_z(.)$, and $G_z(.)$ are the parameters of the filter to be determined later. We define the state estimation error:

$$\tilde{\xi}(t) \triangleq \hat{\xi}(t) - \xi(t) \tag{5.16}$$

From the observer (5.15) with $\eta_2(t) = 0$, we obtain:

$$\hat{\xi}(t) = z(t) + Q_z y(t) \tag{5.17}$$

Substituting the system output (5.2):

$$y(t) = C_\xi \xi(t) + B_h h(\xi(t), u(t)) + D_y \omega(t) \tag{5.18}$$

yields the error expression:

$$\tilde{\xi}(t) = z(t) + Q_z C_\xi \xi(t) + Q_z B_h h(\xi(t), u(t)) + Q_z D_y \omega(t) - \xi(t) \tag{5.19}$$

We begin by defining the state estimation error:

$$\tilde{\xi}(t) \triangleq \hat{\xi}(t) - \xi(t) \tag{5.20}$$

From the observer structure (5.15), with the design choice $\eta_2(t) = 0_{\mathbb{R}^{n_y}}$, we have:

$$y_{\eta_2}(t) = y(t) \quad \text{and} \quad \hat{\xi}(t) = z(t) + Q_z y(t) \tag{5.21}$$

Substituting the system output dynamics from (5.2):

$$y(t) = C_\xi \xi(t) + B_h h(\xi(t), u(t)) + D_y \omega(t) \tag{5.22}$$

into the observer's state estimate yields the explicit error expression:

$$\tilde{\xi}(t) = \underbrace{z(t) - P_z E_\xi \xi(t)}_{\text{State mismatch}} + \underbrace{Q_z D_y \omega(t)}_{\text{Noise propagation}} + Q_z B_h h(\xi(t), u(t)) \tag{5.23}$$

From (5.13), the dynamics of the estimation error 5.23 can be rewritten as follows:

$$\underbrace{\widetilde{\xi}(t) - Q_z D_y \omega(t)}_{\zeta(t)} = z(t) - P_z E_\xi \xi(t). \tag{5.24}$$

The gains P_z, Q_z are designed to satisfy conditions 5.13, thus, the error reduces to:

$$\tilde{\xi}(t) = z(t) - P_z E_\xi \xi(t) + Q_z D_y \omega(t) \tag{5.25}$$

Therefore, we can write

$$\dot{\zeta}(t) = \dot{z}(t) - P_z \dot{\overbrace{E_\xi \xi(t)}} \tag{5.26a}$$

$$\zeta(t) = \tilde{\xi}(t) - Q_z D_y \omega(t). \tag{5.26b}$$

Using the dynamics (5.2) and (5.15) we get the following detailed structure of (5.26):

$$\begin{aligned} \dot{\zeta}(t) = {} & A_z\big(\rho(t)\big)\tilde{\xi}(t) + \Big(A_z\big(\rho(t)\big) - \mathbb{A} + \mathbb{L}C_\xi\Big)\xi \\ & + \Big(B_z - P_z B_f\Big) f(\xi, u) \\ & + \Big(G_z\big(\rho(t)\big) - P_z G_g\big(\rho(t)\big)\Big) g(y, u) \\ & + \Big(\mathbb{E}_\omega - \mathbb{L}\mathbb{D}_\omega\Big)\omega + B_z \delta f_t - A_y B_h \delta h_t \end{aligned} \tag{5.27a}$$

$$\delta f_t = f(\hat{\xi}, u) - f(\xi, u) \tag{5.27b}$$

$$\delta h_t = h(\hat{\xi}, u) - h(\xi, u), \tag{5.27c}$$

$$\mathbb{L} = A_y - A_z Q_z, \quad \mathbb{E}_\omega = -P_z D_\xi, \quad \mathbb{A} = P_z A_\xi, \quad \mathbb{D}_\omega = -D_y. \tag{5.27d}$$

5.3.2 $\mathcal{H}_\infty$ criterion

This subsection is devoted to some definitions related to the $\mathcal{H}_\infty$ performance criterion. The aim consists in finding $\eta_1(t), \eta_2(t)$ and the matrices A_z, A_y, B_z, G_z, and Q_z so that

the estimation error $\tilde{\xi}(t)$ satisfies the criterion:

$$\|\tilde{\xi}\|_{\mathcal{L}_2^{n_\xi}} \leq \sqrt{\alpha\|\omega\|^2_{\mathcal{L}_2^{n_\omega}} + \beta\|\|\tilde{\xi}_0\|^2} \tag{5.28}$$

where $\alpha > 0$ is the disturbance attenuation level and $\beta > 0$ is to be determined. In fact, $\sqrt{\alpha}$ is the disturbance gain from ω to $\tilde{\xi}$. Usually we use Lyapunov functions to get tractable conditions guaranteeing (5.28). In the LMI framework, we take a quadratic Lyapunov function $V(\tilde{\xi})$, such that

$$\vartheta(t) \triangleq \frac{\mathrm{d}V}{\mathrm{d}t}(\tilde{\xi}) + \|\tilde{\xi}\|^2 - \alpha\|\omega\|^2 \leq 0. \tag{5.29}$$

The objective is to develop some LMI conditions under which the inequality (5.29) holds. In the following subsection, we will propose a new LMI-based technique, which ensures the $\mathcal{H}_\infty-$ optimality criterion (5.28).

5.3.3 LMI design procedure

The following theorem summarizes the LMI technique, we propose [176].

Theorem 5.3.3. *Assume that there exist symmetric positive definite matrices* $\mathbb{P} \in \mathbb{R}^{n_\xi \times n_\xi}$, $\mathbb{S}_{ij} \in \mathbb{R}^{n_f^i \times n_f^i}$, $\mathbb{M}_{ij} \in \mathbb{R}^{n_h^i \times n_h^i}$ *and a matrix* $\mathcal{R} \in \mathbb{R}^{n_y \times n_\xi}$ *such that the following convex optimization problem is solvable:*

$$\min(\alpha) \quad \textit{subject to } (5.31) \tag{5.30}$$

$$\begin{bmatrix} \begin{bmatrix} (1,1) & \mathbb{P}\mathbb{E}_\omega - \mathcal{R}_0^T\mathbb{D}_\omega - \Omega_1 - \sum_{j=1}^s \rho_j \mathcal{R}_j^T\mathbb{D}_\omega \\ (\star) & -\left(\Omega_2 + \Omega_2^T\right) - \alpha\mathbb{I}_q \end{bmatrix} & \overbrace{\begin{bmatrix} \Sigma_1^f & \dots & \Sigma_m^f \end{bmatrix}}^{\mathbf{\Sigma_f}} & \overbrace{\begin{bmatrix} \Sigma_1^h & \dots & \Sigma_q^h \end{bmatrix}}^{\mathbf{\Sigma_h}} \\ (\star) & -\Lambda^f\mathbb{S} & 0 \\ (\star) & (\star) & -\Lambda^h\mathbb{M} \end{bmatrix} \leq 0 \tag{5.31}$$

with

$$\mathbb{A}_0^T\mathbb{P}+\mathbb{P}\mathbb{A}_0-C_\xi^T\mathcal{R}_0-\mathcal{R}_0^TC_\xi+\sum_{j=1}^{s}\rho_j\Big(\mathbb{A}_j^T\mathbb{P}+\mathbb{P}\mathbb{A}_j-C_\xi^T\mathcal{R}_j-\mathcal{R}_j^TC_\xi\Big) \tag{5.32}$$

$$\Sigma_i^f=\Big[\mathcal{N}_{i,1}^f\Big(\mathbb{P},\mathbb{S}_{i1}\Big)\dots\ \mathcal{N}_{i,n_f^i}^f\Big(\mathbb{P},\mathbb{S}_{in_f^i}\Big)\Big],\quad \Sigma_i^h=\Big[\mathcal{N}_{i,1}^h\Big(\mathcal{R}_j,\mathbb{M}_{i1}\Big)\dots\ \mathcal{N}_{i,n_h^i}^h\Big(\mathcal{R}_j,\mathbb{M}_{in_h^i}\Big)\Big] \tag{5.33}$$

$$\begin{aligned}\mathcal{N}_{i,k}^f(\mathbb{P},\mathbb{S}_{ik})&=\begin{bmatrix}\mathbb{P}B_z\mathcal{H}_{ik}\\ \bar{D}_y^\top\mathbb{P}B_z\mathcal{H}_{ik}\end{bmatrix}+\begin{bmatrix}H_i^\top\mathbb{S}_{ik}\\ 0\end{bmatrix},\\ \mathcal{N}_{i,k}^h(\mathcal{R}_j,\mathbb{M}_{ik})&=\begin{bmatrix}\mathcal{R}_0^\top B_h\mathcal{F}_{ik}\\ +\sum_{j=1}^{s}\rho_j\mathcal{R}_j^\top B_h\mathcal{F}_{ik}\\ \bar{D}_y^\top\mathcal{R}_0^\top B_h\mathcal{F}_{ik}\end{bmatrix}-\begin{bmatrix}F_i^\top\mathbb{M}_{ik}\\ \\ 0\end{bmatrix}\end{aligned} \tag{5.34}$$

$$\Lambda^f=\textit{block-diag}\Big(\Lambda_1^f,\dots,\Lambda_{n_f}^f\Big),\quad \Lambda_i^f=\textit{block-diag}\left(\frac{2}{b_{i1}}\mathbb{I}_{n_f^i},\dots,\frac{2}{b_{in_f^i}}\mathbb{I}_{n_f^i}\right) \tag{5.35}$$

$$\mathbb{S}=\textit{block-diag}\Big(\mathbb{S}_1,\dots,\mathbb{S}_{n_f}\Big),\quad \mathbb{S}_i=\textit{block-diag}\Big(\overbrace{\mathbb{S}_{i1},\dots,\mathbb{S}_{in_f^i}}^{n_f^i\ \ times}\Big) \tag{5.36}$$

$$\Lambda^h=\textit{block-diag}\Big(\Lambda_1^h,...,\Lambda_{n_h}^h\Big),\quad \Lambda_i^h=\textit{block-diag}\left(\frac{2}{d_{i1}}\mathbb{I}_{n_h^i},\dots,\frac{2}{d_{in_h^i}}\mathbb{I}_{n_h^i}\right) \tag{5.37}$$

$$\mathbb{M}=\textit{block-diag}\Big(\mathbb{M}_1,\dots,\mathbb{M}_{n_h}\Big),\quad \mathbb{M}_i=\textit{block-diag}\Big(\overbrace{\mathbb{M}_{i1},\dots,\mathbb{M}_{in_h^i}}^{n_h^i\ \ times}\Big) \tag{5.38}$$

$$\Omega_1=\mathbb{A}_0^T\mathbb{P}Q_zD_y-C_\xi^T\mathcal{R}_0Q_zD_y+\sum_{j=1}^{s}\rho_j\mathbb{A}_j^T\mathbb{P}Q_zD_y-\sum_{j=1}^{s}\rho_jC_\xi^T\mathcal{R}_jQ_zD_y \tag{5.39}$$

$$\Omega_2=\mathbb{E}_\omega^T\mathbb{P}Q_zD_y-\mathbb{D}_\omega^T\mathcal{R}_0Q_zD_y-\sum_{j=1}^{s}\rho_j\mathbb{D}_\omega^T\mathcal{R}_jQ_zD_y \tag{5.40}$$

$$A_z=\mathbb{A}-\mathbb{L}C_\xi,\quad A_y=\mathbb{L}+A_zQ_z \tag{5.41a}$$

$$B_z=P_zB_f,\quad G_z=P_zG_g \tag{5.41b}$$

Then, the $\mathcal{H}_\infty$ criterion (5.28) is satisfied with $\beta = \lambda_{\max}(\mathbb{P})$. Hence, the observer parameter $\mathbb{L}_j$ is computed by

$$\mathbb{L}_j = \mathbb{P}^{-1}\mathcal{R}_j^T.$$

Proof. From (5.41) and the fact that $Q_z B_h = 0$, the error dynamics (5.27) is reduced to the following one:

$$\begin{aligned}\dot{\zeta}(t) = \Big(\mathbb{A}\big(\rho(t)\big) - \mathbb{L}\big(\rho(t)\big)C_\xi\Big)\tilde{\xi}(t) + B_z\big(\rho(t)\big)\delta f_t \\ - \mathbb{L}\big(\rho(t)\big)B_h\delta h_t + \Big(\mathbb{E}_\omega - \mathbb{L}\big(\rho(t)\big)\mathbb{D}_\omega\Big)\omega.\end{aligned} \tag{5.42}$$

Since $f(.)$ and $h(.)$ are globally Lipschitz, then from lemma 5.2.3, [20] there exist functions

$$\phi_{ij} \ : \ \mathbb{R}^{n_f^i} \times \mathbb{R}^{n_f^i} \longrightarrow \mathbb{R}$$

$$\psi_{ij} \ : \ \mathbb{R}^{n_h^i} \times \mathbb{R}^{n_h^i} \longrightarrow \mathbb{R}$$

and constants a_{ij}, b_{ij}, c_{ij} and d_{ij} such that

$$\delta f_t = \sum_{i,j=1}^{i,j=n_f,n_f^i} \phi_{ij}(t)\mathcal{H}_{ij}H_i\tilde{\xi}(t), \tag{5.43}$$

$$\delta h_t = \sum_{i,j=1}^{i,j=n_h,n_h^i} \psi_{ij}(t)\mathcal{F}_{ij}F_i\tilde{\xi}(t), \tag{5.44}$$

with

$$a_{ij} \leq \phi_{ij}(t) \leq b_{ij}, \tag{5.45}$$

and

$$c_{ij} \leq \psi_{ij}(t) \leq d_{ij}, \tag{5.46}$$

$$\mathcal{H}_{ij} = e_{n_f}(i)e_{n_f^i}^T(j), \quad \mathcal{F}_{ij} = e_{n_h}(i)e_{n_h^i}^T(j).$$

Without loss of generality, we assume that $a_{ij} = c_{ij} = 0$. For more details about this, we

refer the reader to [35]. Hence, the dynamics equation (5.42) becomes

$$\begin{aligned}\dot{\zeta}(t) = &\left(\Big(\mathbb{A}\big(\rho(t)\big) - \mathbb{L}\big(\rho(t)\big)C_\xi\Big) + \sum_{i,j=1}^{i,j=m,n_i}\Big[\phi_{ij}B_z\mathcal{H}_{ij}H_i\Big]\right)\tilde{\xi}(t)\\ &- \left(\sum_{i,j=1}^{i,j=m,n_i}\Big[\psi_{ij}\mathbb{L}\big(\rho(t)\big)B_h\mathcal{H}_{ij}F_i\Big]\right)\tilde{\xi}(t)\\ &+ \Big(\mathbb{E}_\omega - \mathbb{L}\big(\rho(t)\big)\mathbb{D}_\omega\Big)\omega. \end{aligned} \tag{5.47}$$

Now, borrowed from [189], we use the following Lyapunov function:

$$V(\zeta) = \zeta^T(t)\mathbb{P}\zeta(t), \tag{5.48}$$

where $\mathbb{P} = \mathbb{P}^T > 0$. By calculating $\dot{V}(\zeta(t))$ along the trajectory of (5.47), we get $\vartheta(t) \leq 0$ if the following inequality holds:

$$\begin{aligned}&\overbrace{\begin{bmatrix} A_z^\top\big(\rho(t)\big)\mathbb{P} + \mathbb{P}A_z\big(\rho(t)\big) + \mathbb{I}_n & -\Omega_1 + \mathbb{P}\Big(\mathbb{E}_\omega - \mathbb{L}\big(\rho(t)\big)\mathbb{D}_\omega\Big) \\ -\Omega_1 + \Big(\mathbb{E}_\omega - \mathbb{L}\big(\rho(t)\big)\mathbb{D}_\omega\Big)^T\mathbb{P} & -\Big(\Omega_2 + \Omega_2^\top\Big) - \mu_\infty\mathbb{I}_q \end{bmatrix}}^{\text{LINEAR}}\\ &+ \sum_{i,j=1}^{i,j=n_f,n_f^i}\phi_{ij}\left(\overbrace{\begin{bmatrix}\mathbb{P}B_z\mathcal{H}_{ij}\\ \bar{D}_y\mathbb{P}B_z\mathcal{H}_{ij}\end{bmatrix}}^{\mathbb{X}_{ij}^T}\overbrace{\begin{bmatrix}H_i & 0\end{bmatrix}}^{\mathbb{Y}_i} + \mathbb{Y}_i^T\mathbb{X}_{ij}\right)\\ &+ \sum_{i,j=1}^{i,j=n_h,n_h^i}\psi_{ij}\left(\overbrace{\begin{bmatrix}\mathbb{P}\mathbb{L}\big(\rho(t)\big)B_h\mathcal{F}_{ij}\\ \bar{D}_y\mathcal{R}^TB_h\mathcal{F}_{ij}\end{bmatrix}}^{\bar{\mathbb{X}}_{ij}^T}\overbrace{\begin{bmatrix}-F_i & 0\end{bmatrix}}^{\bar{\mathbb{Y}}_i} + \bar{\mathbb{Y}}_i^T\bar{\mathbb{X}}_{ij}\right) \leq 0 \end{aligned} \tag{5.49}$$

where $\bar{D}_y = Q_zD_y$, and

$$\Omega_1 = A_z^T\big(\rho(t)\big)\mathbb{P}Q_zD_y,$$

$$\Omega_2 = \Big(\mathbb{E}_\omega - \mathbb{L}\big(\rho(t)\big)\mathbb{D}_\omega\Big)^T\mathbb{P}Q_zD_y.$$

Using the convenient Young's relation as lemma 5.2.8, we deduce that for all symmetric

positive definite matrices $\mathbb{S}_{ij}$ and $\mathbb{M}_{ij}$ we have introduced recently in [190]

$$\mathbb{X}_{ij}^T\mathbb{Y}_i + \mathbb{Y}_i^T\mathbb{X}_{ij} \leq \frac{1}{2}\Big(\mathbb{X}_{ij} + \mathbb{S}_{ij}\mathbb{Y}_i\Big)^T\mathbb{S}_{ij}^{-1}\overbrace{\Big(\mathbb{X}_{ij} + \mathbb{S}_{ij}\mathbb{Y}_i\Big)}^{\Delta_{ij}} \tag{5.50}$$

$$\bar{\mathbb{X}}_{ij}^T\bar{\mathbb{Y}}_i + \bar{\mathbb{Y}}_i^T\bar{\mathbb{X}}_{ij} \leq \frac{1}{2}\Big(\bar{\mathbb{X}}_{ij} + \mathbb{M}_{ij}\bar{\mathbb{Y}}_i\Big)^T\mathbb{M}_{ij}^{-1}\overbrace{\Big(\bar{\mathbb{X}}_{ij} + \mathbb{M}_{ij}\bar{\mathbb{Y}}_i\Big)}^{\bar{\Delta}_{ij}}. \tag{5.51}$$

Consequently, by following exactly the same steps as in Theorem (5.3.3), [190], we deduce that inequality (5.49) is fulfilled if the LMI (5.31) in Theorem 5.3.3 holds. This ends the proof. □

5.4 Unknown input estimation algorithms

This section is devoted to unknown input estimation for nonlinear systems with nonlinear outputs. The aim consists to use the results of the previous section to estimate, in the $\mathcal{H}_\infty$ sense, unknown inputs occurring in the system. The class of systems concerned by this study is described by the following nonlinear equations:

$$\left\{\begin{array}{rcl} \dot{x} &=& A_x\big(\rho(t)\big)x + A_\mu\mu + B_\sigma\sigma\big(x,\mu,u\big) + G_\varrho\big(\rho(t)\big)\varrho\big(y,u\big) + D_x\omega \\ y &=& C_x x + C_\mu\mu + B_{\ p\varsigma}\big(x,\mu,u\big) + \bar{D}_y\omega \end{array}\right. \tag{5.52}$$

where $x(t) \in \mathbb{R}^{n_x}$ is the system state and $\mu(t) \in \mathbb{R}^{n_\mu}$ is the unknown input vector. The nonlinearities $\sigma(.)$ and $\varsigma(.)$ satisfy the global Lipschitz assumption as in the previous subsection. The matrices B_σ, D_x, C_x, C_μ, B_ς, and $\bar{D}_y$ are known and constant with appropriate dimensions. The matrix $G_\varrho\big(\rho(t)\big)$ is any matrix of appropriate dimension depending on the parameter $\rho(t)$. As for the affine matrices $A_x\big(\rho(t)\big)$ and $A_\mu\big(\rho(t)\big)$, they are assumed to satisfy (5.3) with appropriate constant matrices $A_{x,j}$ and $A_{\mu,j}$, respectively. In the sequel, for sake of brevity, we will omit the LPV parameter $\rho(t)$, which satisfies (5.4). We will present some schemes to estimate simultaneously the system state $x(t)$ and the unknown input $\mu(t)$. In each estimation scheme, we rewrite system (5.52) under the descriptor form (5.2) according to specific assumptions on the parameters of (5.52), namely the matrices $A_\mu, C_\mu, B_\varsigma, C_x$, and the nonlinear function $\varsigma\big(x,u\big)$.

There are several ways to organize the presentation of all the possible scenarios due to

different assumptions required in each scenario. Nevertheless, for practical considerations we will investigate three general cases summarized as follows:

a) $\text{rank}(C_\mu) = n_\mu$;

b) $C_\mu = 0$;

c) $0 < \text{rank}(C_\mu) < n_\mu$.

The organization above is interesting in the sense that it depends on the matrix C_μ which intervenes in the output measurements. Indeed, the different scenarios we will provide strongly depend on the nature and the number of sensors needed to be able to estimate simultaneously the system states and the unknown inputs. This plays a crucial role because from practical point of view, some sensors may be extremely expensive or unavailable at any cost. This organization offers, for a large number of users and a wide field of applications, the possibility to estimate unknown variables according to their sensors availability and accessibility. In the following, we will provide LMI conditions ensuring the asymptotic estimation of the states and the unknown inputs. In each case, after transformation of the model (5.52), we use the preliminary LMI-based design technique 5.31 given in the previous section for descriptor systems.

5.4.1 First case: $\text{rank}(C_\mu) = n_\mu$

System (5.52) can be rewritten under the form (5.2) with

$$E_\xi = \begin{bmatrix} \mathbb{I}_{n_x} & 0_{n_x \times n_\mu} \end{bmatrix}, \; A_\xi = \begin{bmatrix} A_x & A_\mu \end{bmatrix}, \tag{5.53a}$$

$$C_\xi = \begin{bmatrix} C_x & C_\mu \end{bmatrix}, \; \xi = \begin{bmatrix} x \\ \mu \end{bmatrix}, \tag{5.53b}$$

$$\begin{aligned} &B_f = B_\sigma, G_g = G_\varrho, B_h = B_\varsigma, \\ &D_\xi = D_x, D_y = \bar{D}_y, \end{aligned} \tag{5.53c}$$

$$f(\xi,u)=\sigma(x,\mu,u),\ \ h(\xi,u)=\varsigma(x,\mu,u),g(y,u)=\varrho(y,u). \tag{5.53d}$$

Since the matrix C_μ is full column rank then it follows that the condition (5.5) holds. Indeed,

$$\begin{aligned}\operatorname{rank}\left(\begin{bmatrix}E_\xi\\ \\ C_\xi\end{bmatrix}\right)&=\operatorname{rank}\left(\begin{bmatrix}\mathbb{I}_{n_x} & 0_{n_x\times n_\mu}\\ \\ C_x & C_\mu\end{bmatrix}\right)\\ &=n_x+n_\mu=n_\xi.\end{aligned} \tag{5.54}$$

Hence the preliminary result obtained for descriptor systems can be applied according to additional assumptions. Indeed, under Assumption 5.3.2, the observer-based filter (5.15) provides a simultaneous estimation of the state $x(t)$ and the unknown input $\mu(t)$ in the $\mathcal{H}_\infty$ sense defined in (5.28) provided that the filter parameters are given by solving the convex optimization problem (5.30) in Theorem (5.3.3) according to the notations (5.53).

5.4.2 Second case: $C_\mu = 0$

In this case, the transformation (5.53) is not convenient because the rank condition (5.5) or (5.54) does not hold. To be able to use the LMI design method presented for descriptor systems, we need to find a convenient transformation of the system (5.52) into the form (5.2) for which the rank condition (5.5) is fulfilled.

There are some methods in the literature to deal with this issue but it still remains open and some new ideas and improvements are possible even if this may require additional assumptions. These methods are generally established for systems where all the nonlinearities are independent of $\mu(t)$. What we propose in this section is inspired from the basic work in [**?**] developed for linear systems with unknown inputs. The generalization to nonlinear systems with nonlinear outputs, in the presence of disturbances in both the dynamics of the system and the measurements, is not obvious. However, according to the preliminary results and the required assumptions, we need to introduce specific linear

transformations, inspired from [**?**], to get a new system under the form (5.2).

As often required in all unknown input estimation procedures summarized in the three previous items, we need the following assumption on the nonlinearities $\sigma(.,.)$ and $\varsigma(.,.)$:

Assumption 5.4.1. Assume that the nonlinearities $\sigma(.,.)$ and $\varsigma(.,.)$ satisfy the following conditions:

$$\frac{\mathrm{d}\sigma\big(x,\mu,u\big)}{\mathrm{d}\mu} \equiv 0, \tag{5.55}$$

$$\frac{\mathrm{d}\varsigma\big(x,\mu,u\big)}{\mathrm{d}\mu} \equiv 0. \tag{5.56}$$

Assumption 5.4.1 means that the unknown input $\mu(t)$ appears linearly in the system (5.52). Without loss of generality, the matrix A_μ is defined as full column rank. Indeed, if A_μ is not of column rank, then there always exist a full column rank matrix $\bar{A}_{\bar{\mu}}$ and a vector $\bar{\mu}$ such that $A_\mu\mu(t) = \bar{A}_{\bar{\mu}}\bar{\mu}(t)$.

From Assumption 5.4.1 we can write

$$\sigma\big(x,\mu,u\big) \equiv \sigma_{\mu}\big(x,u\big) \text{ and } \varsigma\big(x,\mu,u\big) \equiv \varsigma_{\mu}\big(x,u\big). \tag{5.57}$$

5.4.2.1 Estimation of the system state:

Since A_μ is full column rank, then there is a matrix $\mathbb{T} \in \mathbb{R}^{n_x\times(n_x-n_\mu)}$ such that

$$\mathbb{S} = \begin{bmatrix} \mathbb{T} & A_\mu \end{bmatrix} \tag{5.58}$$

is nonsingular and

$$\mathbb{S}^{-1}A_\mu = \begin{bmatrix} 0_{(n_x-n_\mu)\times n_\mu} \\ \mathbb{I}_{n_\mu} \end{bmatrix}. \tag{5.59}$$

Then using the transformation

$$\xi(t) \triangleq \mathbb{S}^{-1}x(t), \tag{5.60}$$

we get a ξ-system under the descriptor form (5.2) with the following convenient parame-

ters:

$$E_\xi = \begin{bmatrix} \mathbb{I}_{n_x - n_\mu} & 0_{(n_x-n_\mu)\times n_\mu} \end{bmatrix}, \; A_\xi = E_\xi \mathbb{S}^{-1} A_x \mathbb{S}, \tag{5.61a}$$

$$C_\xi = \begin{bmatrix} C_x \mathbb{T} & C_x A_\mu \end{bmatrix}, \; B_f = E_\xi \mathbb{S}^{-1} B_\sigma, \tag{5.61b}$$

$$G_g = E_\xi \mathbb{S}^{-1} G_\varrho, \; B_h = E_\xi \mathbb{S}^{-1} B_\varsigma, \tag{5.61c}$$

$$D_\xi = E_\xi \mathbb{S}^{-1} D_x, \; D_y = E_\xi \mathbb{S}^{-1} \bar{D}_y, \tag{5.61d}$$

$$\begin{aligned} f(\xi, u) &= \sigma_\mu(\mathbb{S}\xi, u), \\ h(\xi, u) &= \varsigma_\mu(\mathbb{S}\xi, u), \\ g(y, u) &= \varrho(y, u), \end{aligned} \tag{5.61e}$$

Thanks to the transformation (5.58)-(5.59) the state vector ξ is decoupled from the unknown input, which vanishes from the system (5.2) corresponding to (5.61). If the rank condition (5.5) is fulfilled, then it is possible to construct an $\mathcal{H}_\infty$ filter providing an estimation of the vector ξ. As we can see, the difference between this case and the case where $\text{rank}(C_\mu) = n_\mu$ is that now condition (5.5) is not a direct consequence of (5.61a)-(5.61b). It depends on the two matrices A_μ and C_x.

Therefore, the following assumption is required : As often required in all unknown input estimation procedures summarized in the three previous items, we need the following assumption on the nonlinearities $\sigma(.,.)$ and $\varsigma(.,.)$:

Assumption 5.4.2. The following condition is fulfilled:

$$\text{rank}\,(C_x A_\mu) = \text{rank}\,(A_\mu) \triangleq n_\mu. \tag{5.62}$$

Assumption 5.4.2 leads to

$$\begin{aligned}\operatorname{rank}\left(\begin{bmatrix} E_\xi \\ \\ C_\xi \end{bmatrix}\right) &\triangleq \operatorname{rank}\left(\begin{bmatrix} \mathbb{I}_{n_x-n_\mu} & 0_{(n_x-n_\mu)\times n_\mu} \\ \\ C_x\mathbb{T} & C_xA_\mu \end{bmatrix}\right) \\ &= \operatorname{rank}\left(\mathbb{I}_{n_x-n_\mu}\right) + \operatorname{rank}\left(C_xA_\mu\right) \\ &= n_x - n_\mu + \operatorname{rank}\left(A_\mu\right) \\ &= n_x. \end{aligned} \tag{5.63}$$

Finally, we can apply the design procedure given in the preliminary results. It follows that under Assumption 5.3.2 and Assumption 5.4.2, the observer-based filter (5.15) provides an estimation of the state $\xi(t) \triangleq \mathbb{S}^{-1}x(t)$ in the $\mathcal{H}_\infty$ sense defined in (5.28) provided that the filter parameters are given by solving the convex optimization problem (5.30) in Theorem 5.3.3 according to the notations (5.61). The system state $x(t)$ is estimated by

$$\hat{x}(t) = \mathbb{S}\hat{\xi}(t) \tag{5.64}$$

which satisfies the $\mathcal{H}_\infty$ inequality

$$\|\tilde{x}\|_{\mathcal{L}_2^{n_x}} \leq \sqrt{\mu_x\|\omega\|^2_{\mathcal{L}_2^{n_\omega}} + \nu_x\|\tilde{x}_0\|^2} \tag{5.65}$$

where $\tilde{x}(t) = x(t) - \hat{x}(t)$ and

$$\mu_x = \alpha\|\mathbb{S}\|^2,\ \nu_x = \beta\|\mathbb{S}\|^2\|\mathbb{S}^{-1}\|^2.$$

5.4.2.2 Estimation of the unknown input:

Now that the state of the system is estimated, it remains to estimate the unknown input $\mu(t)$, which was not estimated simultaneously with $x(t)$. To do that, we will exploit $\hat{x}(t)$, but we need to use its derivative $\dot{\hat{x}}(t)$, which may be calculated numerically online. Introducing the notations

$$\xi_2 = \begin{bmatrix} 0_{n_\mu\times(n_x-n_\mu)} & \mathbb{I}_{n_\mu} \end{bmatrix}\xi \triangleq \mathbb{S}_2\xi, \quad A_{2,\xi} = \mathbb{S}_2\mathbb{S}^{-1}A_x\mathbb{S}$$

$$B_{2,f} = \mathbb{S}_2\mathbb{S}^{-1}B_\sigma, \quad G_{2,h} = \mathbb{S}_2\mathbb{S}^{-1}G_\varrho, \quad D_{2,\xi} = \mathbb{S}_2\mathbb{S}^{-1}D_x,$$

then from the transformation (5.58)-(5.59), we get

$$\mu(t) = \dot{\xi}_2 - A_{2,\xi}\xi - B_{2,f}\sigma_{\mu}(\mathbb{S}\xi, u) - G_{2,g}\varrho(y,u) + D_{2,\xi}\omega \tag{5.66}$$

Then, we propose to estimate the unknown input by:

$$\boxed{\hat{\mu}(t) = \dot{\hat{\xi}}_2 - A_{2,\xi}\hat{\xi} - B_{2,f}\sigma_{\hat{\mu}}\big(\mathbb{S}\hat{\xi}, u\big) - G_{2,g}\varrho\big(y,u\big)} \tag{5.67}$$

Now we can state two propositions related to the estimation of the unknown input $\mu(t)$. To simplify, we first present the results in the output disturbance-free case, i.e: $\bar{D}_y = 0$. Later, we will provide new bounds for $\bar{D}_y \neq 0$, where the derivative of the disturbance will appear in the formulas.

Proposition 5.4.3. *Under Assumption 5.3.2 and Assumption 5.4.2, if the convex optimization problem (5.30) in Theorem 5.3.3 according to the notations (5.61) is solvable, then the observer-based filter (5.15) and the unknown input estimation (5.67) guarantee the following $\mathcal{L}_2$ bound:*

$$\|\mu - \hat{\mu}\|_{\mathcal{L}_2^{n_\mu}} \leq \sqrt{\lambda_\omega(\epsilon)\|\omega\|^2_{\mathcal{L}_2^{n_\omega}} + \lambda_0(\epsilon)\|\tilde{\xi}_0\|^2} \tag{5.68}$$

where

$$\begin{aligned}\lambda_\omega(\epsilon) = &\left(\left\|\mathbb{S}_2\big(\mathbb{A} - \mathbb{L}C_\xi\big) - A_{2,\xi}\right\| + \gamma_f\left\|\mathbb{S}_2\big(B_z - B_{2,f}\big)\right\|\right.\\ &\left.+ \gamma_h\left\|\mathbb{S}_2\mathbb{L}B_h\right\|\right)^2\Big(1 + \frac{1}{\epsilon}\Big)\alpha\\ &+ \big(1+\epsilon\big)\left\|\mathbb{S}_2\mathbb{E}_\omega + D_{2,\xi}\right\|^2,\end{aligned} \tag{5.69a}$$

$$\begin{aligned}\lambda_0(\epsilon) = &\left(\left\|\mathbb{S}_2\big(\mathbb{A} - \mathbb{L}C_\xi\big) - A_{2,\xi}\right\| + \gamma_f\left\|\mathbb{S}_2\big(B_z - B_{2,f}\big)\right\|\right.\\ &\left.+ \gamma_h\left\|\mathbb{S}_2\mathbb{L}B_h\right\|\right)^2\Big(1 + \frac{1}{\epsilon}\Big)\beta.\end{aligned} \tag{5.69b}$$

5.4.3 Third case: $0 < \text{rank}(C_\mu) < n_\mu$

In this section, we combine the two previous cases, namely the case $\text{rank}(C_\mu) = n_\mu$ and $\text{rank}(C_\mu) = 0$. In such a situation, $0 < \text{rank}(C_\mu) < n_\mu$, there exist a matrix $C_{\mu_1} \in \mathbb{R}^{n_y \times n_{\mu_1}}$ and a variable $\mu_1(t) \in \mathbb{R}^{n_{\mu_1}}$ such that

$$C_\mu \mu(t) = C_{\mu_1} \mu_1(t) \text{ and } \text{rank}\big(C_{\mu_1}\big) = n_{\mu_1}. \tag{5.70}$$

The nonlinear functions may depend on the vector μ_1. Then Assumption 5.4.1 is replaced by the following one: Assume that the nonlinearities $\sigma(.,.)$ and $\varsigma(.,.)$ satisfy the following conditions:

$$\frac{\partial \sigma\big(x,\mu,u\big)}{\partial \mu} \equiv \frac{\partial \sigma\big(x,\mu,u\big)}{\partial \mu_1}, \tag{5.71}$$

$$\frac{\partial \varsigma\big(x,\mu,u\big)}{\partial \mu} \equiv \frac{\partial \varsigma\big(x,\mu,u\big)}{\partial \mu_1}. \tag{5.72}$$

From Assumption 5.4.2 and since each of the n_μ unknown inputs should appear in system equations (5.52), then there exist matrices $A_{\mu_2} \in \mathbb{R}^{n_x \times n_{\mu_2}}$, $\mathcal{T}_{\mu_1} \in \mathbb{R}^{n_\mu \times n_{\mu_1}}$, $\mathcal{T}_{\mu_2} \in \mathbb{R}^{n_\mu \times n_{\mu_2}}$, and a variable $\mu_2(t) \in \mathbb{R}^{n_{\mu_2}}$ such that

$$A_\mu \mu(t) = A_{\mu_1} \mu_1(t) + A_{\mu_2} \mu_2(t) \tag{5.73}$$

$$\text{rank}\big(A_{\mu_2}\big) = n_{\mu_2}, n_\mu = n_{\mu_1} + n_{\mu_2} \tag{5.74}$$

$$\mu(t) = \mathcal{T}_{\mu_1} \mu_1(t) + \mathcal{T}_{\mu_2} \mu_2(t). \tag{5.75}$$

Notice that equations (5.73)-(5.75) are not possible only if at least one of the unknown inputs in the vector $\mu(t)$ does not appear in the system (5.52). However, such a case is useless because there is no unknown input to estimate.

Since A_{μ_2} is full column rank, then there is a matrix $\mathbb{N} \in \mathbb{R}^{n_x \times (n_x - n_{\mu_1})}$ such that

$$\mathbb{M} = \begin{bmatrix} \mathbb{N} & A_{\mu_2} \end{bmatrix} \tag{5.76}$$

is nonsingular and

$$\mathbb{M}^{-1}A_{\mu_2} = \begin{bmatrix} 0_{(n_x-n_{\mu_2})\times n_{\mu_2}} \\ \mathbb{I}_{n_{\mu_2}} \end{bmatrix}. \tag{5.77}$$

Then, as in the previous section, after transforming the system (5.52), the dynamics of the augmented vector

$$\xi(t) \triangleq \begin{bmatrix} \mathbb{M}^{-1}x(t) \\ \mu_1(t) \end{bmatrix} \tag{5.78}$$

can be written under the descriptor form (5.2) with the following parameters:

$$E_\xi = \begin{bmatrix} \mathbb{I}_{n_x-n_{\mu_2}} & 0_{(n_x-n_{\mu_2})\times n_{\mu_2}} & 0_{(n_x-n_{\mu_2})\times n_{\mu_1}} \end{bmatrix}, \tag{5.79a}$$

$$\mathbb{K}_\xi = \begin{bmatrix} \mathbb{I}_{n_x-n_{\mu_2}} & 0_{(n_x-n_{\mu_2})\times n_{\mu_2}} \end{bmatrix}, \tag{5.79b}$$

$$A_\xi = \mathbb{K}_\xi\mathbb{M}^{-1}\begin{bmatrix} A_x\mathbb{M} & A_{\mu_1} \end{bmatrix}, \tag{5.79c}$$

$$C_\xi = \begin{bmatrix} C_x\mathbb{N} & C_xA_{\mu_2} & C_{\mu_1} \end{bmatrix}, \; B_f = \mathbb{K}_\xi\mathbb{M}^{-1}B_\sigma, \tag{5.79d}$$

$$G_g = \mathbb{K}_\xi\mathbb{M}^{-1}G_\varrho, \; B_h = \mathbb{K}_\xi\mathbb{M}^{-1}B_\varsigma, \tag{5.79e}$$

$$D_\xi = \mathbb{K}_\xi\mathbb{M}^{-1}D_x, \; D_y = \mathbb{K}_\xi\mathbb{M}^{-1}\bar{D}_y, \tag{5.79f}$$

$$f(\xi,u) = \sigma_\mu(\mathbb{M}\xi,u), \; h(\xi,u) = \varsigma_\mu(\mathbb{M}\xi,u), g(y,u) = \varrho(y,u). \tag{5.79g}$$

Now let us introduce the following assumption.

Assumption 5.4.4. The following condition is fulfilled:

$$\operatorname{rank}(C_xA_{\mu_2}) = \operatorname{rank}(A_{\mu_2}) \triangleq n_{\mu_2}. \tag{5.80}$$

Under Assumption 5.4.4 and the fact that C_{μ_1} is full column rank, it is easy to show

that

$$\operatorname{rank}\left(\begin{bmatrix} E_\xi \\ \\ C_\xi \end{bmatrix}\right) = n_x + n_{\mu_1} \triangleq n_\xi.$$

Hence, we can apply the preliminary results to deduce an estimation of the unknown input $\mu(t)$. From (5.75), the unknown input $\mu(t)$ is estimated in the $\mathcal{H}_\infty$ sense as follows:

$$\hat{\mu}(t) = \mathcal{T}_{\mu_1}\hat{\mu}_1(t) + \mathcal{T}_{\mu_2}\dot{\hat{\xi}}_{\mu_2} - \mathcal{T}^A_{\mu_2}\hat{\xi} - \mathcal{T}^B_{\mu_2}\sigma_{\hat{\mu}}\big(\mathbb{M}_{\mu_1}\hat{\xi}, u\big) - \mathcal{T}^G_{\mu_2}\varrho\big(y, u\big) \tag{5.81}$$

where

$$\hat{\xi}_{\mu_2} \triangleq \overbrace{\begin{bmatrix} 0_{n_{\mu_2}\times(n_x-n_{\mu_2})} & \mathbb{I}_{n_{\mu_2}} \end{bmatrix}}^{\mathbb{M}_{\mu_2}}\hat{\xi}, \tag{5.82}$$

$$\mathcal{T}^A_{\mu_2} \triangleq \mathbb{M}_{\mu_2}\mathbb{M}^{-1}A_x\mathbb{M},\ \mathcal{T}^B_{\mu_2} \triangleq \mathbb{M}_{\mu_2}\mathbb{M}^{-1}B_f, \tag{5.83}$$

$$\mathcal{T}^G_{\mu_2} \triangleq \mathbb{M}_{\mu_2}\mathbb{M}^{-1}G_g,\ \mathbb{M}_{\mu_1} \triangleq \begin{bmatrix} \mathbb{M} & 0 \\ \\ 0 & \mathbb{I}_{n_{\mu_1}} \end{bmatrix}. \tag{5.84}$$

Remark 5.4.5. To avoid repetition, the detailed mathematical calculations, which we can get by following exactly the same steps as in the previous sections, are omitted. In addition, Proposition 5.4.3 still remains valid with convenient λ_ω and λ_0 corresponding to the new vector $\xi(t)$ defined in (5.78) and the new matrices defined in (5.82)-(5.84).

Remark 5.4.6. Since the matrix A_{μ_2} in (5.73)-(5.74) is not unique, then we have the possibility to choose the one that satisfies Assumption 5.4.4.

Remark 5.4.7 (Discussion on the assumptions). Notice that the assumptions introduced in this section are needed to apply the general LMI-based technique given in Theorem 5.3.3. Assumption 5.4.1 and Assumption 5.4.3 are introduced because we need the nonlinear function to depend on the corresponding vector $\xi(t)$ in each case, as in the system (5.2), where the nonlinear functions $f(.)$ and $g(.)$ depend on the state vector $\xi(t)$. Since in the second case, the vector $\xi(t) \triangleq \mathbb{S}^{-1}x(t)$ defined in (5.60), is not depending on $\mu(t)$, then we need $\sigma(.)$ and $\varsigma(.)$ to not depending on $\mu(t)$. We apply the same analogy in Assump-

tion 5.4.3. Since the corresponding state vector is the $\xi(t)$ defined in (5.78), then we need $\sigma(.)$ and $\varsigma(.)$ to be independent from $\mu_2(t)$. As for Assumption 5.4.2 and Assumption 5.4.4, by analogy, they are similar to Assumption 5.3.2. They look like Assumption 5.3.2 corresponding to system (5.2) with (5.60)-(5.61) and (5.78)-(5.79), respectively.

Remark 5.4.8. We should mention that in the the second and third cases, the new system matrices depend on new LPV parameters due to the presence of products between matrices depending on $\rho(t)$. For instance, if we focus on the third case, the matrix $\mathbb{M}$ in (5.76) depends on $\rho(t)$. Then its inverse $\mathbb{M}^{-1}$ depends on $\rho(t)$. Consequently, the new state matrix A_ξ in (5.79c) depends on a new LPV parameter $\rho_{\mathbb{M}}(t) \triangleq \kappa(\rho(t))$. Such a new parameter $\rho_{\mathbb{M}}(t)$ is determined after determining the matrix $\mathbb{M}$. This depends on the model at hand of the user. For instance, in the wastewater treatment model presented in the next section, we have $\kappa(\rho(t)) \equiv \rho(t)$, i.e.: $\rho_{\mathbb{M}}(t) \equiv \rho(t)$.

5.5 Application to Wastewater Treatment

Wastewater treatment plants (WWTP) are nonlinear systems subject to large perturbations in flows and load, together with uncertainties on the composition of the incoming wastewater mainly due to the impact of rain events and industrial charges. The Benchmark model has been proposed by the European program COST 624 for the evaluation of control strategies in wastewater treatment plants [8]. The wastewater treatment plants are usually composed of one or a set of biological tanks: anoxic and aerobic in closed loop with settler. The simulation benchmark plant design is comprised of five reactors in series with a10-layer secondary settling tank. Figure 5.1 shows a schematic representation of the layout. The Benchmark is based on the most common wastewater treatment plant: a continuous flow activated sludge plant, performing nitrification and pre-nitrification. For simplicity, we will take only the case of one aerated tank with a settler. In order to illustrate the effectiveness of the proposed nonlinear estimation algorithms we use a

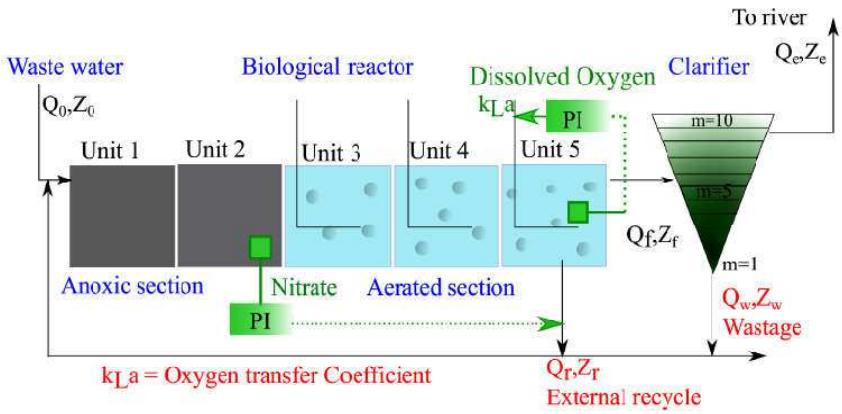

Figure 5.1: The benchmark simulation model no. 1 (BSM1) plant [6].

Table 5.1: Definition of the state variables in the reduced model

Variable	**Description**
X_{DCO}	Biodegradable substrate
S_{NO}	Nitrate and nitrite nitrogen concentration $[\text{mg} \cdot \text{l}^{-1}]$
S_{NH}	Ammonia nitrogen concentration $[\text{mg} \cdot \text{l}^{-1}]$
S_{ND}	Soluble biodegradable organic nitrogen concentration $[\text{mg} \cdot \text{l}^{-1}]$
S_O	Dissolved oxygen concentration $[\text{mg} \cdot \text{l}^{-1}]$

nonlinear reduced model described in Section 2.7, it contains five state variables :

$$x = \begin{bmatrix} X_{DCO} & S_{NO} & S_{NH} & S_{ND} & S_O \end{bmatrix}^\top$$

where the dynamical equations of the reduced model are given in equations 2.51. The objective is to estimate the measured states or concentrations S_O, S_{NO} and S_{NH} that are available fro measurement. However, the inlet concentrations S_{NO}^{in}, and S_{NH}^{in} are not measured online, they will be treated as unknown inputs and will be estimated.

5.5.1 Third case $0 < \text{rank}(C_\mu) < n_\mu$:

Since the unknown input estimation algorithms given in the previous section, the third case, is the more general one, then it is sufficient to provide simulations result. To this end, in addition to the model unknown inputs S_{NO}^{in} and S_{NH}^{in}, we consider that the S_O sensor is affected by a fault $d(t)$ given by:

$$d(t) \triangleq \begin{cases} 10\sin(4\pi t) & \text{if } \ 4(\text{day}) < d(t) < 7(\text{day}) \\ 0 & \text{otherwise.} \end{cases}$$

In a compact form, by adding $d(t)$ as unknown input, the model is described under the form (5.52) with the following parameters [47]:

$$E_\xi = \begin{bmatrix} 1 & 0 & 0 & 0 & 0 & 0 & 0 & 0 \\ 0 & 1 & 0 & 0 & 0 & 0 & 0 & 0 \\ 0 & 0 & 1 & 0 & 0 & 0 & 0 & 0 \\ 0 & 0 & 0 & 1 & 0 & 0 & 0 & 0 \\ 0 & 0 & 0 & 0 & 1 & 0 & 0 & 0 \end{bmatrix} \tag{5.85a}$$

$$A_x = \begin{bmatrix} -0.7955\rho(t) & 0 & 0 & 0 & 0 \\ 0 & -\rho(t) & 0 & 0 & 0 \\ 0 & 0 & -\rho(t) & \theta_4 & 0 \\ 0 & 0 & 0 & -\rho(t) - \theta_4 & 0 \\ 0 & 0 & 0 & 0 & \rho(t) - k_{La} \end{bmatrix},$$

$$A_\mu = \begin{bmatrix} 0 & 0 & 0 \\ 1 & 0 & 0 \\ 0 & 1 & 0 \\ 0 & 0 & 0 \\ 0 & 0 & 0 \end{bmatrix}, G_\varrho = \begin{bmatrix} 1 & 0 & \rho(t) & 0 \\ 0 & 0 & 0 & 0 \\ 0 & 0 & 0 & 0 \\ 0 & 0 & 0 & \rho(t) \\ 0 & SO_{sat} & 1 & 0 \end{bmatrix}, B_\varsigma = \begin{bmatrix} 0 \\ 0 \\ 0 \\ 0 \\ 0 \end{bmatrix}$$

$$B_\sigma = \begin{bmatrix} -1.49 & -1.49 & 0 & 0 \\ 0 & 0.17 & 4.16 & 0 \\ -0.08 & -0.08 & -4.16 & 0 \\ 0 & 0 & 0 & 1.0 \\ 0 & 0 & -19.04 & -10.00 \end{bmatrix},$$

$$C_x = \begin{bmatrix} 0 & 1 & 0 & 0 & 0 \\ 0 & 0 & 1 & 0 & 0 \\ 0 & 0 & 0 & 0 & 1 \end{bmatrix}, C_\mu = \begin{bmatrix} 0 & 0 & 0 \\ 0 & 0 & 0 \\ 0 & 0 & 1 \end{bmatrix},$$

$$D_x = \begin{bmatrix} 0.2 & 0.2 & 1.1 & 0.1 & 0 \end{bmatrix}^\top, \bar{D}_y = \begin{bmatrix} 0.1 \\ 0.2 \\ 0.3 \end{bmatrix},$$

where

- $\rho(t) = D^{in}$ is the influent flow rate;
- $\mu = \begin{bmatrix} \rho(t)S_{NO}^{in} & \rho(t)S_{NH}^{in} & d \end{bmatrix}^\top$ is the unknown input vector;
- The matrices D_x and D_y represent the distribution of the disturbances added in the process and in the sensors. We assume that a uniformly distributed random noise is injected in the system according to matrices D_x and D_y.

The nonlinear functions of the system are given by

$$\begin{aligned}
\rho(u,u) &= [\theta_2 \quad k_La \quad X_{DCO}^{in} \quad S_{ND}^{in}]^\top, \\
\varsigma(x,\mu,u) &= 0 \\
\sigma_1(x,\mu,u) &= \theta_1 \frac{X_{DCO}}{220+X_{DCO}} \frac{S_O}{0.2+S_O} \\
\sigma_2(x,\mu,u) &= \theta_1 \frac{X_{DCO}}{220+X_{DCO}} \frac{0.2}{0.2+S_O} \frac{S_{NO}}{0.2+S_{NO}} \eta_{NO,g} \\
\sigma_3(x,\mu,u) &= \theta_3 \frac{S_{NH}}{S_{NH}+1} \frac{S_O}{S_O+0.4} \\
\sigma_4(x,\mu,u) &= \theta_4 \frac{X_{DCO}}{X_{DCO}+258} \frac{S_O}{0.2+S_O} \eta_{NO,h} \frac{0.2}{0.2+S_O} \frac{S_{NO}}{0.5+S_{NO}}.
\end{aligned}$$

The values of the parameters are given in Table 2.5, [6]. After calculating the partial derivatives of the nonlinearities, we find that all the lower and upper bounds a_{ij} and b_{ij} are equal to 0 and 0.186, respectively.

We have $\text{rank}(C_\mu) = 1$, then we will write :

$$C_\mu \mu = C_{\mu_1} \mu_1, \text{ with } C_{\mu_1} = \begin{bmatrix} 0 & 0 & 1 \end{bmatrix}^{\mathrm{T}}, \ \mu_1 = d(t)$$

Hence, we can get (5.73)-(5.75) with $\mu_2 = \begin{bmatrix} S_{NO}^{in} & S_{NH}^{in} \end{bmatrix}^\top$,

$$A_{\mu_1} = \begin{bmatrix} 0 \\ 0 \\ 0 \\ 0 \\ 0 \end{bmatrix}, A_{\mu_2} = \begin{bmatrix} 0 & 0 \\ 1 & 0 \\ 0 & 1 \\ 0 & 0 \\ 0 & 0 \end{bmatrix}, \tag{5.86}$$

$$\mathcal{T}_{\mu_1} = \begin{bmatrix} 0 \\ 0 \\ 1 \end{bmatrix}, \mathcal{T}_{\mu_2} = \begin{bmatrix} 1 & 0 \\ 0 & 1 \\ 0 & 0 \end{bmatrix}, \ \mu_2 = \begin{bmatrix} \rho(t) S_{NO}^{in} \\ \\ \rho(t) S_{NH}^{in} \end{bmatrix}. \tag{5.87}$$

It is obvious that $\text{rank}(C_x A_{\mu_2}) = \text{rank}(A_{\mu_2}) = n_{\mu_2} = 2$. Then Assumption 5.4.4 holds, which means that we can apply the estimation algorithm (5.81) to estimate the whole unknown input μ, after estimating the vector $\xi(t)$ given by

$$\xi(t) \triangleq \begin{bmatrix} \mathbb{M}^{-1} x(t) \\ \\ \mu_1(t) \end{bmatrix}, \tag{5.88}$$

where $\mathbb{M}$ comes from (5.76) with $\mathbb{N} = \begin{bmatrix} 1 & 0 & 0 \\ 0 & 0 & 0 \\ 0 & 0 & 0 \\ 0 & 0 & 1 \\ 0 & 1 & 0 \end{bmatrix}$.

By expressing the matrix $\mathbb{M}$, the new state vector $\xi(t)$ in (5.88) contains the following six components:

$$\hat{\xi}(t) = \begin{bmatrix} X_{\text{DCO}} & S_{NO} & S_{NH} & S_{ND} & S_O & \mu_1(t) = d(t) \end{bmatrix}$$

The remaining unknown input $\mu_2(t)$ is defined by $\mu_2(t) = \begin{bmatrix} \mu_2^1(t) & \mu_2^2(t) \end{bmatrix}^\top$, where

- $\mu_2^1(t) = \rho(t) S_{NO}^{in} \Longrightarrow S_{NO}^{in} = \frac{1}{\rho(t)} \mu_2^1(t)$;
- $\mu_2^2(t) = \rho(t) S_{NH}^{in} \Longrightarrow S_{NH}^{in} = \frac{1}{\rho(t)} \mu_2^2(t)$.

5.5.1.1 Estimation of the system state :

The matrices in (5.79), corresponding to the model, are expressed as follows:

$$E_\xi = \begin{bmatrix} 1 & 0 & 0 & 0 & 0 & 0 \\ 0 & 1 & 0 & 0 & 0 & 0 \\ 0 & 0 & 1 & 0 & 0 & 0 \end{bmatrix}, \quad \mathbb{K}_\xi = \begin{bmatrix} 1 & 0 & 0 & 0 & 0 \\ 0 & 1 & 0 & 0 & 0 \\ 0 & 0 & 1 & 0 & 0 \end{bmatrix}, \quad A_\xi = A_{\xi,0} + \rho(t) A_{\xi,1}$$

$$A_{\xi,0} = \begin{bmatrix} 0 & 0 & 0 & 0 & 0 & 0 \\ 0 & -240 & 0 & 0 & 0 & 0 \\ 0 & 0 & -124 & 0 & 0 & 0 \end{bmatrix}, \quad A_{\xi,1} = \begin{bmatrix} -0.79545 & 0 & 0 & 0 & 0 & 0 \\ 0 & 1 & 0 & 0 & 0 & 0 \\ 0 & 0 & -1 & 0 & 0 & 0 \end{bmatrix}, \quad D_\xi = \begin{bmatrix} 0.1 \\ 0 \\ 0.1 \end{bmatrix}$$

$$C_\xi = \begin{bmatrix} 0 & 0 & 0 & 1 & 0 & 0 \\ 0 & 0 & 0 & 0 & 1 & 0 \\ 0 & 1 & 0 & 0 & 0 & 1 \end{bmatrix}, \quad B_f = \begin{bmatrix} -1.4925 & -1.4925 & 0 & 0 \\ 0 & 0.17221 & 4.1666 & 0 \\ -0.0800 & -0.0800 & -4.1666 & 0 \\ 0 & 0 & 0 & 1 \\ 0 & 0 & -19.04166 & -10 \end{bmatrix}$$

$$G_g = \begin{bmatrix} 80.49277 & 0 & 0 & 0 \\ 0 & 0 & 0 & 0 \\ 0 & 0 & 0 & 0 \\ 0 & 0 & 0 & 0 \\ 0 & 804.927 & 0 & 0 \end{bmatrix}$$

By applying the proposed method on the descriptor system obtained by using the

transformations (5.76)-(5.79), the corresponding matrices P_z and Q_z are computed as

$$P_z = \begin{bmatrix} 1 & 0 & 0 \\ 0 & 1 & 0 \\ 0 & 0 & 1 \\ 0 & 0 & 0 \\ 0 & 0 & 0 \\ 0 & -1 & 0 \end{bmatrix}, \; Q_z = \begin{bmatrix} 0 & 0 & 0 \\ 0 & 0 & 0 \\ 0 & 0 & 0 \\ 1 & 0 & 0 \\ 0 & 1 & 0 \\ 0 & 0 & 1 \end{bmatrix} \tag{5.90}$$

By solving the convex optimization problem (5.30) under the LMI constraints (5.31), obtained the following observer gains:

$$L_0 = \begin{bmatrix} 77.753917580392596 & 77.590764343566065 & 86.448115850653011 \\ -16.155882009902044 & -16.251586703905026 & -27.557130104509650 \\ 85.352145624391426 & 85.160755970375561 & 86.214355923684906 \\ 0.695078261107510 & 0.673725541278918 & 0.589954562677434 \\ 0.673310982825319 & 0.697562725269364 & 0.593805507810576 \\ 18.932074731886665 & 19.026436234148044 & 30.345947271073964 \end{bmatrix} \tag{5.91}$$

$$L_1 = \begin{bmatrix} 4.547964299638846 & 4.574707154824896 & 4.952407964141358 \\ -2.683593046776394 & -2.711428170654091 & -3.123810441999024 \\ 2.797374814491731 & 2.799233269628079 & 2.888686742653718 \\ 0.114022478939181 & 0.107220641929511 & 0.049097276015912 \\ 0.107858764286684 & 0.114930763813435 & 0.049764130074496 \\ 2.962453090284253 & 2.990669028123705 & 3.322378577027695 \end{bmatrix} \tag{5.92}$$

The optimal value of the disturbance attenuation level is $\alpha = 0.42711$.

To run simulation, the system and the observer are initialized, respectively, by :

$$\xi(0) = [52, 5, 5, 1, 1, 0, 0, 0], z_i = [0, 0, 0, 0, 0, 0, 0, 0]$$

The simulation results over a horizon of $T = 14$ days are depicted in Figure 5.2, which shows quite clearly the efficiency of the proposed unknown input observer design method. This scenario confirms the applicability of the observer in faulty environments, while keeping some measurements available. which is crucial for fault-tolerant control. The estimation of the system states and the sensor fault, ($\xi_6 = \mu_1(t) = f(t)$), is accurate as exhibit the behavior of the states in Figure (e) 5.2.

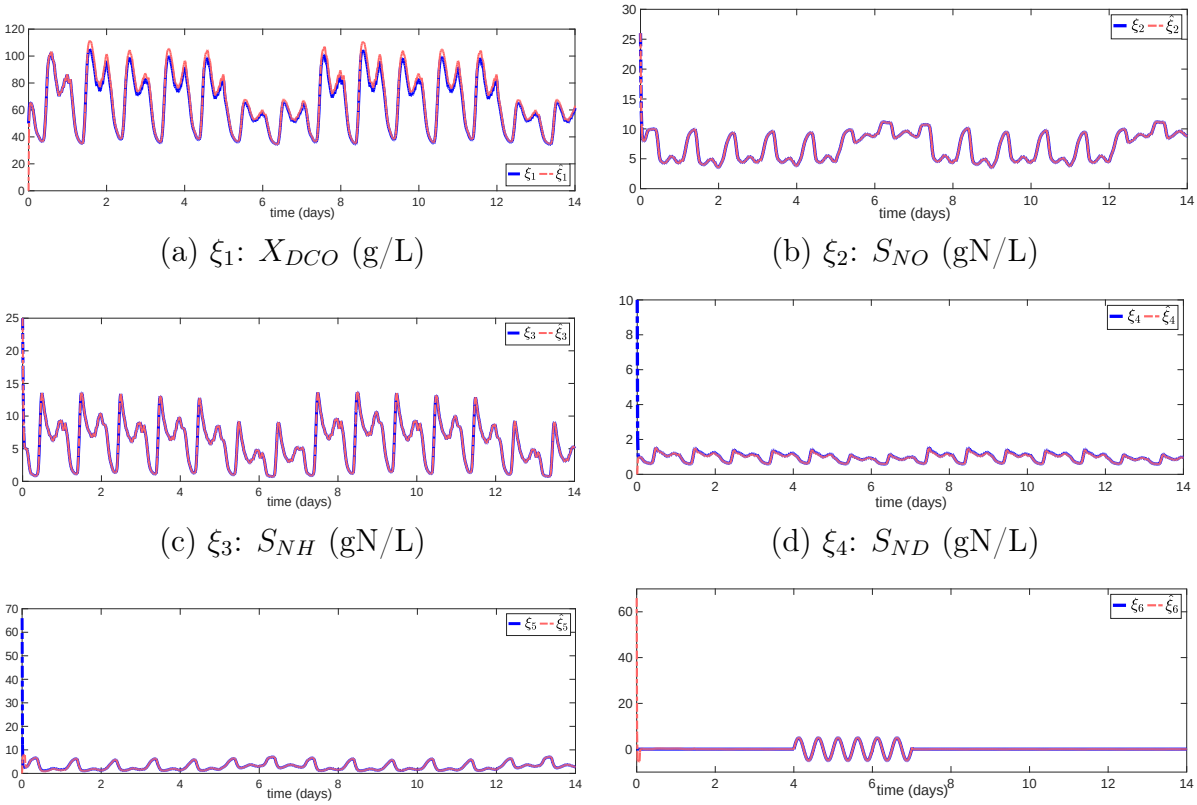

(a) ξ_1: X_{DCO} (g/L)

(b) ξ_2: S_{NO} (gN/L)

(c) ξ_3: S_{NH} (gN/L)

(d) ξ_4: S_{ND} (gN/L)

(e) ξ_5: S_O (g/L)

(f) $\xi_6 = \mu_1(t) = d(t)$: Sensor fault (g/L)

Figure 5.2: System states and their estimates:(a) organic concentration X_{DCO}, (b) nitrate/nitrite nitrogen concentration S_{NO}, (c) ammonium nitrogen concentration S_{NH}, (d) soluble organic nitrogen S_{ND}, (e) dissolved oxygen concentration S_O, and (f) sensor fault estimation $\xi_6 = \mu_1(t) = f(t)$.

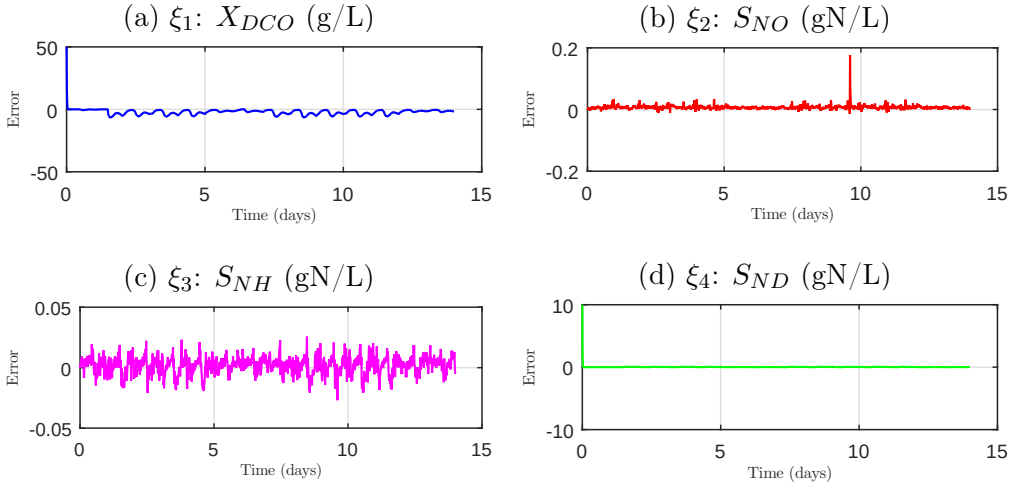

(a) ξ_1: X_{DCO} (g/L)

(b) ξ_2: S_{NO} (gN/L)

(c) ξ_3: S_{NH} (gN/L)

(d) ξ_4: S_{ND} (gN/L)

Figure 5.3: Estimation errors of the system states: (a) organic matter concentration X_{DCO}, (b) nitrate/nitrite nitrogen S_{NO}, (c) ammonium nitrogen S_{NH}, and (d) soluble organic nitrogen S_{ND}.

The estimation errors of the states remain low, showing the observer's resilience to partial sensor degradation. The fault signal d (i.e., ξ_8) is successfully estimated, which

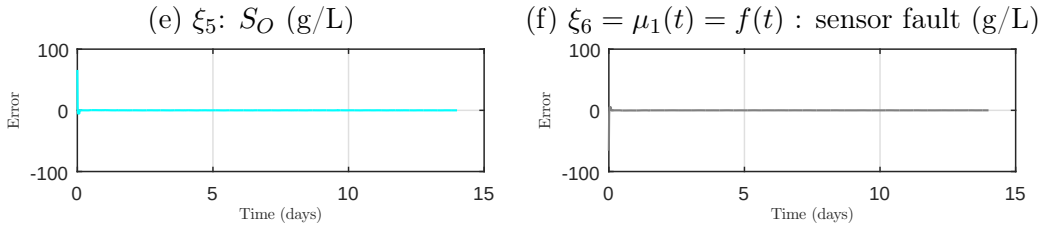

Figure 5.4: Estimation errors of the remaining system states : (e) dissolved oxygen concentration S_O, and (f) fault signal estimation $\xi_6 = \mu_1(t) = f(t)$.

demonstrates the observers potential for fault detection and isolation (FDI).

5.5.1.2 Estimation of the remaining unknown inputs :

Hence, we can apply the results of step one to estimate the remaining unknown inputs in the absence available sensors $\mu_2(t) = [D^{in}S^{in}_{NO}, D^{in}S^{in}_{NH}]^T$. The simulation results can be depicted in Figures 5.5 .

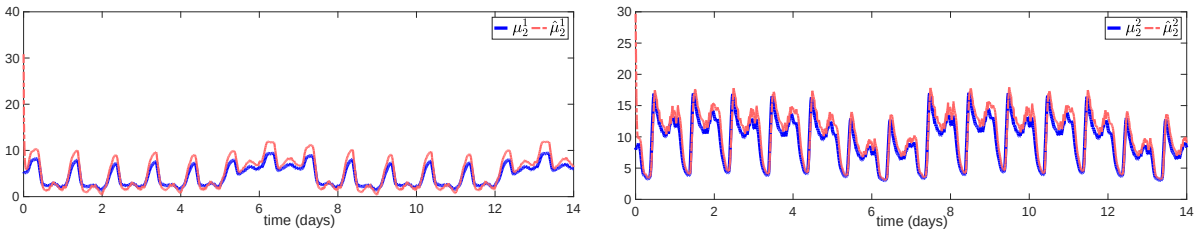

(a) $\mu_2^1(t)$ estimation (b) $\mu_2^2(t)$ estimation

Figure 5.5: Unknown inputs $\mu_2^1(t)$ and $\mu_2^2(t)$ with their respective estimations.

Overall, the simulation results show the effectiveness and performances of the proposed design methods despite the presence of the disturbances. and the derivatives of $\hat{\xi}(t)$, see equation 5.81. Moreover, the estimation given here is raw, without any filtering. We can improve the estimation by introducing filters or numerical differentiators.

5.5.2 A favorable case rank$(C_\mu) = n_\mu$

This condition implies that all components of the unknown input $\mu(t)$ have a direct and independent influence on the measured output $y(t)$. Physically, this corresponds to a situation where the number and configuration of sensors are sufficient to make all unknown inputs observable. Hence, the estimation vector in this case is defined as:

$$\hat{\xi} = \left[X_{DCO},\ S_{NO},\ S_{NH},\ S_{ND},\ S_O,\ D_{in}S^{in}_{NO},\ D_{in}S^{in}_{NH},\ d\right]^\top$$

We have $n_x = 5, n\mu = 3$ and the $(rank(C_\mu) = 3)$ then the condition (5.5) holds, where;

$$\text{rank}\left(\begin{bmatrix} E_\xi \\ C_\xi \end{bmatrix}\right) = 8 = n_x + n_\mu$$

Hence, we can apply the results of Section 5.4.1, to deduce the estimation of the unknown input $\mu(t)$ and state variables $x(t)$ in the estimation vector $\hat{\xi}$, where the equations of reduced nonlinear model $ASM1$ can be rewritten under the descriptor from (5.2) by using the following parameters :

$$E_\xi = \begin{bmatrix} 1 & 0 & 0 & 0 & 0 & 0 & 0 & 0 \\ 0 & 1 & 0 & 0 & 0 & 0 & 0 & 0 \\ 0 & 0 & 1 & 0 & 0 & 0 & 0 & 0 \\ 0 & 0 & 0 & 1 & 0 & 0 & 0 & 0 \\ 0 & 0 & 0 & 0 & 1 & 0 & 0 & 0 \end{bmatrix} \tag{5.93a}$$

$$A_x(\rho(t)) = \begin{bmatrix} -0.7954\rho(t) & 0 & 0 & 0 & 0 \\ 0 & -\rho(t) & 0 & 0 & 0 \\ 0 & 0 & -\rho(t) & 0 & 0 \\ 0 & 0 & 0 & -\rho(t) & 0 \\ 0 & 0 & 0 & 0 & 1 \end{bmatrix} \tag{5.93b}$$

$$A_\mu(\rho(t)) = \begin{bmatrix} 0 & 0 & 0 \\ \rho(t) & 0 & 0 \\ 0 & \rho(t) & 0 \\ 0 & 0 & 0 \\ 0 & 0 & 1 \end{bmatrix}, G_g(\rho(t)) = \begin{bmatrix} 1 & 0 & 0 & 0 \\ 0 & 0 & 0 & 0 \\ 0 & 0 & 0 & 0 \\ 0 & 0 & 0 & 0 \\ 0 & SO_{sat} & 1 & 0 \end{bmatrix}, \tag{5.93c}$$

$$B_f(\rho(t)) = \begin{bmatrix} -1.49 & -1.49 & 0 & 0 \\ 0 & 0.17 & 4.16 & 0 \\ -0.08 & -0.08 & -4.16 & 0 \\ 0 & 0 & 0 & 1.0 \\ 0 & 0 & -19.04 & -10.00 \end{bmatrix} \tag{5.93d}$$

$$C_x = \begin{bmatrix} 0 & 1 & 0 & 0 & 0 \\ 0 & 0 & 1 & 0 & 0 \\ 0 & 0 & 0 & 0 & 1 \end{bmatrix}, \; C_\mu = \begin{bmatrix} 1 & 0 & 0 \\ 0 & 1 & 0 \\ 0 & 0 & 1 \end{bmatrix}, \; D_\xi = \begin{bmatrix} 0.2 \\ 0.2 \\ 1.1 \\ 0.1 \\ 0 \end{bmatrix}, \; D_y = \begin{bmatrix} 0.1 \\ 0.2 \\ 0.3 \end{bmatrix} \tag{5.93e}$$

Note that matrix C_μ, $\text{rank}(C_\mu) = n_\mu = 3$ is of full column rank, then the condition (5.5)(2) is fulfilled. From (6), there exist two matrices P_z and Q_z

$$P_z = \begin{bmatrix} 1 & 0 & 0 & 0 & 0 \\ 0 & 1 & 0 & 0 & 0 \\ 0 & 0 & 1 & 0 & 0 \\ 0 & 0 & 0 & 1 & 0 \\ 0 & 0 & 0 & 0 & 1 \\ 0 & -1 & 0 & 0 & 0 \\ 0 & 0 & -1 & 0 & 0 \\ 0 & 0 & 0 & 0 & -1 \end{bmatrix}, \; Q_z = \begin{bmatrix} 0 & 0 & 0 \\ 0 & 0 & 0 \\ 0 & 0 & 0 \\ 0 & 0 & 0 \\ 0 & 0 & 0 \\ 1 & 0 & 0 \\ 0 & 1 & 0 \\ 0 & 0 & 1 \end{bmatrix} \tag{5.94}$$

Therefore, we can build the proposed two-stage observer (5.15) after solving the LMI (5.31) conditions for the $\mathcal{H}_\infty$ optimal criterion, given by Theorem (5.3.3), which have been found to be feasible by using the YALMIP toolbox in Matlab/Simulink, we obtained the following observer gains:

$$L_0 = \begin{bmatrix} 1.0\text{e}{+05} & & \\ 0.26 & 0.11 & 0.04 \\ -2.44 & -0.05 & 0.71 \\ -2.47 & 0.95 & 1.89 \\ 0.37 & 0.16 & 0.08 \\ 0.33 & 0.20 & 0.06 \\ 2.44 & 0.05 & -0.71 \\ 2.47 & -0.95 & -1.89 \\ -0.33 & -0.20 & -0.063 \end{bmatrix}, \quad L_1 = \begin{bmatrix} 1.0\text{e}{+03} & & \\ -0.29 & -0.12 & -0.03 \\ 0.19 & -1.24 & -1.73 \\ -0.98 & -3.19 & -3.79 \\ 0.05 & 0.03 & 0.02 \\ -1.44 & -0.68 & -0.30 \\ -0.19 & 1.24 & 1.73 \\ 0.98 & 3.19 & 3.79 \\ 1.44 & 0.68 & 0.30 \end{bmatrix} \tag{5.95}$$

The best optimal values of the disturbance attenuation level are $\mu_\infty = 0.140483$ and $\nu_\infty = 1.904e^{07}$.

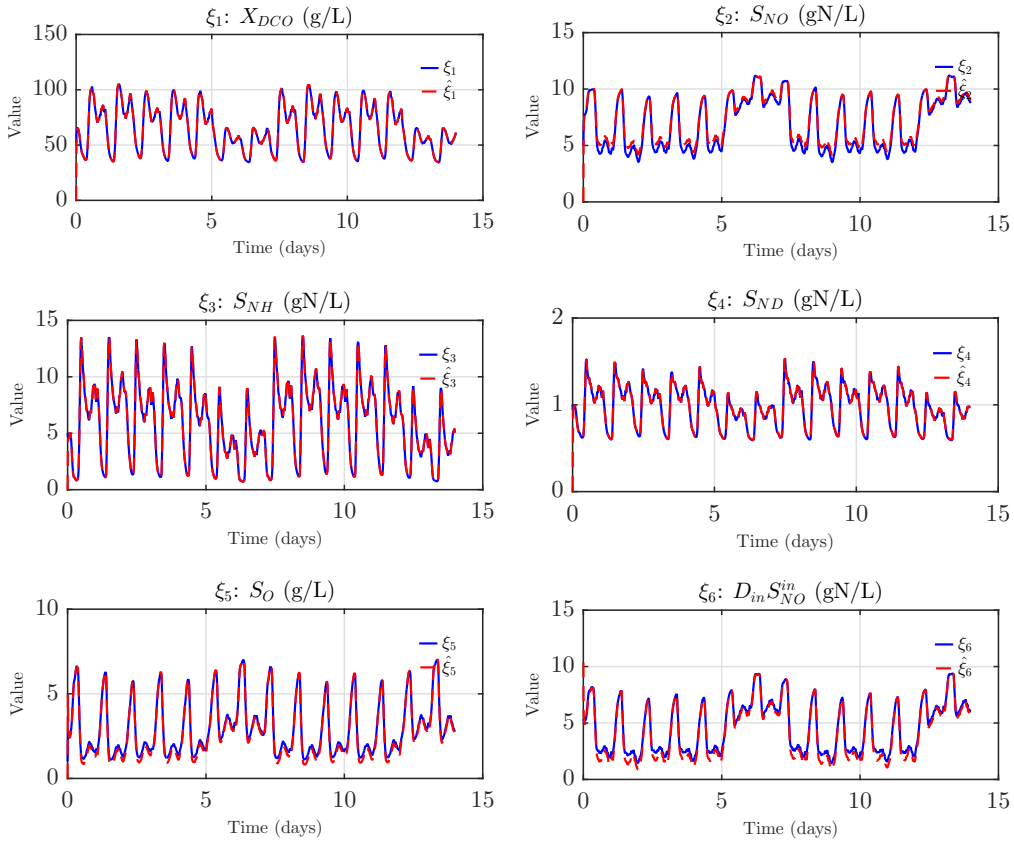

Figure 5.6: Comparison between true values and estimates of system states (First case) (a) X_{DCO}, (b) S_{NO}, (c) S_{NH}, (d) S_{ND}, (e) S_O, (f) $D_{in}S^{in}_{NO}$.

In this observation scenario, full information available, all system outputs are available, and the unknown inputs have a direct influence on the measured outputs. The estimation errors for all states (ξ_1 to ξ_8) remain small, bounded, and tend to converge towards zero

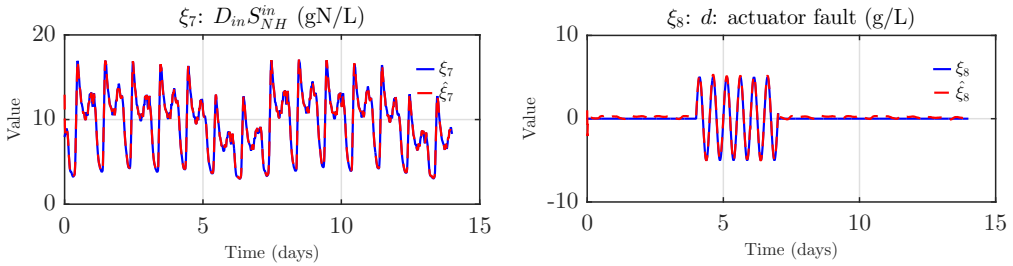

Figure 5.7: Behavior of state variables and their estimates : (g) inflow ammonium concentration $D_{in}S_{NH}^{in}$, (h) sensor fault d.

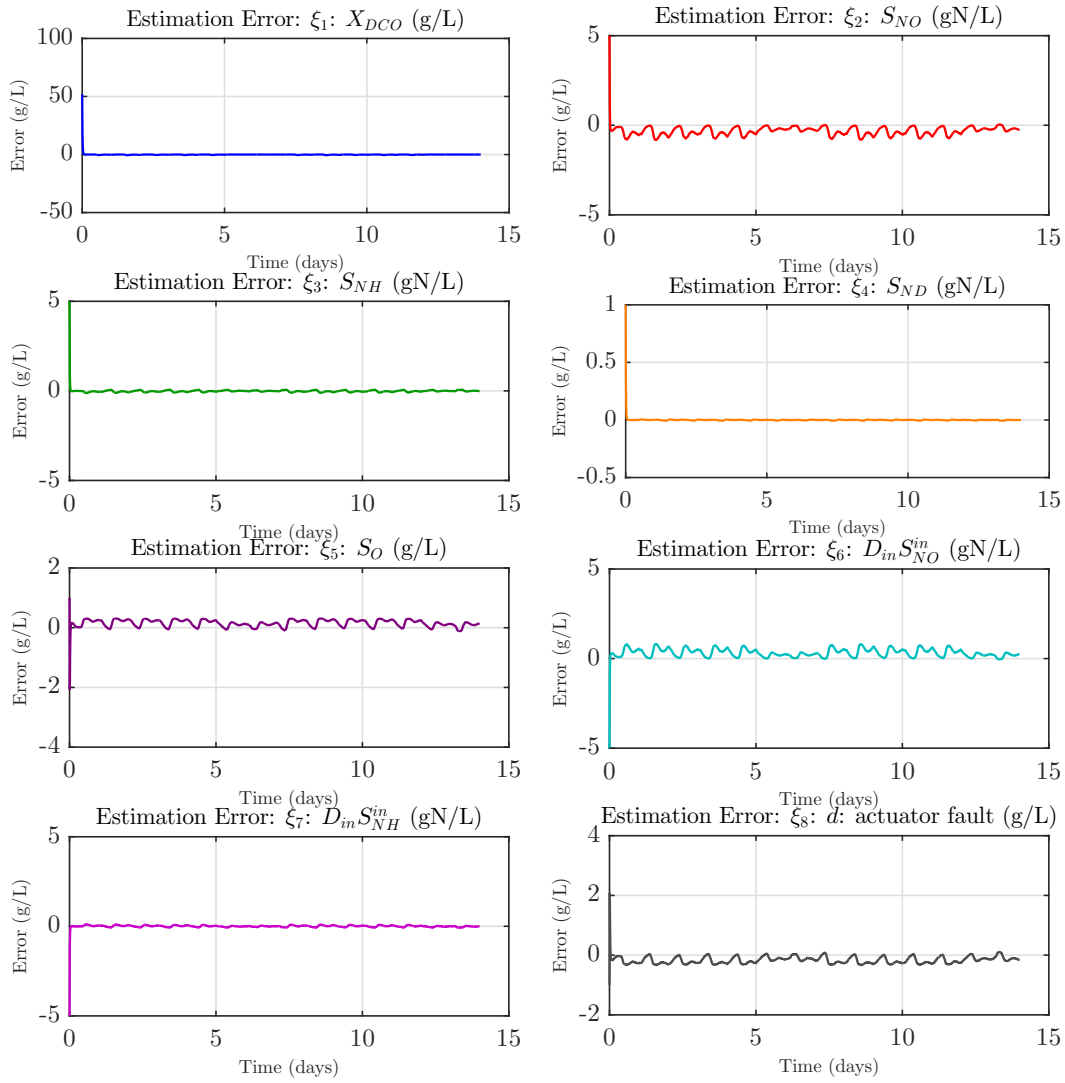

Figure 5.8: Estimation errors of the system states ξ_1 to ξ_8 under the first case scenario.

see Figures 5.8. This result confirms that the observer accurately tracks both the state dynamics and the unknown inputs. Particularly, ξ_6 to ξ_8 (representing inflow disturbances and sensor fault) are well reconstructed as Figures (5.6) and (5.7), which validates the effectiveness of the unknown input decoupling strategy. Overall, the observer performance

is excellent, with fast convergence and negligible steady-state errors.

5.5.3 Second case: $C_\mu = 0$

In this scenario meaning that the unknown inputs $\mu(t)$ have no direct influence on the system outputs. In practice, this case corresponds to disturbances or faults that do not appear in the outputs, but still affect the internal dynamics of the system. then the state vector is decoupled from the unknown input and the estimation vector $\hat{\xi}$ is given as :

$$\xi(t) \triangleq S^{-1}x(t)$$

$$\hat{\xi} = \left[X_{DCO},\ S_{NO},\ S_{NH},\ S_{ND},\ S_O\right]^\top$$

And the following condition (Assumption 5.4.2) is fulfilled:

$$\operatorname{rank}\left(C_x A_\mu\right) = \operatorname{rank}\left(A_\mu\right) = 3. \tag{5.96}$$

then the condition (5.5) holds, where;

$$\operatorname{rank}\left(\begin{bmatrix} E_\xi \\ \\ C_\xi \end{bmatrix}\right) = n_x = 5. \tag{5.97}$$

Through the use of appropriate transformations (5.58)–(5.59), the system can be reformulated into a convenient structure (Equation (5.2)).

5.5.3.1 Estimation of the system state :

To enable the estimation of the system state, by introducing the following parameters :

$$T = \begin{bmatrix} 0.9000 & 0 \\ 0 & 0 \\ 0 & 0 \\ 0 & 0.6000 \\ 0 & 0 \end{bmatrix} \qquad S = \begin{bmatrix} 0.9000 & 0 & 0 & 0 & 0 \\ 0 & 0 & 79.4928 & 0 & 0 \\ 0 & 0 & 0 & 79.4928 & 0 \\ 0 & 0.6000 & 0 & 0 & 0 \\ 0 & 0 & 0 & 0 & 1.0000 \end{bmatrix}$$

$$S^{-1}A_\mu = \begin{bmatrix} 0 & 0 & 0 \\ 0 & 0 & 0 \\ 1 & 0 & 0 \\ 0 & 1 & 0 \\ 0 & 0 & 1 \end{bmatrix} \qquad E_t = \begin{bmatrix} 1 & 0 & 0 & 0 & 0 \\ 0 & 1 & 0 & 0 & 0 \end{bmatrix} \qquad A_{\xi,0} = \begin{bmatrix} 0 & 0 & 0 & 0 & 0 \\ 0 & -124 & 0 & 0 & 0 \end{bmatrix}$$

$$A_{\xi,1} = \begin{bmatrix} -0.7955 & 0 & 0 & 0 & 0 \\ 0 & -1.0000 & 0 & 0 & 0 \end{bmatrix} \quad A_\xi = \begin{bmatrix} 0 & 0 & -79.4928 & 0 & 0 \\ 0 & 0.9359 & 0 & -79.4928 & 0 \\ 0 & 0 & 0 & 0 & -1.6051 \end{bmatrix}$$

$$C_\xi = \begin{bmatrix} 0 & 0 & 79.4928 & 0 & 0 \\ 0 & 0 & 0 & 79.4928 & 0 \\ 0 & 0 & 0 & 0 & 1.0000 \end{bmatrix} \qquad G_g = \begin{bmatrix} 0 & 0 & 0 & 0 \\ 0 & 0 & 0 & 0 \\ 0 & 0.1000 & 0 & 0 \end{bmatrix}$$

$$B_f = \begin{bmatrix} 0 & 0.0022 & 0.0524 & 0 \\ -0.0010 & -0.0010 & -0.0524 & 0 \\ 0 & 0 & -0.1904 & -0.1000 \end{bmatrix} \qquad D_\xi = \begin{bmatrix} 0.2222 \\ 0.1667 \end{bmatrix}$$

Given Assumption 5.3.2, then there exist matrices $P_z \in \mathbb{R}^{n_\xi \times n_d}$ and $Q_z \in \mathbb{R}^{n_\xi \times n_y}$.

$$P_z = \begin{bmatrix} 1 & 0 \\ 0 & 1 \\ 0 & 0 \\ 0 & 0 \\ 0 & 0 \end{bmatrix} \qquad Q_z = \begin{bmatrix} 0 & 0 & 0 \\ 0 & 0 & 0 \\ 0.0126 & 0 & 0 \\ 0 & 0.0126 & 0 \\ 0 & 0 & 1.0000 \end{bmatrix}$$

The $\mathcal{H}_\infty$ criterion (5.28) is satisfied with $\alpha = 2.0982e^{-05}$, $\beta = 23.2110$, $\mu_x = 0.0033$,. Hence, the observer gains were determined by solving the convex optimization problem (5.30), subject to the LMI constraints (5.31).

$$L_0 = \begin{bmatrix} 0.3307 & 0.3309 & 27.0624 \\ 0.2828 & 0.2829 & 19.1704 \\ 0.0405 & 0.0366 & 0.7676 \\ 0.0366 & 0.0404 & 0.7677 \\ 0.0412 & 0.0412 & 0.8536 \end{bmatrix} \qquad L_1 = \begin{bmatrix} 0.0054 & 0.0054 & 0.3718 \\ 0.0045 & 0.0045 & 0.3276 \\ 0.0005 & 0.0005 & 0.0446 \\ 0.0005 & 0.0005 & 0.0447 \\ 0.0006 & 0.0006 & 0.0639 \end{bmatrix}$$

The matrices of the observer in (5.6) are computed as follows :

$$A_z = \begin{bmatrix} -55.0373 & 0 & -56.1007 & -56.1372 & -52.7902 \\ 0 & -193.1898 & -47.1872 & -47.2059 & -41.8367 \\ 0 & 0 & -6.2394 & -5.7178 & -3.8566 \\ 0 & 0 & -5.7178 & -6.2251 & -3.8575 \\ 0 & 0 & -6.5057 & -6.5085 & -5.2773 \end{bmatrix}$$

$$A_y = \begin{bmatrix} 0 & 0 & 0 \\ 0 & 0 & 0 \\ 0 & 0 & 0 \\ 0 & 0 & 0 \\ 0 & 0 & 0 \end{bmatrix} \qquad G_z = \begin{bmatrix} 1.1111 & 0 & 76.8776 & 0 \\ 0 & 0 & 0 & 115.3163 \\ 0 & 0 & 0 & 0 \\ 0 & 0 & 0 & 0 \\ 0 & 0 & 0 & 0 \end{bmatrix}$$

The simulation results are depicted in Figure (5.9) and (5.10).

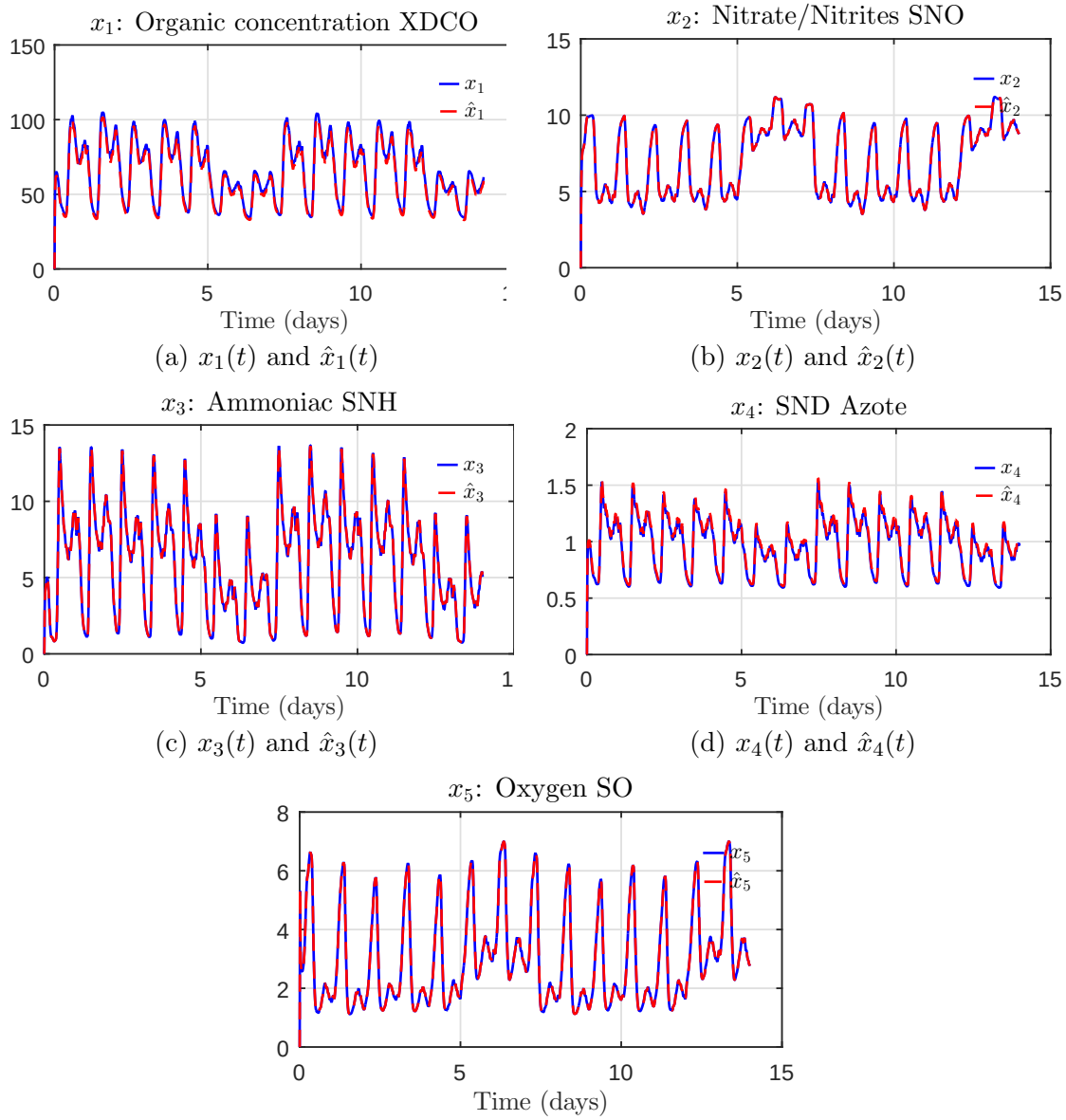

(a) $x_1(t)$ and $\hat{x}_1(t)$

(b) $x_2(t)$ and $\hat{x}_2(t)$

(c) $x_3(t)$ and $\hat{x}_3(t)$

(d) $x_4(t)$ and $\hat{x}_4(t)$

(e) Oxygen concentration $x_5(t)$ and its estimate $\hat{x}_5(t)$

Figure 5.9: Reconstruction of state variables x_1 to x_5 and their estimations.

The state estimation errors for ξ_1 to ξ_5 remain within acceptable bounds, showing that the observer can still track the system states even in the absence of full input observability.

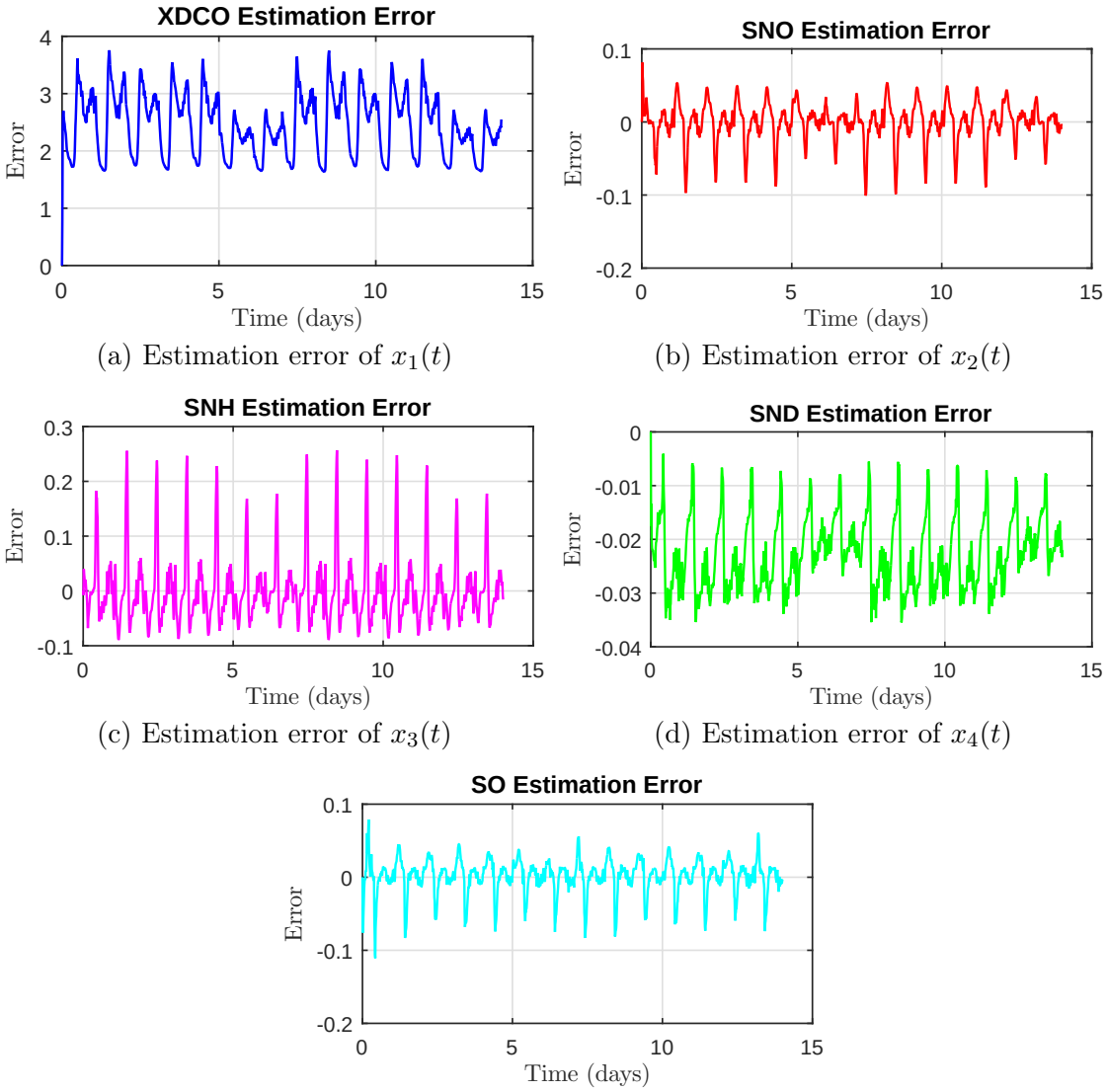

(a) Estimation error of $x_1(t)$

(b) Estimation error of $x_2(t)$

(c) Estimation error of $x_3(t)$

(d) Estimation error of $x_4(t)$

(e) Estimation error of $x_5(t)$

Figure 5.10: Estimation errors of the state variables x_1 to x_5.

5.5.3.2 Estimation of the unknown inputs :

Once the state $\hat{x}(t)$ is estimated, the unknown input $\mu(t)$ can be determined using its derivative $\dot{\hat{x}}(t)$, computed numerically in real time as in (5.66) and (5.67) . We now introduce the some necessary matrices.

$$S_2 = \begin{bmatrix} 0 & 0 & 1 & 0 & 0 \\ 0 & 0 & 0 & 1 & 0 \\ 0 & 0 & 0 & 0 & 0.01 \end{bmatrix} \quad A_{2,\xi} = \begin{bmatrix} 0 & 0 & -79.49 & 0 & 0 \\ 0 & 0.94 & 0 & -79.49 & 0 \\ 0 & 0 & 0 & 0 & -1.61 \end{bmatrix} \quad D_{2,t} = \begin{bmatrix} 0.0025 \\ 0.0138 \\ 0 \end{bmatrix} \tag{5.98}$$

Figures 5.11 present the results obtained from the simulation.

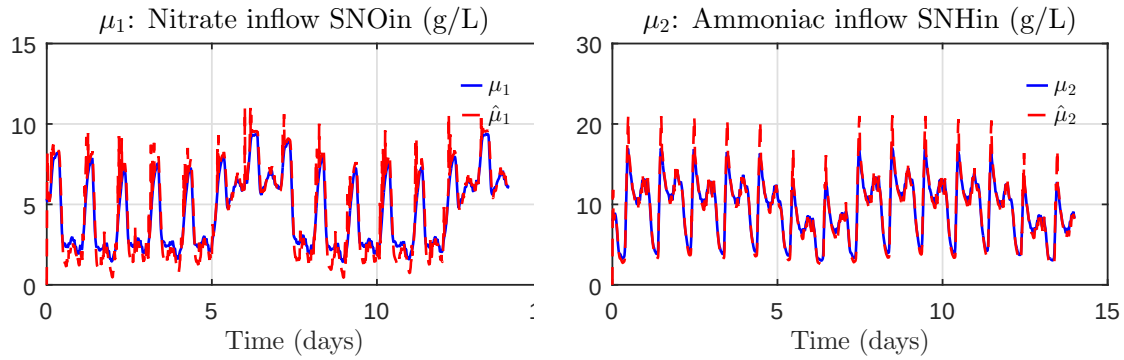

(a) Estimation of $\mu_1 = S_{NO}^{in}$ (b) Estimation of $\mu_2 = S_{NH}^{in}$

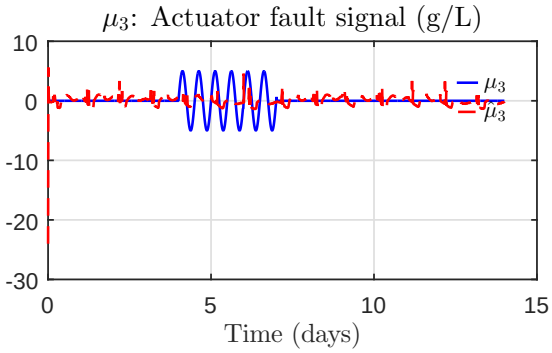

(c) Estimation of $\mu_3(t) = d$ fault)

Figure 5.11: Reconstruction of the unknown inputs: nitrate inflow $\mu_1(t)$, ammoniac inflow $\mu_2(t)$ and fault $\mu_3(t)$

In this observation scenario, the unknown inputs do not directly affect the measured outputs (i.e., $C_\mu = 0$). As expected, the estimation of μ_1, μ_2, and μ_3 becomes more challenging, leading to higher errors in the reconstructed variables ξ_6 to ξ_8, as illustrated in Figure 5.11, particularly in the case of the fault signal $\mu_3(t)$. This case highlights the limitations of observability and the importance of the rank condition in the design of unknown input observers. Despite the degraded performance compared to other scenarios, the estimation remains acceptable from a practical perspective.

Overall, despite the injected disturbances, the simulation results show that the designed two-stage state observer (5.6) converges to the true values after a very short transient period and effectively rejects the disturbances affecting both the system dynamics and measurements. Moreover, the results clearly demonstrate that, across the three scenarios, the estimation errors of the state variables, the unknown inputs, and the fault remain within a very narrow range. These satisfactory outcomes highlight the robustness of the proposed observer in rejecting perturbations, as well as its effectiveness in simultaneously estimating the state variables and the unknown inputs with high accuracy.

5.6 Conclusion

In this chapter, we have developed a comprehensive framework for unknown input estimation in nonlinear descriptor systems characterized by both LPV dynamics and Lipschitz nonlinearities. The proposed methodology introduces a general $\mathcal{H}_\infty$ observer design approach based on Linear Matrix Inequalities (LMIs), supported by advanced mathematical tools such as reformulated Lipschitz constraints, strategic use of Youngs inequality, and a Lyapunov function that eliminates disturbance derivatives. These innovations allow for less conservative synthesis conditions and broader applicability. A major contribution lies in the formulation of three adaptive estimation algorithms, each precisely tailored to the rank structure of the distribution matrix C_μ:

- **Case where C_μ is full rank:** Allows direct algebraic estimation of unknown inputs.
- **Case where C_μ is zero rank:** Requires a change of basis and matrix decomposition to restore observability.
- **Case where $0 < \text{rank}(C_\mu) < n_\mu$:** Combines the above approaches to handle partial observability of unknown inputs.

This classification ensures that the proposed algorithms are not limited to idealized cases but are instead applicable to a wide range of realistic industrial configurations. The proposed estimation strategies were rigorously validated through their application to a

biological wastewater treatment plant (COST 624 benchmark), involving state variables such as organic substrate, nitrogen, and dissolved oxygen concentrations. The observers demonstrated accurate estimation performance maintaining estimation errors below 0.5% even in the presence of actuator and sensor faults, as well as external disturbances. These results underscore the robustness and practical value of the proposed observers in fault diagnosis and system monitoring. Beyond validation, this chapter lays a solid methodological foundation for the development of fault-tolerant control schemes. The theoretical results established here will be directly leveraged in the next chapter, where we will explore how the estimated states and unknown inputs can be integrated into a control architecture capable of maintaining system performance despite faults and uncertainties.

Chapter 6

Integrated FTC and Neural MPC for DO Control in WWTP

"The art of research is the art of persistent questioning."
(Albert Einstein)

6.1 Introduction

The precise regulation of dissolved oxygen (DO) concentration in biological wastewater treatment plants (WWTPs) is a major challenge to ensure the quality of water treatment while controlling energy consumption. Indeed, a low oxygen concentration slows down the microbial activity essential for organic matter degradation, whereas excessive oxygen leads to significant energy costs associated with aeration. This delicate trade-off lies at the heart of process control, which is characterized by nonlinear, multi-scale dynamics and high sensitivity to external disturbances and model uncertainties [191], [192, 193]. Maintaining this concentration around a critical setpoint fixed at $2mg/L$, with an appropriate tolerance, is essential to reconcile biological performance and energy cost management related to aeration. Traditionally, proportional-integral (PI) controllers are used within the Benchmark Simulation Model No. 1 (BSM1). However, due to the complexity of the phenomena and variable operating conditions, such fixed-parameter linear controllers often fail to provide satisfactory regulation performance across the full operating range [194]. Therefore, advanced control strategies, such as Nonlinear Model Predictive Control (NMPC), have emerged as promising solutions. NMPC, also known as receding horizon control, relies on an accurate model of the process behavior, which can be a classical state-space mathematical model or a neural network-based model. These techniques enable real-time optimization of a cost function under complex constraints but face significant challenges due to nonlinearity, high-dimensional variables, and sensitivity to optimization initial conditions [195]. To address these challenges, nature-inspired metaheuristic algorithms, such as Genetic Algorithms (GA) and Particle Swarm Optimization (PSO), are employed to efficiently solve these complex optimization problems, with PSO being preferred for its lower computation time [196, 197]. Furthermore, system robustness against faults and disturbances remains a critical challenge. To meet this requirement, we propose a Dynamic Output Feedback Fault-Tolerant Control (DOFFTC) strategy. This approach relies on a precise prior estimation of faults and unknown inputs, obtained using the estimation algorithm developed in the previous chapter. This

algorithm, based on advanced observer techniques, enables real-time identification of disturbances and anomalies affecting the system, providing essential information for robust controller design. The DOFFTC uses these estimations to design a control law capable of actively compensating dynamic faults while ensuring system stability, effective disturbance rejection, and precise regulation of the dissolved oxygen concentration. The control synthesis is based on a reformulation into Linear Matrix Inequalities (LMIs) through a Lyapunov-based approach, thus guaranteeing a convex mathematical framework and efficient resolution using modern optimization tools. This chapter is organized as follows. It first details the design of the Nonlinear Neural Model Predictive Control (NNMPC), including NNARX modeling and optimization using PSO and GA algorithms. Building on this, the chapter then presents the Active Fault-Tolerant Control (AFTC) architecture, which is formulated through Lyapunov-based Linear Matrix Inequalities (LMIs) to ensure system stability and fault rejection. Finally, the proposed control strategies are validated through simulations on the Benchmark Simulation Model No. 1 (BSM1), demonstrating superior performance compared to PI control in terms of setpoint tracking, disturbance rejection, and fault resilience

6.2 The activated sludge waste-water treatment plant (AS-WWTP)

This section focuses on the structural layout of the BSM1 plant, the biological treatment based on the activated sludge process has already been detailed in the chapter 2.2.2.1.

6.2.1 Plant Layout

The BSMl consists of two parts, one is the biochemical reaction tank and the other is the secondary sedimentation tank. Biochemical reaction tank is divided into five units, where the first two units are non-aerated compartments (denitrification) whereas the last three units are aerated compartments (nitrification) as shown in Figure 5.1 [198] [199]. Reactors 3 and 4 have a fixed oxygen transfer coefficient ($KLa_{3,4} = 240[d^{-1}]$), and the DO

of reactor five should be maintained at a predetermined set point value $2[g(COD).m^{-3}]$ by manipulation of the oxygen transfer process KLa_5. A general survey of the benchmark model and a technical description is provided by [200]. In each unit, the mass fraction x_k of each component in the k^{th} compartment is expressed as shown in Equation (2.26). Due to the influence of DO concentration by aeration, the material balance equation was special, as Equation 2.28. where, $S_{O,sat} = 8[mg/L]$, $S_{O,sat}$ is the saturation concentration of dissolve oxygen [200].

6.3 Control of the ASWWTP

6.3.1 The PI dissolved oxygen controller

For PI controller a recursive discrete PI algorithm with antiwindup protection was used

$$u_k = u_{k-1} + K_p(e_k - e_{k-1}) + K_p\frac{T_s}{T_i}e_{k-1} - \frac{T_s}{T_i}(u_{k-1} - u_{lim}) \tag{6.1}$$

With

$$\begin{cases} u_{lim} = u_{min}, if, u_{k-1} < u_{min} \\ u_{k-1}, if, u_{min} \leqslant u_{k-1} \leqslant u_{max} \\ u_{max}, if, u_{k-1} > u_{min} \end{cases} \tag{6.2}$$

where u_{min} and u_{max} are minimal and maximal DO set-point values.

6.3.2 The neural network model predictive controller (NNMPC)

6.3.2.1 Linear MPC controller

In general, MPC consists of the following three key elements [201]:

- Explicit use of a model and on-line measurements to predict the process output along a future prediction horizon (H_p).
- Minimization a chosen cost function to find a sequence of manipulated input moves over a control horizon (H_c) where the predicted response moves to the set point
- Only the first of the calculated input sequence is implemented and the whole opti-

mization is repeated at the next sampling time.

The MPC methodology is characterized by the strategy represented in Figure 6.1 [201].

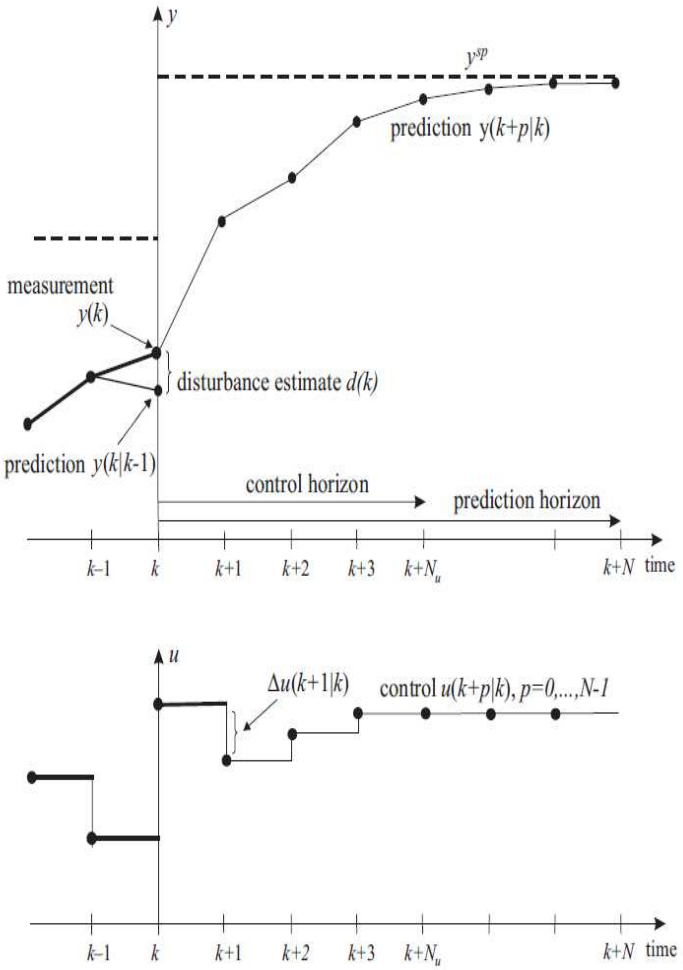

Figure 6.1: Model predictive control problem formulation

The following quadratic cost function is typically used:

$$\min_{u(k)} J = \sum_{p=1}^{H_p} (e(k+p/k))^2 + \lambda * \sum_{p=1}^{H_c} (\Delta u(k+p/k))^2 \tag{6.3}$$

where

$$e(k+p/k) = w(k+p/k) - y_m(k+p/k), (H_p) > (H_c) \tag{6.4}$$

- $e(k+p/k)$: represent the deviation of the predicted values of the output $y_m(k+p/k)$ from the respective reference $w(k+p/k)$ over the prediction horizon.
- $\Delta u(k+H_c-1/k)$: The control increments

- λ: is the positive weight factor of the control signal.

In MPC is usually used in combination with input and output constraints

$$\begin{cases} \triangle U(t+k-1) = 0, for, k > H_c \\ U_{min} \leqslant U(k) \leqslant U_{max} \\ \triangle U_{min} \leqslant \triangle U(k) \leqslant \triangle U_{max} \\ y_{min} \leqslant y(k) \leqslant y_{max} \end{cases} \tag{6.5}$$

6.3.2.2 Nonlinear Model Predictive Control

One limitation to the LMPC methods is that they are based on linear system theory and may not perform on highly nonlinear system. Hence a Nonlinear (NMPC) an extension of the LMPC is considered. The neural Network auto-regressive with exogenous inputs NNARX model is a powerful modeling and validation tool that offers simplicity and flexibility of network architecture and time series predictions [202].

The general form of regression vector for the NARX model is

$$\varphi(k+1) = [y(k), ..., y(k+1-du), u(k+1-d), ..., u(k+1-d-dy)]^T \tag{6.6}$$

As the above model takes as inputs ny past outputs and nu past control inputs and has delay d. A neural model structure in Figure 6.2 [203] was developed with a multi-layer preceptor with only one hidden layer containing k neurons with hyperbolic tangent activation function, an output layer with one neuron with a linear activation function [204] [205] [206]. The general NNARX neural network equation can be written as:

$$\hat{y}_p(k+1) = w_0^2 + \sum_{h=1}^{k} w_h^2 \varphi(w_{k,0}^1 + \sum_{i=0}^{du} w_i^1 u_1(k-i) + \sum_{j=0}^{dy} w_j^1 \hat{y}_1(k-j)) \tag{6.7}$$

w_h^2,w_i,w_j are the weights and $w_{k,0}^1$; w_0^2 are the biases.

The training phase is offline, the learning rule for the NNARX network is the Levenberg-Marquardt back-propagation (LMBP) algorithm was used for adjusting the network biases and weights.

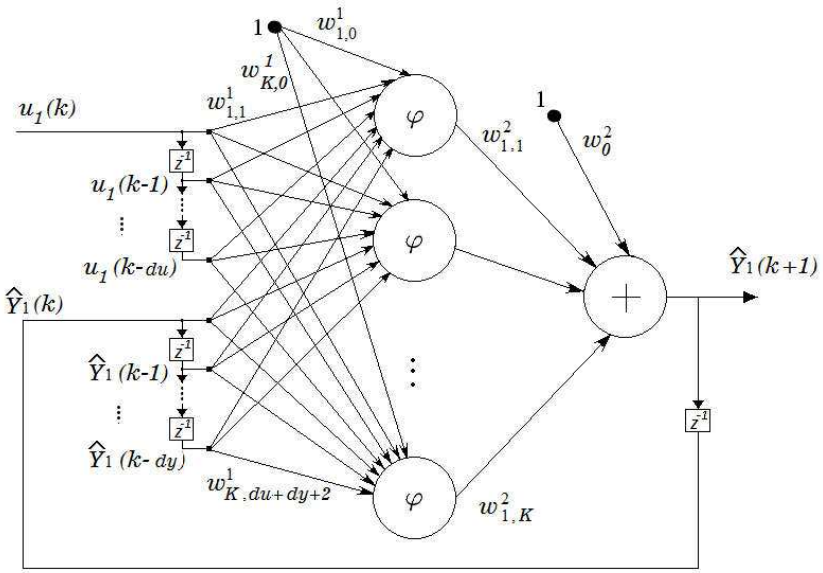

Figure 6.2: The structure of the NNARX neural network: SISO model.

6.4 NNMPC optimization cost function

This section copes the problem of optimization , where three algorithms are proposed, starting with the classical one which is Levenberg-Marquardt algorithm then two meta-heuristic will used.

6.4.1 Newton based Levenberg Marquardt method

It is necessary to apply an iterative search method to minimize the above performance index J, see equation (6.3), at each iteration. Since fast convergence is crucial for real-time control, a Newton based Levenberg-Marquardt minimization method is chosen [203]which can be expressed as follows:

$$f^{(i)} = -G[U^{(i)}](H[U^{(i)}(k)] + \lambda^{(i)} I)^{(-1)} \tag{6.8}$$

Where $f^{(i)}$: the search direction.

The algorithm is summarized below [203] [207] [208]:

1. Initialize λ, Select initial sequence of future control inputs, $U^{(0)}$ and evaluate the criterion $J(U^{(0)}); i = 0$.

2. Compute the gradient vector $G(U^{(i)})$ and the Hessian matrix $H(U^{(i)})$.
3. Using the Cholesky factorization on $(H[U^{(i)}(k)] + \lambda^{(i)} I)$ the to check the positive definiteness of the Hessian matrix and if the factorization fails (the matrix is not positive definite), set $\lambda = 4\lambda$ and go to 2.
4. Determine the search direction,$f^{(i)}$.
5. Evaluate the criterion $J(U^{(i)} + f^{(i)})$ and determine the ratio between actual and predicted decrease in the criterion $r^{(i)}$:

$$r^{(i)} = 2\frac{J(U^{(i)}) - J(U^{(i)} + f^{(i)})}{\lambda(f^{(i)})^T f^{(i)} - (f^{(i)})^T G[U^{(i)}]} \tag{6.9}$$

6. if $r^{(i)} > 0.75$ then Reduce λ, $\lambda = \lambda/2$ and go to 2.
7. if $r^{(i)} < 0.25$ then Increase λ, $\lambda = 2\lambda$
8. if $r^{(i)} > 0$ then $U^{(i+1)} = U^{(i)} + f^{(i)}$, $i = i + 1$
9. If stopping criteria: $U^{(i)} - U^{(i-1)} < \delta$ or i>maxiter is not satisfied, go to 2.
10. Otherwise, accept the current iterate as the sequence of future optimal control signal, U^*, and end the iteration.

view that the Levenberg Marquardt method require vast cost in the complex calculation of the Hessian or Jocabian matrices, the Particle swarm optimization (PSO) method is more appropriate to reduce the computation load.

6.4.2 Particle swarm optimization

The PSO heuristic search method is applied to perform the nonlinear optimization in NNMPC to enhance the convergence and accuracy. The PSO a heuristic search method that was developed by Kennedy and Eberhart (1995) [209], conceptually based on social behavior of flocks of birds, while attempting to simulate the motion of swarms of birds, investigating the notion of collective intelligence in biological populations.

- The particle flies towards a position with a velocity at each time step, which depends

on its own previous best position or solution x_{pbest} and the position of the best of its neighbors

- The best value of all the particles in the swarm called x_{gbest}
- The quality of a particle position depends on a specific objective function (fitness).
- The swarm contain of $p_i(k)$ particle which it position denotes $x_i(k)$, where the position for each particle changes by adding a velocity $v_i(k)$ to the current position [209] [210] [211].

The update of each particle and its velocity is accomplished by the following relations as shown in Figure 6.3 [212].

$$v_i(k+1) = \chi[\omega_j * v_i(k) + c_1 \cdot r_1(x_{pbest} - x_i(k)) + c_2 \cdot r_2(x_{gbest} - x_i(k))] \tag{6.10}$$

$$\chi = \frac{2k}{\left|2 - \Phi - \sqrt{\Phi^2 - 4\Phi}\right|} \quad \text{avec} \quad \begin{cases} 0 \leqslant k \leqslant 1, \\ \Phi = \Phi_1 + \Phi_2 \geqslant 4, \\ k = 1, \ \Phi_1 = \Phi_2 = 2.05 \end{cases} \tag{6.11}$$

$$x_i(k+1) = x_i(k) + v_i(k+1) \tag{6.12}$$

Where:

- $c1 > 0, c2 > 0$: represent cognitive and social components respectively that means how much the particle is directed towards good positions
- $r1, r2$ are the uniform distribution numbers in the range [0,1];
- ω_j is an inertia weight, determining how much of the previous velocity of the particle is preserved,
- χ: is the constriction coefficient.

Each particles position in the swarm represents a solution to the MPC optimization problem, i.e the inclusion of the control sequence over the control horizon. The effectiveness of each solution (particle) is calculated through the considered cost function of the MPC

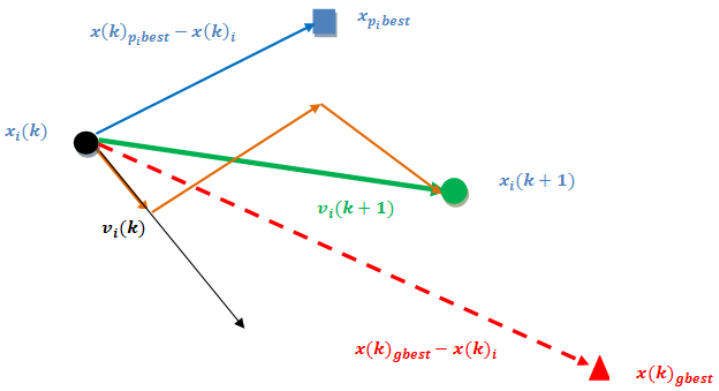

Figure 6.3: Updating the position and the velocity.

controller see equation (6.3). Where :

- The constraints over the control signal can be implemented by limiting the search space of PSO $x(k) \in [x_{min}, x_{max}]$
- The constraints over the control signal variation

can be represented as follows:

$$v_i(k) = \begin{cases} v_i(k) & if v_i(k) \leqslant V_{max} \\ V_{max} & if v_i(k) > V_{max} \end{cases}$$

where V_{max} is the maximum allowable control variation for the control element [213] [212] [214] [215] [216]

6.4.3 Genetic Algorithm (GA)

The Genetic Algorithm (GA) is a non-deterministic, iterative, heuristic optimization technique inspired by Darwinian evolution. It solves problems by imitating natural evolutionary processes. In the context of MPC, the fitness function used by the optimizer is defined by the objective or cost function [217, 218].

GA starts with an initial population of chromosomes, each representing a possible solution to the optimization problem. New generations are produced using genetic operators such as selection, crossover, and mutation.

The algorithm terminates after a predefined maximum number of generations or when

the allowed computation time has elapsed [219–223].

The algorithm proceeds according to the following steps:

1. **Initial population generation**: A number of individual solutions are randomly generated to form the initial population. The population size N_{ind}, typically set by the user, is an important factor that affects the scalability and performance of the algorithm.

   Encoding: An individual s_i, representing a candidate solution, is defined as a sequence of control inputs with the following structure:

$$s_i = [u(k), u(k+1), \ldots, u(k+N_u-1)]$$

2. **Fitness function evaluation**: The objective function provides a measure of how well individuals perform in the problem domain. In the MPC problem, the fittest individuals are those with the lowest numerical value of the objective function given in equation (6.3).

3. **Selection operation**: The goal of selection is to choose the fittest individuals from the current population to generate offspring for the next generation.

4. **Crossover (recombination) operation**: For each chromosome s_i, a random number r is generated. If r is less than the crossover probability P_c, crossover is performed; otherwise, the chromosome remains unchanged [221, 224]. Assuming that crossover is applied to two parent chromosomes s_i and s_{i+1} at position z, the operation can be represented as:

$$\begin{aligned}
s_i &= [u_i(k), \ldots, u_i(k+z-1) \mid u_i(k+z), \ldots, u_i(k+N_u-1)] \\
s_{i+1} &= [u_{i+1}(k), \ldots, u_{i+1}(k+z-1) \mid u_{i+1}(k+z), \ldots, u_{i+1}(k+N_u-1)] \\
&\Downarrow \textbf{Crossover operation} \\
s_i^{\text{new}} &= [u_i(k), \ldots, u_i(k+z-1) \mid u_{i+1}(k+z), \ldots, u_{i+1}(k+N_u-1)] \\
s_{i+1}^{\text{new}} &= [u_{i+1}(k), \ldots, u_{i+1}(k+z-1) \mid u_i(k+z), \ldots, u_i(k+N_u-1)] \quad (6.13)
\end{aligned}$$

5. **Mutation operation**: Mutation introduces random changes to parts of the offspring with a low probability P_m, typically ranging from 0.001 to 0.01. It modifies elements in the chromosomes generated by crossover and helps prevent the algorithm from getting trapped in local optima.

6.5 Results

In this section, the proposed control scheme is tested and compared with the PI controller as specified in BSM1. In order to get the simulation of BSM1 The ordinary differential equations for describing activated sludge reactions and the clarifier were completed by C-program in S-function of SIMULINK with MATLAB version R2015a, and run on a PC with a clock speed of 2.90 GHz and 4 GB RAM, in a Microsoft Windows 10.0 environment.

Since disturbances play an important role in the evaluation of controller performances, influent disturbances are defined for dry-weather conditions which diurnal variations and weekly trends (lower peaks in weekend data) are also depicted by these data as shown in Figure 6.4

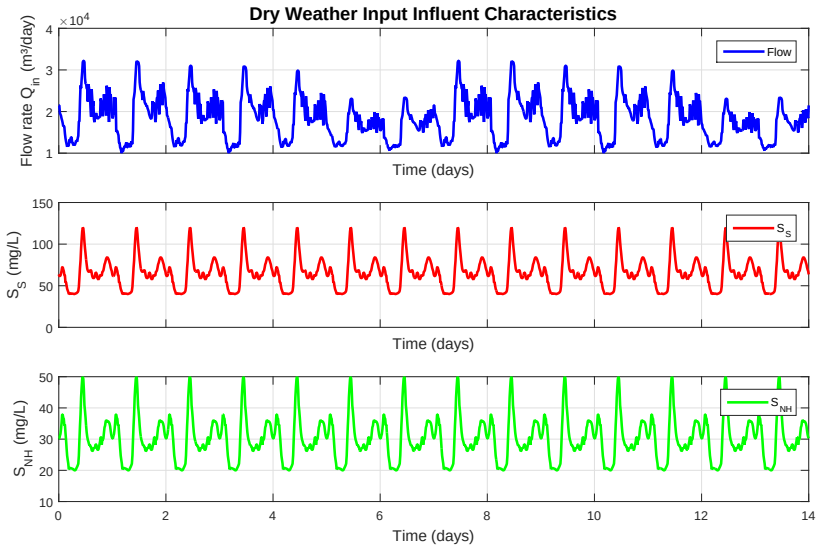

Figure 6.4: Dry weather input influent characteristics.

The BSM1 model consist of thirteen states defined in vector as follows:

$$[S_I, S_S, X_I, X_S, X_{BH}, X_{BA}, X_P, S_O, S_{NO}, S_{NH}, S_{ND}, X_{ND}, S_{ALK}] \tag{6.14}$$

The main goal of the control is to maintain the dissolved oxygen concentration at the $2mg/l$ level by manipulation of the oxygen transfer coefficient KLa_5 in the last compartment. The efficiency of NNMPC algorithm in the WWTPs is validated by comparison with the baseline PI controller.

6.5.1 The PI controller

The PI controller parameters are set as $kp = 150$, $ki = 1000$, respectively, which is the default setting in the benchmark BSM1. The simulation result obtained with PI controller on real time is presented in Figure 6.5. The dissolved oxygen concentration response is

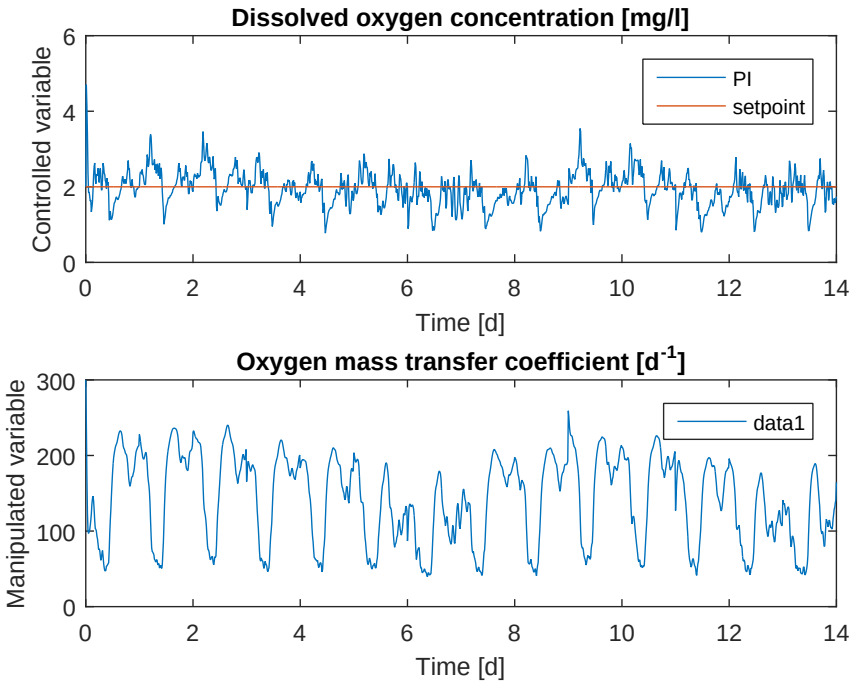

Figure 6.5: the dissolved oxygen concentration response and the manipulated input u_{Kla_5} with PI conroller.

trying to maintain the desired set-point but the result of the regulation with PI controller is bad.

6.5.2 The NNMPC controller

The proposed predictive control scheme is implemented using a Neural Network NNARX model as discussed in section 6.3.2.2

6.5.2.1 The NNARX model

- The selected optimal architecture of NNARX model corresponds to multilayer perceptron with five neurons in hidden layer of the hyperbolic tangent transfer function and one linear unit for the output layer.
- The order of the line memories are selected as follwing:

  $(nu = 2)$ past control input $u(k) = [u_{kla_5}]^T$.

  $(ny = 2)$ for past output $y(k) = [y_{s_o}(k)]^T$.
- The training algorithm for adjust The weights and bias values of the NNARX model is Levernberg-Marquardt back-propagation algorithm.

The response of the trained NNARX model and the plant are presented in Figure 6.6. The result from the system identification depicted in Figure 6.6 show the predicted value

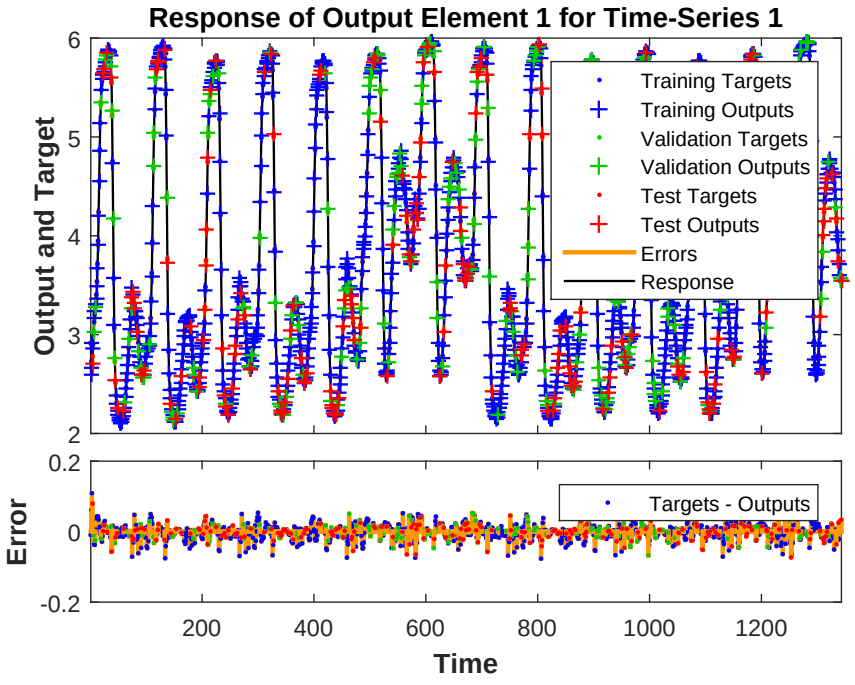

Figure 6.6: The response of the analytic model of the biological wastewater plant and the trained NNARX model.

are very close to the true value and low estimation error. The identified NNARX structure is chosen for their excellent one-step-ahead approximation to estimate with accuracy the prediction values of dissolved oxygen in a future time horizon N_y needed for the NNMPC.

6.5.2.2 The tuning parameters of NNARX-MPC

The controller tuning parameters are chosen as follows:

- The prediction horizon $Ny = 7$
- The control horizon $Nu = 2$
- The penalty factor on difference control signal $\delta = 0.9$

Minimization of the NNARX-MPC cost function is done using a Newton based Levenberg-Marquardt algorithm with its parameters are chosen as :

- The learning rate $\lambda = 0.1$
- The stopping criteria $\delta = 1e^(- 4)$
- The initial control input $u(k) = 143[d^{-1}]$

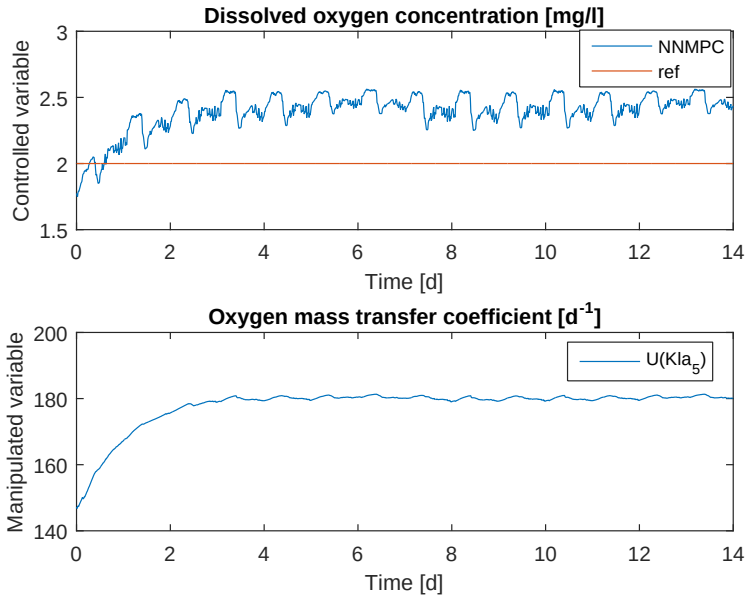

Figure 6.7: The dissolved oxygen concentration response and the manipulated input u_{Kla5} with NNARX-MPC controller.

The simulation obtained with the proposed advance NNARX-MPC is shown in Figure 6.7. NNARX-MPC control system has the best control effect in the WWTPs. So as to exhibit the advantages of the NNARX-MPC controller compared to the PI, we are used the evaluation criteria for the control schemes namely:

- **Integral Square Error (ISE)**:

$$\mathrm{ISE} = \int_{t=1}^{t=14} e^2(t)\,\mathrm{d}t \tag{6.15}$$

- **Integral Absolute Error (IAE)**:

$$\mathrm{IAE} = \int_{t=1}^{t=14} |e(t)|\,\mathrm{d}t \tag{6.16}$$

- **Maximum Deviation (MaxDev)**:

$$\mathrm{MaxDev} = \max |e(t)| \tag{6.17}$$

where $e(t)$ represents the output error between the measured controlled dissolved oxygen (DO) value and the desired or reference signal.

Table 6.1: Evaluation of NNARX-MPC and PI Controllers Based on Performance Criteria.

Controller	**IAE**	**ISE**	**MaxDev**
PI	5.0050	2.9850	2.7012
NNARX-MPC	4.8900	2.4529	0.5636

Furthermore, a detailed comparison of performance criteria for both control schemes is shown in Table 6.1. It is observed that the NNARX-MPC controller performs better than the PI controller. The values of IAE, ISE, and MaxDev obtained for the NNARX-MPC are the smallest, indicating higher control accuracy and improved dynamic performance. As illustrated in Figure 6.8, the output error range of the NNARX-MPC based on the LevenbergMarquardt (LM) optimization method is narrower than that of the PI controller, which confirms that the NNARX-MPC ensures more precise tracking of the desired dissolved oxygen (DO) concentration. This improved precision means that the NNARX-MPC can maintain the DO level closer to its reference value with smaller de-

viations and faster convergence, which is particularly important for maintaining optimal biological activity in wastewater treatment processes. In order to improve the perfor-

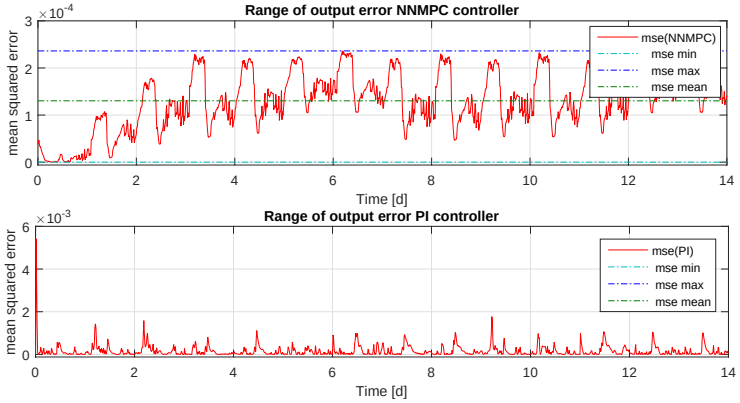

Figure 6.8: The range of regulation errors of NNARXMPC and PI controller.

mance for NNARX-MPC controller, two metaheuristics optimization methods, PSO and GA, are investigated to deal with the associated multi-objective optimization problem.

6.5.3 The PSO optimization method for NNARXMPC controller

Particle Swarm Optimization (PSO) is a well established algorithm and is often cited in the literature and reported to have been applied to solve many control problems. Here, we apply PSO algorithm to find optimal solutions for the NNARX-MPC controller. In the design, we use the control parameters of table 6.2, were derived empirically through successive simulations.

The response of DO with the Manipulated variable $u[KLa_5]$ of PSO NNARX MPC controller based on PSO optimization algorithm is presented in Figure 6.9, it can be seen that the proposed controller is able successfully to correct the evolution of the output and to track smoothly the set point most of the time.

6.5.4 The GA optimization method for NNARXMPC controller

Genetic algorithms (GA) are a well-known optimization technique in solving many practical problems. We will use this technique for NNARX-MPC controller. An appropriate choice of the parameters affects the speed of the convergence of GA. The basic

Table 6.2: PSO parameters used in NNARX-MPC controller.

Parameter	**Value**
Number of Decision Variables N_u	10
Lower control signal constraint $x_{\min}$	155
Upper control signal constraint $x_{\max}$	160
Prediction step k	1
ϕ_1 (Cognitive coefficient)	2.05
ϕ_2 (Social coefficient)	2.05
$\Phi = \phi_1 + \phi_2$	4.10
Constriction factor χ	Computed based on $\Phi = 2.1$
Population Size	50
Number of Iterations	10
Cognitive Acceleration Coefficient	$\chi \cdot \phi_1$
Social Acceleration Coefficient	$\chi \cdot \phi_2$
Max Velocity $v_i(k) = \Delta U_{\max}$	$0.4 \cdot (x_{\max} - x_{\min})$
Min Velocity $\Delta U_{\min}$	0

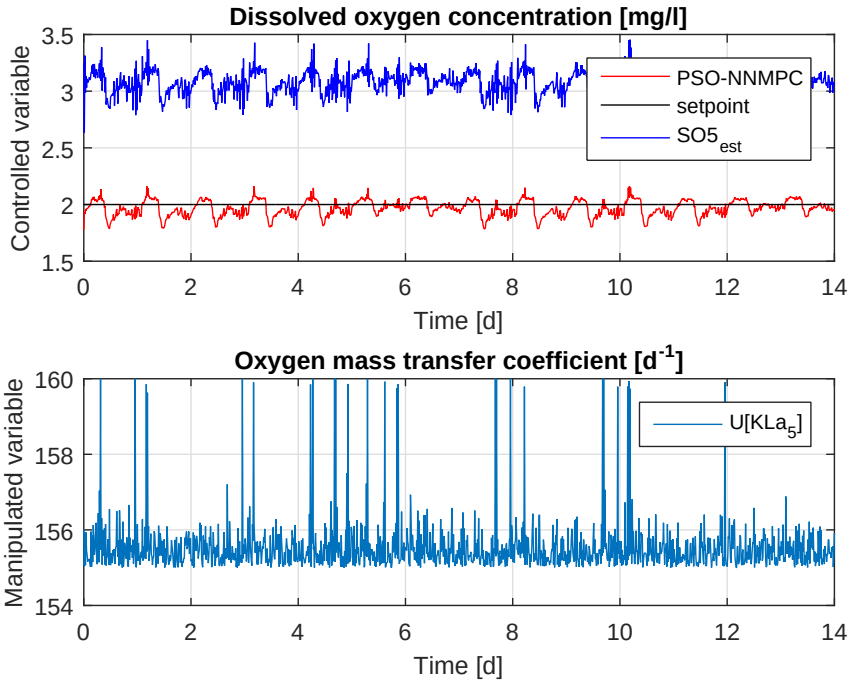

Figure 6.9: The dissolved oxygen concentration response and the manipulated input u_{Kla_5} with PSO-NNMPC-controller.

binary encode with tournament selection was used. The parameters required to be specified in Table 6.3

As illustrated in Figure 6.10 the simulations of the proposed GA-NNMPC controller with genetic algorithm optimization can track the reference signal reasonably good under

Table 6.3: Genetic Algorithm parameters used in controller optimization.

Parameter	**Value**
Number of Decision Variables N_u	2
Lower control signal constraint	150
Upper control signal constraint	155
Crossover rate	0.8
Mutation rate	0.01
Population Size	30
Number of Iterations	15

the defined constraints.

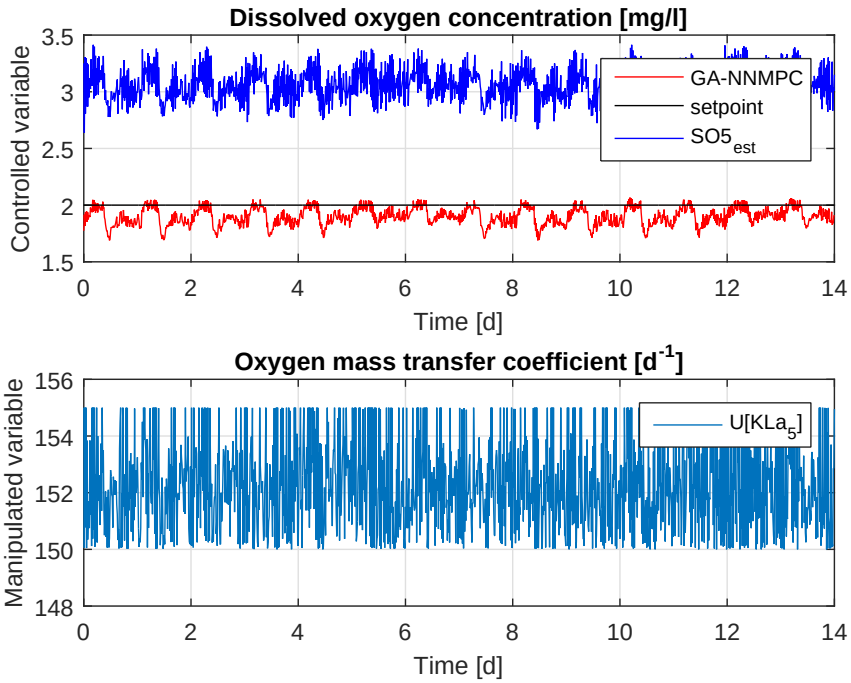

Figure 6.10: Dissolved oxygen concentration.GA-NNMPC-controlled process response in aeration tank 5.

The comparative analysis is based upon various performance measures such as execution time, real-time implementation feasibility, and the control performance (ISE, IAE) are compared. Table 6.4 indicates that the execution time of the PSO-NNMPC algorithm works tow times faster than that of GA-NNMPC algorithm.

Moreover, the performances of controller ISE and IAE of PSO-NNMPC are lower than those of GA-NNMPC and LM-NNMPC as are depicted in table 6.5. It can be concluded that the PSO-NNMPC strategy can realize satisfied optimization performance and high-

Table 6.4: Execution time for PSO-MPC, GA-MPC and LM-MPC controllers

Controllers	**Elapsed Time [s]**
PSO-NNMPC	685.321
GA-NNMPC	1364.772
LM-NNMPC	111.893

accuracy tracking control.

Table 6.5: Performance Comparison of NNMPC Controllers

Controller	**IAE**	**ISE**	**MaxDev**
PSO-NNMPC	0.8823	0.0820	0.2258
GA-NNMPC	1.5001	0.2288	0.3106
LM-NNMPC	4.8900	2.4529	0.5636

6.6 The proposed architecture of active fault tolerant control

The goal of this section is to develop a novel Fault-Tolerant Control (FTC) strategy based on robust fault estimation and compensation of a sensor fault (f_s), in order to maintain the performance and stability of the baseline (nominal) control system under both faulty and fault-free conditions. The proposed FTC scheme is based on a combination of:

- (a) robust control design, and
- (b) independent estimation of the sensor fault.

The controller must be robust to expected sensor fault estimation errors as well as to a bounded reference signal. As shown in the architecture in Figure 6.11, the scheme incorporates dedicated unknown input estimation observers, as described in Equation 5.15, which were synthesized in the previous chapter. These observers are designed to ensure accurate estimation and effective compensation of the sensor fault. This section also introduces a Dynamic Output Feedback Controller (DOFC) that serves as the robust baseline controller. Furthermore, it develops the theoretical framework for applying the proposed FTC strategy to nonlinear systems described by the model in Equation 5.52.

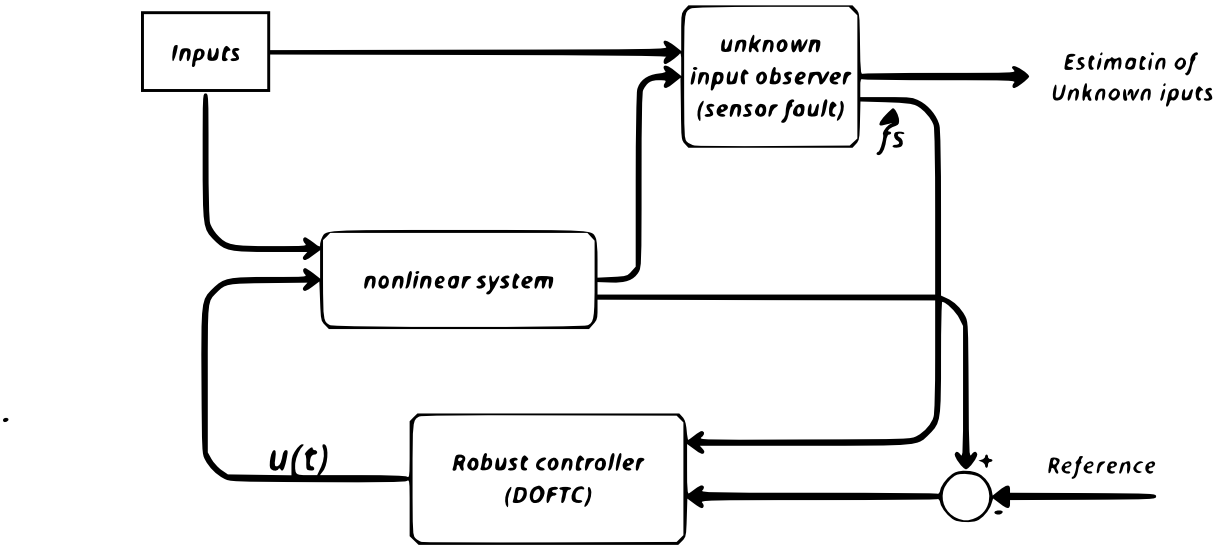

Figure 6.11: Proposed active dynamic output feedback fault tolerant controller DOFFTC system architecture

Remark 6.6.1. In the literature, most FTC strategies assume constant fault signals (i.e, $\dot{f}(t) = 0$) [225] [226] [227].

This work proposes an **Active FTC (AFTC)** system that overcomes this limitation by accommodating *time-varying faults*, thereby addressing a broader class of practical fault scenarios.

Lemma 6.6.2. *Given a scalar $\mu > 0$ and symmetric positive definite (SPD) matrix $G \succ 0$, the following inequality holds for any matrices R and X of compatible dimensions:*

$$X^{\mathsf{T}}R + R^{\mathsf{T}}X \preceq X^{\mathsf{T}}GX + R^{\mathsf{T}}G^{-1}R \tag{6.18}$$

Lemma 6.6.3. *Given $\mu > 0$ and $G \succ 0$, $\forall R, X \in \mathbb{R}^{n\times m}$:*

$$X^{\top}R + R^{\top}X \preceq \mu X^{\top}GX + \mu^{-1}R^{\top}G^{-1}R$$

6.7 Problem Formulation and Preliminary Results

The control objective is to synthesize a Dynamic Output Feedback Controller (DOFC) that guarantees the output of the nonlinear LPV plant tracks a bounded time-varying reference signal, under both fault-free and faulty operating conditions. To achieve this goal, an augmented system is constructed, consisting of : The original plant dynamics, as

given in Equation 5.52:

$$\begin{cases} \dot{x} = A_x\big(\rho(t)\big)x + A_\mu\mu + B_\sigma\sigma(x,\mu,u) + G_\varrho\big(\rho(t)\big)\varrho(y,u) + D_x\omega \\ y = C_x x + C_\mu\mu + B_\varsigma\varsigma(x,\mu,u) + \bar{D}_y\omega \end{cases} \tag{6.19}$$

where : $x \in \mathbb{R}^n$ is the state vector, $u \in \mathbb{R}^m$ is the control input vector, $y \in \mathbb{R}^l$ is the output vector, $\mu \in \mathbb{R}^{n_\mu}$ represents unknown inputs, $A_x \in \mathbb{R}^{n\times n}$, $G_\varrho \in \mathbb{R}^{n\times m}$, $C_x \in \mathbb{R}^{l\times n}$, $C_\mu \in \mathbb{R}^{l\times n_\mu}$. The integral of the tracking error is defined as:

$$\dot{e}(t) = y_r(t) - y(t) \Rightarrow e_{tr}(t) = \int (y_r(t) - Sy(t))\, dt \tag{6.20}$$

where $S \in \mathbb{R}^{q\times l}$ is the output selection matrix that determines which plant outputs track the reference signal (q being the number of regulated outputs). Substituting the plant output into Equation 6.20 yields:

$$e_{tr}(t) = y_r(t) - S\left(C_x x + C_\mu\mu + B_\varsigma\varsigma(x,\mu,u) + \bar{D}_y\omega\right) \tag{6.21}$$

The augmented system, composed of the original system in Equation 5.52 and the integral of the tracking error, is then defined as follows:

$$\begin{cases} \bar{\dot{x}} &= \bar{A}_x\big(\rho(t)\big)x + \bar{A}_\mu\mu + \bar{B}_\sigma\sigma\big(x,\mu,u\big) + \bar{G}_\varrho\big(\rho(t)\big)\varrho\big(y,u\big) + \bar{D}_x\omega \\ \bar{y} &= \bar{C}_x x + \bar{C}_\mu\mu + \bar{B}_\varsigma\varsigma\big(x,\mu,u\big) + \bar{D}_y\omega \end{cases} \tag{6.22}$$

Where the augmented state vector is given by $\overline{x} = \begin{bmatrix} e_{tr} \\ x \end{bmatrix}$ and:

$$\overline{A}(\rho) = \begin{bmatrix} 0 & -SC_x \\ 0 & A_x(\rho) \end{bmatrix}, \quad \overline{A_\mu}(\rho) = \begin{bmatrix} -SC_\mu \\ A_\mu(\rho) \end{bmatrix}, \quad \overline{G}_\varrho(\rho) = \begin{bmatrix} 0 \\ G(\rho) \end{bmatrix}, \quad \overline{B}_\sigma = \begin{bmatrix} 0 \\ B_f \end{bmatrix}$$

$$R = \begin{bmatrix} -I \\ 0 \end{bmatrix}, \quad D_x = \begin{bmatrix} -SD_y \\ D_x \end{bmatrix}, \quad \overline{C} = \begin{bmatrix} I & 0 \\ 0 & C_x \end{bmatrix}, \quad \overline{C}_\mu(\rho) = \begin{bmatrix} 0 \\ C_\mu(\rho) \end{bmatrix}$$

$$\overline{D}_y = \begin{bmatrix} 0 \\ D_y \end{bmatrix}$$

As the system in Equation 6.22 has a common output matrix C, the tracking and stabilization are achieved using a quadratically parametrized Dynamic Output Feedback Controller, defined as :

$$\begin{cases} \dot{x}_c(\rho) = A_c(\rho)x_c(\rho) + B_c(\rho)(\bar{y} - S_r y_r), \\ \quad u = C_c(\rho)x_c(\rho) + D_c(\rho)(\bar{y} - S_r y_r) - F\mu(\rho) \end{cases} \tag{6.23}$$

where x_c denotes the controller state, $A_c(p) \in \mathbb{R}^{(n+q)\times(n+q)}$, $B_c(p) \in \mathbb{R}^{(n+q)\times(l+q)}$, $C_c(p) \in \mathbb{R}^{m\times(n+q)}$, and $D_c(p) \in \mathbb{R}^{m\times(l+q)}$ represent the parameter-dependent controller matrices. The matrices $R \in \mathbb{R}^{(n+q)\times q}$ and $F \in \mathbb{R}^{(n+q)\times\mu}$ are design parameters, while $S_r \in \mathbb{R}^{(l+q)\times q}$ is introduced to ensure dimensional compatibility between y_r and $\bar{y}$. Aggregation of Equations 6.22 and 6.23 gives the following system :

$$\begin{cases} \dot{x}_a = A_a(\rho)x_a + E_a(\rho)d + \bar{B}_f f(x_a, \mu, u) \\ y_a = C_a x_a + D_a d \end{cases} \tag{6.24}$$

The augmented system matrices are defined as:

$$A_a(\rho) = \begin{bmatrix} \bar{A}(\rho) + \bar{G}_\rho(\rho) D_c(\rho) \bar{C}_x & \bar{G}_\rho(\rho) C_c(\rho) \\ B_c(\rho) \bar{C}_x & A_c(\rho) \end{bmatrix}, \tag{6.25}$$

$$E_a = \begin{bmatrix} \bar{A}_\mu + \bar{G}_\rho(\rho) D_c(\rho) \bar{C}_\mu - \bar{G}_\rho(\rho) F & R - \bar{G}_\rho(\rho) D_c(\rho) S_r & \bar{D}_x + \bar{G}_\rho(\rho) D_c(\rho) \bar{D}_y \\ B_c(\rho) \bar{C}_\mu & -B_c(\rho) S_r & B_c(\rho) \bar{D}_y \end{bmatrix}, \tag{6.26}$$

$$x_a = \begin{bmatrix} \bar{x} \\ x_c \end{bmatrix}, \quad \bar{B}_f(x_a, \mu, u) = \begin{bmatrix} \bar{B}_\sigma \\ 0 \end{bmatrix}, \quad \bar{d} = \begin{bmatrix} \mu \\ y_r \\ w \end{bmatrix}, \tag{6.27}$$

$$C_a = \begin{bmatrix} \bar{C} & 0 \end{bmatrix}, \quad D_a = \begin{bmatrix} \bar{C}_\mu & 0 & \bar{D}_y \end{bmatrix} \tag{6.28}$$

where: $n_a = n+q+n_c$, $A_a(\rho) \in \mathbb{R}^{n_a \times n_a}$ is the augmented state matrix, $E_a \in \mathbb{R}^{(n_a) \times (n_\mu + q + n_w)}$ is the disturbance input matrix, $d \in \mathbb{R}^{n_\mu + q + n_w}$ aggregates sensor fault, reference and disturbance.

Theorem 6.7.1. *Consider the closed-loop system described by Equation 6.24, the closed-loop system achieves tracking of the reference signal with a guaranteed $\mathcal{H}_\infty$ performance with an attenuation level γ_m, provided the augmented disturbance signal d is bounded, if there exist symmetric positive definite (SPD) matrices X, Y, and matrices $A_c(\rho)$, $B_c(\rho)$, $D_c(\rho)$, $C_c(\rho)$, such that the following LMI constraint is satisfied:*

$$\min(\gamma_c) \quad \textit{subject to} \tag{6.29}$$

$$LMI = \begin{bmatrix} (1,1) & \Pi_2^T B_f(\rho) & \Pi_1^T Hi & \Pi_2^T E_a & \Pi_1^T C_a^T & -\Pi_1^T C_a^T & \mathbf{0} \\ * & -\delta^{-1} I & \mathbf{0} & \mathbf{0} & \mathbf{0} & \mathbf{0} & J^T \\ * & * & -\delta^{-1} I & \mathbf{0} & \mathbf{0} & \mathbf{0} & \mathbf{0} \\ * & * & * & J^T J - \gamma_c^2 I & \mathbf{0} & \mathbf{0} & \mathbf{0} \\ * & * & * & * & -I_{n+q} & \mathbf{0} & \mathbf{0} \\ * & * & * & * & * & -g^{-1} I_{n+q} & \mathbf{0} \\ * & * & * & * & * & * & -g I_{n+q} \end{bmatrix} \prec 0 \tag{6.30}$$

where:

$$(1,1) = \Pi_1^T A_a^T \Pi_2 + \Pi_2^T A_a \Pi_1 = \begin{bmatrix} \bar{A}X + X^T \bar{A}^T + \hat{C}^\top \bar{G}_f^T + \bar{G}_f \hat{C} & \hat{A}^\top + \bar{A} + \bar{G}_f D_c \bar{C}_x \\ \hat{A} + \bar{A}^T + \bar{C}_x^T D_c^T \bar{G}_f^T & \bar{A}^T Y + Y^T \bar{A} + \bar{C}_x^T \hat{B}^T + \hat{B} \bar{C}_x \end{bmatrix} \tag{6.31}$$

$$\Pi_1^T Hi = \begin{bmatrix} XHi \\ Hi \end{bmatrix} \tag{6.32}$$

$$\Pi_1^T C_a^T = \begin{bmatrix} X\overline{C}^T \\ \overline{C}^T \end{bmatrix} \tag{6.33}$$

$$\Pi_2^T E_a = \begin{bmatrix} \bar{A}_\mu + \bar{G}_f D_c(\rho) \bar{C}_\mu - \bar{G}_f F & R - \bar{G}_f D_c(\rho) S_r & \bar{D}_x + \bar{G}_f D_c(\rho) \bar{D}_y \\ Y^T \bar{A}_\mu + \hat{B} \bar{C}_\mu - Y^T \bar{G}_f F & Y^T R - \hat{B} S_r & Y^T \bar{D}_x + \hat{B} \bar{D}_y \end{bmatrix} \tag{6.34}$$

$$\Pi_2^T B_f = \begin{bmatrix} \bar{B}_f \\ Y \bar{B}_f \end{bmatrix} \tag{6.35}$$

$$J = (D_a - E_r)^T \tag{6.36}$$

The controller gains are thus calculated as follows:

$$D_c(\rho) = \hat{D}(\rho) \tag{6.37}$$

$$C_c(\rho) = (\hat{C} - D_c\bar{C}_x X)(M^T)^{-1} \tag{6.38}$$

$$B_c(\rho) = N^{-1}(\hat{B} - Y^T\bar{G}_f D_c) \tag{6.39}$$

$$A_c(\rho) = N^{-1}\Big(\hat{A} - Y^T(\bar{A} + \bar{G}_f D_c\bar{C}_x)X + NB_c(\rho)\bar{C}_x X + Y^T\bar{G}_f C_c(\rho)M^T\Big)(M^T)^{-1} \tag{6.40}$$

M and N satisfy $MN^T = I - XY^T$

Proof. : Following the $\mathcal{H}_\infty$ performance specification, the controller's robustness against augmented disturbance inputs d is quantified through minimization of the following performance criterion:

$$\frac{\|e_{tr}\|_2}{\|d\|_2} \leq \gamma_c \quad \text{(Performance specification)} \tag{6.41}$$

$$J = e_{tr}^T e_{tr} - \gamma_c^2 d^T d \leq 0 \quad \text{(Cost function)} \tag{6.42}$$

where the performance output $e_{tr} = y_a - S_r y_r$ satisfies:

$$\begin{aligned} e_{tr}^T e_{tr} = {} & x_a^T C_a^T C_a x_a + x_a^T C_a^T D_a d + d^T D_a^T C_a x_a \\ & + d^T D_a^T D_a d - x_a^T C_a^T E_r d - d^T D_a^T E_r d \\ & - d^T E_r^T C_a x_a - d^T E_r^T D_a d + d^T E_r E_r^T d \end{aligned} \tag{6.43}$$

With, the disturbance vector d and reference shaping matrix E_r are defined as:

$$d = \begin{bmatrix} \mu \\ y_r \\ w \end{bmatrix}, \qquad E_r = \begin{bmatrix} 0 & S_r & 0 \end{bmatrix} \tag{6.44}$$

Thus

$$\begin{aligned} J = {} & x_a^\intercal C_a^\intercal C_a x_a + x_a^\intercal [C_a^\intercal D_a - C_a^\intercal E_r] d \\ & + d^\intercal [D_a^\intercal C_a - E_r^\intercal C_a] x_a \\ & + d^\intercal [E_r E_r^\intercal + D_a^\intercal D_a - E_r^\intercal D_a - D_a^\intercal E_r - \gamma_c^2 I] d \end{aligned} \tag{6.45}$$

Then

$$J = \begin{bmatrix} x_a \\ d \end{bmatrix}^{\mathsf{T}} \begin{bmatrix} C_a^{\mathsf{T}} C_a & C_a^{\mathsf{T}} D_a - C_a^{\mathsf{T}} E_r \\ D_a^{\mathsf{T}} C_a - E_r^{\mathsf{T}} C_a & E_r E_r^{\mathsf{T}} + D_a^{\mathsf{T}} D_a - E_r^{\mathsf{T}} D_a - D_a^{\mathsf{T}} E_r - \gamma_c^2 I \end{bmatrix} \begin{bmatrix} x_a \\ d \end{bmatrix} \tag{6.46}$$

where

6.7.0.1 Lyapunov Stability Analysis

Consider the augmented system (6.24) with the Lyapunov function candidate:

$$v(x_a) = x_a^{\mathsf{T}} \bar{P} x_a, \quad \bar{P} \succ 0 \tag{6.47}$$

Performance Criterion

The $\mathcal{H}_\infty$ performance requirement is encoded in:

$$\begin{bmatrix} x_a \\ d \end{bmatrix}^{\mathsf{T}} \begin{bmatrix} C_a^{\mathsf{T}} C_a & C_a^{\mathsf{T}} J \\ J^{\mathsf{T}} C_a & J^{\mathsf{T}} J - \gamma_c^2 I \end{bmatrix} \begin{bmatrix} x_a \\ d \end{bmatrix} < 0 \tag{6.48}$$

where $J = D_a - E_r$ is the performance channel mixing matrix.

Stability Condition

The combined stability and performance requirement gives:

$$\dot{v}(x_a) + e_{tr}^{\mathsf{T}} e_{tr} - \gamma_c^2 d^{\mathsf{T}} d < 0 \tag{6.49}$$

Lyapunov Derivative Analysis : The derivative expands as:

$$\begin{aligned} \dot{v}(x_a) = {} & x_a^{\mathsf{T}} \left(A_a^{\mathsf{T}}(\rho) \bar{P} + \bar{P} A_a(\rho) \right) x_a \\ & + 2 x_a^{\mathsf{T}} \bar{P} \bar{G}_f f(x_a, \mu, u) \\ & + 2 x_a^{\mathsf{T}} \bar{P} E_a(\rho) d \end{aligned} \tag{6.50}$$

The Lipschitz-bounded nonlinear term satisfies:

$$\| f(x_a, \mu, u) \| \leq \| H x_a \| \tag{6.51}$$

where H contains the Lipschitz constants.

Applying Young's inequality with parameter $\delta > 0$ yields:

$$2x_a^\top \bar{P}\bar{G}_f f \leq \delta x_a^\top \bar{P}\bar{G}_f \bar{G}_f^\top \bar{P}x_a + \delta^{-1} f^\top f \tag{6.52}$$

Combining with the Lipschitz condition $f^\top f \leq x_a^\top H^\top H x_a$ gives:

$$2x_a^\top \bar{P}\bar{G}_f f \leq \delta x_a^\top \bar{P}\bar{G}_f \bar{G}_f^\top \bar{P}x_a + \delta^{-1} x_a^\top H^\top H x_a \tag{6.53}$$

6.7.0.2 Matrix Formulation

Substituting (6.53) into (6.50) yields:

$$\begin{bmatrix} x_a \\ d \end{bmatrix}^\mathsf{T} \begin{bmatrix} \Theta_{11} & \bar{P}E_a(\rho) \\ E_a^\mathsf{T}(\rho)\bar{P} & 0 \end{bmatrix} \begin{bmatrix} x_a \\ d \end{bmatrix} \tag{6.54}$$

where $\Theta_{11} = A_a^\mathsf{T}(\rho)\bar{P} + \bar{P}A_a(\rho) + \delta \bar{P}\bar{G}_f\bar{G}_f^\mathsf{T}\bar{P} + \delta^{-1}H_i^\mathsf{T}H_i$. Combining with the performance criterion gives the complete LMI:

$$\begin{bmatrix} \Theta_{11} + C_a^\mathsf{T}C_a & \bar{P}E_a(\rho) + C_a^\mathsf{T}J \\ * & J^\mathsf{T}J - \gamma_c^2 I \end{bmatrix} \prec 0 \tag{6.55}$$

We have the matrix relation:

$$P\begin{bmatrix} X \\ M^\mathsf{T} \end{bmatrix} = \begin{bmatrix} I \\ 0 \end{bmatrix} \Rightarrow P\begin{bmatrix} X & I \\ M^\mathsf{T} & 0 \end{bmatrix} = \begin{bmatrix} I & Y \\ 0 & N^\mathsf{T} \end{bmatrix} \tag{6.56}$$

Define the transformation matrices:

$$\Pi_1 = \begin{bmatrix} X & I \\ M^\mathsf{T} & 0 \end{bmatrix}; \quad \Pi_2 = \begin{bmatrix} I & Y \\ 0 & N^\mathsf{T} \end{bmatrix} \tag{6.57}$$

Based on Lemma 6.18, and the Schur Complement Theorem, inequality 6.55 implies that LMI 6.30.

6.8 Simulation result to WWTP

In this section, we implement our Fault-Tolerant Control (FTC) strategy on a simplified version of the ASM1 model, reduced to five key variables. The objective is to precisely regulate the dissolved oxygen concentration (S_O) at **2 mg/L**, a critical threshold for op-

timizing biological treatment while minimizing energy consumption. The reduced model captures the essential dynamics of the components, while accounting for sensor faults affecting S_O as shown in Figure 6.12. The FTC Dynamic Output Feedback Controller

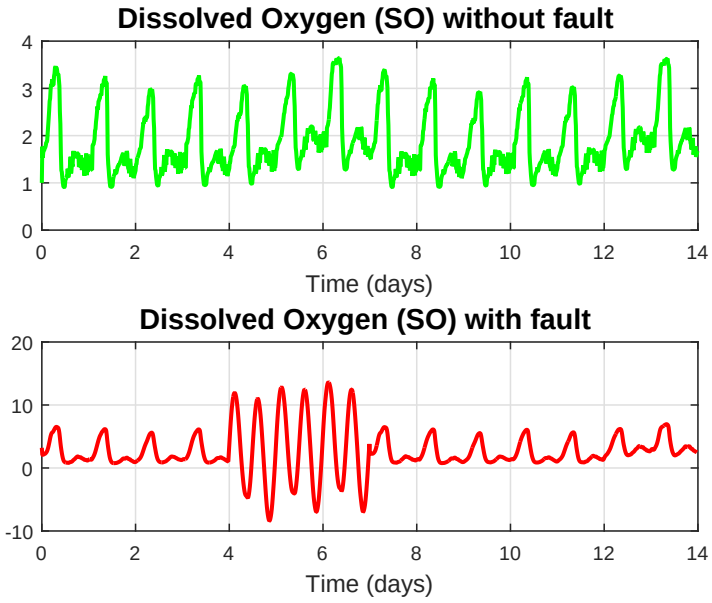

Figure 6.12: Dissolved oxygen measurement (healthy and faulty sensors)

(DOFC), previously developed, is deployed here with : Real-time estimation of additive faults (bias, drift) via an unknown input observer (see Section 5.15), where :

$$\bullet\ \mu = \begin{bmatrix} \rho(t) S_{NO}^{in} & \rho(t) S_{NH}^{in} & d(t) \end{bmatrix}^{\top}$$

Here, $d(t)$ is an unknown input added to the model, in addition to the unknown influent concentrations $S_{\mathrm{NO}}^{\mathrm{in}}$ and $S_{\mathrm{NH}}^{\mathrm{in}}$. We consider that the S_{O} sensor is affected by a fault $d(t)$ defined as:

$$d(t) \triangleq \begin{cases} 10\sin(4\pi t) & \text{if } 4 < t < 7 \\ 0 & \text{otherwise} \end{cases} \tag{6.58}$$

The model is subjected to process and measurement noise through disturbance matrices D_x and D_y, which inject uniformly random perturbations system dynamics and outputs, respectively.

$$X \sim \mathrm{Uniform}(a, b)$$

By solving the convex optimization problem (5.30) under the LMI constraints (6.30), obtained the following DOFFTC controller matrices:

$$X = \begin{bmatrix} 0 & 0 & 0 & 0 & 0 & 0 \\ 0 & 1.6798 & 0 & 0 & 0 & 0 \\ 0 & 0 & 0 & 0 & 0 & 0 \\ 0 & 0 & 0 & 0 & -0.0009 & 0 \\ 0 & 0 & 0 & -0.0009 & 0.7974 & 0 \\ 0 & 0 & 0 & 0 & 0 & 0.0004 \end{bmatrix} \times 10^8 \tag{6.59}$$

$$Y = 10^8 \times \begin{bmatrix} 1.3703 & 0 & 0 & 0 & 0 & 0 \\ 0 & 0.0047 & 0.0032 & -0.0030 & 0.0143 & 0 \\ 0 & 0.0032 & 0.0122 & -0.0124 & -0.0099 & 0 \\ 0 & -0.0030 & -0.0124 & 0.0125 & 0.0119 & 0 \\ 0 & 0.0143 & -0.0099 & 0.0119 & 0.1499 & 0 \\ 0 & 0 & 0 & 0 & 0 & 0 \end{bmatrix} \tag{6.60}$$

And the optimal value of the disturbance attenuation level is $\gamma_c = 2.0051$.

To run simulation, the system and the controller are initialized, respectively, by :

$$\mathbf{x}_{ci} = [0,\ 0.07,\ 0.01,\ 0.01,\ 0.04,\ 0]$$

After the synthesis process, the state-space matrices of the DOFFTC A_c, B_c, C_c, D_c controller are given as follows.

$$A_c = 10^{12} \times \begin{bmatrix} 0 & 0 & 0 & 0 & 0 & 0 \\ 0 & 0 & 0 & 0 & 0 & 0 \\ 0 & 0 & 0 & 0 & 0 & -0.0002 \\ 0 & 0 & 0 & 0 & 0 & 0.0003 \\ 0 & 0 & -0.0005 & 0 & 0.0014 & 0.0172 \\ 0.0001 & 0 & -0.1173 & 0.0011 & 0.3255 & 4.1007 \end{bmatrix}$$

$$B_c = 10^8 \times \begin{bmatrix} 0 & 0 & 0 & 0 \\ 0 & 0 & 0 & 0 \\ -0.0004 & 0 & 0 & 0 \\ 0.0009 & 0 & -0.0001 & 0 \\ -0.0075 & -0.0024 & 0.0020 & -0.0247 \\ 8.4306 & -0.0096 & -0.0750 & -0.0413 \end{bmatrix}$$

$$C_c = 10^5 \times \begin{bmatrix} 0 & 0 & 0 & 0.0008 & -0.0006 & 0.0003 \\ 0 & 0 & 0.0002 & 0.1738 & -0.1492 & -0.0074 \\ 0 & -0.0001 & 0 & 0 & 0 & 0 \\ 0 & 0 & -0.0347 & 0.0003 & 0.0964 & 1.2150 \end{bmatrix}$$

$$D_c = \begin{bmatrix} 0.1198 & 2.8680 & 9.5199 & 24.0664 \\ 2.8680 & -0.0143 & -0.0353 & 0.0374 \\ 9.5199 & -0.0353 & -0.1202 & -0.3013 \\ 24.0664 & 0.0374 & -0.3013 & -0.1226 \end{bmatrix}$$

The figure 6.13 depicts the system response under a DOFFTC strategy regulating the dissolved oxygen (DO) concentration in the presence of a sensor fault. A sensor fault affecting DO measurement is introduced between days four and seven. Despite this perturbation, the system maintains stable and accurate performance, reflecting the robustness of the control strategy. The tracking error (upper subplot) shows a slight amplitude increase during the fault period, bounded within $\pm 1 * 10^{-3}$ g/l and symmetrically centered around zero, indicating rapid fault detection and compensation without inducing instability. The

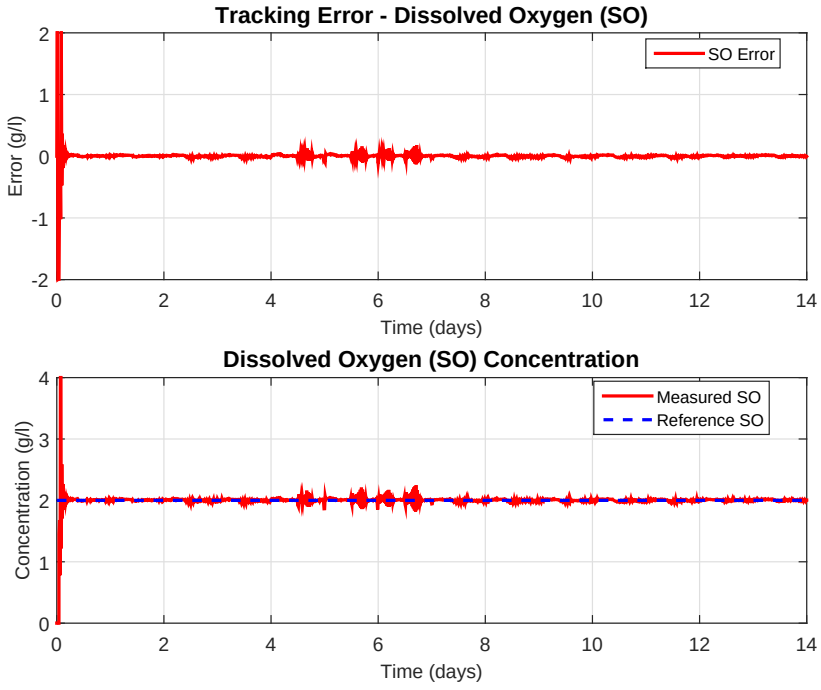

Figure 6.13: System behavior under a sensor fault with dynamic output feedback FTC

lower subplot confirms that the measured DO concentration (red curve) closely follows the reference (dashed blue curve at 2 mg/l), with minimal overshoot and no sustained oscillations, even during the fault. These results demonstrate the DOFFTC strategy's effectiveness in reconfiguring control to ensure accurate reference tracking and minimal

transient error in the presence of sensor faults and disturbances in dynamic and measurement equation system . The figure 6.14 illustrates the temporal evolution of the oxygen

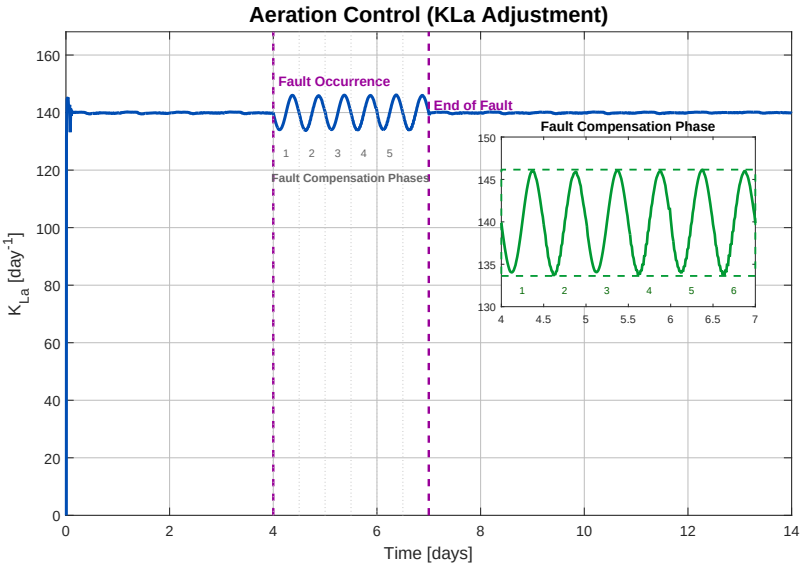

Figure 6.14: DOFFTC Strategy via KLa Manipulation: Simultaneous Sensor Fault Compensation and Aeration Energy Optimization

transfer coefficient K_La, used here as the aeration control signal, within the context of dissolved oxygen regulation under a sensor fault. Three distinct phases can be clearly identified:

Before the fault (Day 0 to Day 4): The control signal remains stable around a nominal value (approximately 140 day^{-1}), reflecting the proper functioning of the system in steady-state conditions without disturbances.

During the fault (Day 4 to Day 7): From Day 4, a sensor fault is introduced into the system, affecting the measurement of dissolved oxygen. In response, the K_La signal becomes oscillatory and shows significant periodic variations around the nominal value. This dynamic behavior indicates the activation of the fault compensation mechanism embedded in the dynamic feedback control law. The controller detects an inconsistency between the measured output and the expected dynamics, and reacts by adjusting the aeration rate (through K_La) to maintain the actual oxygen concentration close to the setpoint of 2 mg/L, despite the erroneous measurement. The oscillations in the control signal result from the bias correction effort, which is typical of an additive fault compen-

sation strategy where a corrective term is dynamically introduced to cancel out the sensor fault effect.

After the fault (After Day 7): Once the fault is resolved, the system quickly returns to a stabilized control regime, with the $K_L a$ signal returning to its baseline level. This demonstrates the reversibility of the compensation mechanism and the resilience of the controller.

The inset (zoomed view between Day 4 and Day 7) allows a closer observation of the compensation phase. It shows regular oscillations, indicating an adaptive control mechanism in action, adjusting the aeration rate in real time to cope with the uncertainty introduced by the fault.
Simulation results confirm the effectiveness of the proposed DOF-FTC strategy in regulating the dissolved oxygen concentration (S_O) within a tight range of ± 2 mg/L around the setpoint, despite the presence of sensor faults and external disturbances.

These results validate the proposed controller, which ensures:

- **Active compensation** via adjustment of the oxygen transfer coefficient (KLa),
- **Robustness** against hydraulic and organic load variations,
- Prevention of energy overconsumption (linked to excessive aeration),
- Protection against biological performance degradation (due to under-oxygenation).

The results highlight the method's compatibility with wastewater treatment plant operational constraints while providing a reproducible framework for more complex models.

6.9 conclusion

This chapter explored an advanced approach to dissolved oxygen (DO) regulation in wastewater treatment plant. I independently implemented a neural network-based model predictive control (NNMPC) as well as an active fault-tolerant control (FTC) strategy, with the aim of ensuring accurate DO regulation while minimizing energy costs associ-

ated with aeration, represented by the volumetric oxygen transfer coefficient K_{La}. The study allowed me to compare several variants of intelligent controllers and to assess their performance under both normal conditions and in the presence of faults. The results first highlighted the limitations of the conventional PI controller, which, although providing a certain level of stability, remained inefficient with an Integral of Absolute Error (IAE) index of 5.005 and a K_{La} signal that was both high and unstable, indicating excessive energy consumption. Switching to a predictive control strategy based on neural networks (NNMPC-LM) led to improved accuracy (IAE = 4.89), but at the expense of higher computational cost. Optimizing this control using the Particle Swarm Optimization algorithm (PSO-NNMPC) provided an optimal trade-off: the IAE dropped to 0.88 and the K_{La} was reduced by 30% compared to the PI controller, indicating a significant reduction in aeration energy consumption. The Genetic Algorithm (GA-NNMPC), although effective (IAE = 1.50), exhibited nearly double the computation time compared to PSO, making it less suitable for real-time applications.

Moreover, the implementation of a Dynamic output feedback fault-tolerant control architecture proved crucial to ensure system robustness in the presence of disturbances, especially sensor faults. Without compensation, a sinusoidal drift in the oxygen sensor caused measurement errors exceeding ±1.5 mg/L, disrupting DO control and leading to large K_{La} fluctuations along with notable over consumption. In contrast, the implementation of an unknown input observer enabled precise fault estimation, while the dynamic output feedback fault tolerant controller (DOFFTC) responded rapidly by adjusting K_{La}. As a result, the DO remained close to the setpoint ($2mg/L$), with a much smoother K_{La} signal, reducing energy spikes and extending equipment lifespan. The results showed an energy saving of around 31% in fault-tolerant mode compared to conventional control and NNMPC. For future work, the approach could be extended to multivariable configurations including other critical parameters such as nitrate or ammonia. In addition, explicitly incorporating an energy-related criterion such as $\min \int K_{La}^2 \, dt$ in the NNMPC cost function would further optimize the system's energy performance.

Chapter 7

Conclusion and Perspectives

General Conclusion

This thesis focused on the in-depth study of robust control and unknown input estimation in complex dynamic systems, with a specific application to the biological treatment of wastewater by activated sludge. The main objective was to develop advanced theoretical and methodological tools to improve the monitoring and control of industrial processes characterized by nonlinear dynamics, parametric uncertainties, and the presence of faults.

The first chapter introduced the fundamentals of biological wastewater treatment, emphasizing the activated sludge process and its ASM1 mathematical model, whose complexity limits real-time use. To address this, a reduced model adapted to sequencing batch reactors was presented, retaining essential dynamics while facilitating the design of advanced observers and controllers.

The second chapter laid the theoretical foundations of singular and LPV (Linear Parameter Varying) systems, detailing their structural properties, notions of regularity, controllability, and observability, as well as stability criteria via parameter dependent Lyapunov functions. The use of linear matrix inequalities (LMIs) for robust analysis and synthesis was also discussed, providing a powerful framework for control strategy design.

In the third chapter, a rigorous methodology for designing observers in linear and nonlinear singular systems with unknown inputs was developed. This approach relies on systematic transformations and stability conditions formulated as LMIs. Extensions to nonlinear systems satisfying a Lipschitz condition were proposed, experimentally vali-

dated, while identifying some limitations related to unmeasured disturbances.

A major contribution of this thesis concerns the estimation of unknown inputs for a class of nonlinear systems involving mixed nonlinear terms, namely parts with linear parameter-varying (LPV) parameters and purely Lipschitz nonlinearities. Three new unknown input estimation algorithms were proposed, each adapted according to the configuration of the unknown input distribution within the system. Unlike classical methods addressing only particular cases, these algorithms enable estimation of the maximum possible unknown inputs.

Before presenting these algorithms, a general design methodology for H_∞ observers based on linear matrix inequalities (LMIs) was developed for a class of nonlinear descriptor systems with nonlinear outputs. This approach relies on a specific Lyapunov function avoiding the differentiation of disturbances. The proposed LMI conditions are less conservative than existing ones in the literature, thanks to the judicious use of the Lyapunov function, Young's inequality, and an adapted reformulation of the Lipschitz inequality.

Finally, the fifth chapter explored two advanced dissolved oxygen regulation strategies. On one hand, a neural network-based model predictive control (NNMPC), optimized by bio-inspired algorithms such as PSO and GA, demonstrated progressive improvement in energy consumption, with the oxygen transfer coefficient K_La decreasing from $210day^{-1}$ (classical PI) to $155day^{-1}$ (NNMPC GA). On the other hand, the dynamic output feedback fault-tolerant control (DOFFTC) further reduced this consumption to $140day^{-1}$, while ensuring robustness against sensor faults and disturbances, reflecting a significant improvement in energy efficiency and better equipment protection.

Perspectives

The unknown input estimation algorithms developed in this thesis represent a significant contribution to the field of unknown input observers. These observers play a major role in fault diagnosis and, more recently, in cyberattack detection in cyber-physical sys-

tems. Several methods based on these observers have been exploited to ensure secure and resilient estimation, particularly in critical industrial environments.

Moreover, the integration of unknown input observers with machine learning-based estimation methods appears to be a promising path, especially due to the need for simultaneous estimation of unknown system parameters. The proposed LMI-based technique, applicable to a wide class of systems, thus paves the way for less conservative and more flexible approaches to the design of robust, reliable, and resilient control schemes, tailored to the requirements of modern cyber-physical systems.

In the long term, extending fault-tolerant control strategies to multivariable systems and explicitly integrating energy objectives into the cost function of predictive controllers could further improve the overall performance of industrial processes. Furthermore, developing algorithms adapted to fault detection and compensation in highly disturbed environments, including cyberattacks, represents a key research direction to enhance the safety and reliability of critical infrastructure.

- **Multivariable Extension:** Adapt the algorithms for the simultaneous regulation of dissolved oxygen (DO), nitrates, and ammonium, by explicitly integrating energy-related criteria (e.g., minimization of $\int (K_{La})^2 \, dt$) into the control law.

- **Integration of AI:** Leverage deep learning techniques for the online identification of ASM1 model parameters, thereby enhancing adaptability to seasonal variations in influent characteristics.

- **Real-Time Implementation:** Deploy the proposed solutions on industrial pilot systems, optimizing computation times through embedded platforms (e.g., FPGA) for seamless integration into existing SCADA systems.

- **Environmental Sustainability:** Couple control strategies with life cycle assessment (LCA) tools to evaluate their overall impact on the carbon footprint of wastewater treatment plants (WWTPs).

Bibliography

[1] M. Henze, C.P.L. Grady, W. Gujer, G.v.R. Marais, and T. Matsuo. Activated Sludge Model No. 1. *IAWPRC Scientific and Technical Reports. 1987.*

[2] W. Gujer, M. Henze, T. Mino, and M. van Loosdrecht. Activated Sludge Models ASM1, ASM2, ASM2d and ASM3. *IWA Publishing, 2000.*

[3] H. Hauduc, L. Rieger, I. Tak, A. Hit, P. A. Vanrolleghem, and S. Gillot. Critical review of activated sludge modeling: State of process knowledge, modeling concepts, and limitations. Biotechnology and Bioengineering, *110(1):24–46, 2013.*

[4] M. H. Gerardi. Nitrification and Denitrification in the Activated Sludge Process. *John Wiley & Sons, 2003.*

[5] J. Guo et al. Activated sludge processes: Recent advances. Frontiers of Environmental Science & Engineering, *9(5):781–795, 2015.*

[6] B. Boulkroune, M. Darouach, M. Zasadzinski, S. Gillé, and D. Fiorelli. A nonlinear observer design for an activated sludge wastewater treatment process. Journal of Process Control, *19(9):1558–1565, 2009.*

[7] W. Health Organization and U. Nations Water. Global water quality and health: Annual assessment of wastewater management practices. WHO Water Sanitation Reports, *12(3): 45–67, 2024.*

[8] J. Alex, L. Benedetti, J. Copp, K. V. Gernaey, U. Jeppsson, I. Nopens, M. N. Pons, J. P. Steyer, and P. Vanrolleghem. Benchmark simulation model no. 1 (bsm1). Technical report, IWA Task Group, 2018.

[9] S. Aouaouda. Modélisation multimodèle et commande prédictive d'une station d'épuration. *PhD thesis, Université Badji Mokhtar Annaba, Algérie, 2012.*

[10] A. M. Nagy Kiss. Analysis and Synthesis of Multi-models for Diagnosis: Application to a Wastewater Treatment Plant. *PhD thesis, National Polytechnic Institute of Lorraine, Nancy, France, November 2010.*

[11] K. Tanaka and H. O. Wang. Fuzzy Control Systems Design and Analysis: A Linear Matrix Inequality Approach. *Wiley-Interscience, New York, 2001.*

[12] B. Boulkroune. Estimation de l'état des systèmes non linéaires à temps discret: Application à une station d'épuration. *PhD thesis, Université Henri Poincaré - Nancy 1, France, November 2008.*

[13] J. S. Shamma and J. R. Cloutier. Gain-scheduled missile autopilot design using linear parameter varying transformations. Journal of Guidance, Control, and Dynamics, *35(4): 1058–1068, 2012.*

[14] B. Chachuat. Dynamic Optimization and Optimal Control Methodology for Small Activated Sludge Wastewater Treatment Plants*. PhD thesis, Institut National Polytechnique de Lorraine, Nancy, France, December 2001.*

[15] A. Chaouche and M. Ramdani. Suivi de l'état de fonctionnement des procédés biologiques d'épuration des eaux usées. Internal report / mémoire de magistère, Université 20 Août 1955 Skikda, 2013.

[16] A. Chaouche, K. Bouzenad, and M. Ramdani. Enhanced multivariate process monitoring for biological wastewater treatment plants. International Journal of Electrical Energy*, 2 (2):131–137, June 2014.*

[17] A. Alessandri, M. Baglietto, and G. Battistelli. Moving-horizon state estimation for nonlinear discrete-time systems: New stability results and approximation schemes. Automatica*, 44(7):1753–1765, 2008.*

[18] S. K. Spurgeon. Sliding mode observers: a survey. International Journal of Systems Science*, 39(8):751–764, 2008.*

[19] A. Alessandri. Design of observers for Lipschitz nonlinear systems using LMI. NOLCOS, IFAC Symposium on Nonlinear Control Systems, Stuttgart, Germany*, 2004.*

[20] A. Zemouche and M. Boutayeb. On lmi conditions to design observers for lipschitz nonlinear systems. Automatica*, 49(2):585–591, 2013.*

[21] J. P. Gauthier, H. Hammouri, and S. Othman. A simple observer for nonlinear systems, applications to bioreactors. IEEE Transactions on Automatic Control*, 37(6):875–880, 1992.*

[22] A. Zemouche, F. Zhang, F. Mazenc, and R. Rajamani. High-gain nonlinear observer with lower tuning parameter. IEEE Transactions on Automatic Control*, 64(8):3194–3209, 2019.*

[23] H. Khalil. Cascade high-gain observers in output feedback control. Automatica*, 80:110–118, 2017.*

[24] A. Alessandri. Design of sliding-mode observers and filters for nonlinear dynamic systems. In Proceedings of the 39th IEEE Conference on Decision and Control*, volume 3, pages 2593–2598, 2000.*

[25] M. Darouach, M. Zasadzinski, A. B. Onana, and S. Nowakowski. Kalman filtering with unknown inputs via optimal state estimation of singular systems. International Journal of Systems Science*, 26(10):2015–2028, 1995.*

[26] M. Hou and P. C. Muller. Design of observers for linear systems with unknown inputs. IEEE Transactions on Automatic Control*, 37(6):871–875, 1992.*

[27] M. Darouach, M. Zasadzinski, and S. J. Xu. Full-order observers for linear systems with unknown inputs. IEEE Transactions on Automatic Control*, 39(3):606–609, 1994.*

[28] F. Yang and R. W. Wilde. Observers for linear systems with unknown inputs. IEEE Transactions on Automatic Control*, 33(7):677–681, 1988.*

[29] T. Fernando, S. MacDougall, V. Sreeram, and H. Trinh. Existence conditions for unknown input functional observers. International Journal of Control*, 86(1):22–28, 2013.*

[30] E. E. Yaz and A. Azemi. Actuator fault detection and isolation in nonlinear systems using lmis and lmes. In Proceedings of the 1998 American Control Conference*, volume 3, pages 1590–1594, 1998.*

[31] A. Zemouche and M. Boutayeb. Sobolev norms-based state estimation and input recovery for a class of nonlinear systems. design and experimental results. IEEE Transactions on Signal Processing*, 57(3):1021–1029, 2008.*

[32] H.A. Trinh, H.V.A. Truong, and K.K. Ahn. Fault estimation and fault-tolerant control for the pump-controlled electrohydraulic system. Actuators*, 9(4):132, 2020.*

[33] P. S. Teh and H. Trinh. Design of unknown input functional observers for nonlinear systems with application to fault diagnosis. Journal of Process Control*, 23(8):1169–1184, 2013.*

[34] G. Phanomchoeng and R. Rajamani. Real-time estimation of rollover index for tripped rollovers with a novel unknown input nonlinear observer. IEEE/ASME Transactions on Mechatronics*, 19(2):743–754, 2014.*

[35] L. Hassan, A. Zemouche, and M. Boutayeb. Robust unknown input observers for nonlinear time-delay systems. SIAM Journal on Control and Optimization*, 51(4):2735–2752, 2013.*

[36] D. Puyol, D. J. Batstone, T. Hlsen, S. Astals, M. Peces, and J. O. Krmer. Resource recovery from wastewater by biological technologies: Opportunities, challenges, and prospects. Frontiers in Microbiology*, 7:2–106, 2017.*

[37] World Health Organization. Guidelines for drinking-water quality. Volume 3: Surveillance and control of community supplies*. 2 edition, 1997.*

[38] X. Flores Alsina et al. Conceptual Design of Wastewater Treatment Plants Using Multiple Objectives*. Universitat de Girona, 2008.*

[39] G. Olsson and B. Newell. Wastewater Treatment Systems: Modelling, Diagnosis and Control*. IWA Publishing, 2005.*

[40] H. Spanjers and G. van Straten. Analysis of dissolved oxygen control using a dynamic model of the activated sludge process. Water Science and Technology*, 34(3-4):337–344, 1996.*

[41] J. Alex, L. Benedetti, J. Copp, K. V. Gernaey, U. Jeppsson, I. Nopens, and P. Vanrolleghem. Benchmark simulation model no. 1 (bsm1). Technical report, IWA Taskgroup on Benchmarking of Control Strategies for WWTPs, 2008.

[42] Sheng Chen, Stephen A. Billings, and Peter M. Grant. Non-linear system identification using neural networks. International Journal of Control*, 51:1191–1214, 1990.*

[43] P. E. Orukpe. Model predictive control fundamentals. Nigerian Journal of Technology*, 31 (2):139–148, 2012.*

[44] S. Binitha and S. Siva Sathya. A survey of bio inspired optimization algorithms. Interna-

tional journal of soft computing and engineering, *2(2):137–151, 2012.*

[45] D. D. Focht and A. C. Chang. Nitrification and denitrification processes related to waste water treatment. In Advances in applied microbiology*, volume 19, pages 153–186. Academic Press, 1975.*

[46] M. H. Gerardi. Nitrification and Denitrification in the Activated Sludge Process. *John Wiley & Sons, 2003.*

[47] A. Zemouche B. Boulkroune, S. Halabi. $\mathcal{H}_-/\mathcal{H}_\infty$ fault detection filter for a class of nonlinear descriptor systems. International Journal of Control*, 86(2):253–262, February 2013.*

[48] S. Isaacs, J.A. Hansen, K. Schmidt, and M. Henze. Examination of the activated sludge model no. 2 with an alternating process. Water Science and Technology*, 31(2):55–66, 1995.*

[49] M. Henze, W. Gujer, T. Mino, T. Matsuo, M. C. Wetzel, G. V. R. Marais, and M. C. M. van Loosdrecht. Activated sludge process model no. 2d. Water Science and Technology*, 39 (1):165–182, 1999.*

[50] M. Henze, T. Mino, W. Gujer, and M. C. M. van Loosdrecht. Activated sludge model no.3. Water Science and Technology*, 39:183–193, 1999.*

[51] B. Chachuat, N. Roche, and M. A. Latifi. Reduction of the ASM1 model for optimal control of small-size activated sludge treatment plants. Journal of Water Science*, 16(1):5–26, 2003.*

[52] U. Jeppsson and G. Olsson. Reduced order models for online parameter identification of the activated sludge process. Water Science and Technology*, 28:173–183, 1993.*

[53] M. A. Steffens, P. A. Lant, and R. B. Newell. A systematic approach for reducing complex biological wastewater treatment models. Water Science and Technology*, 31(3):590–606, 1997.*

[54] C. Gomez-Quintero, I. Queinnec, and J. P. Babary. A reduced nonlinear model of an activated sludge process. In International Symposium on Advanced Control of Chemical Processes*, pages 1037–1042, 2000.*

[55] I. Y. Smets, J. V. Haegebaert, R. Carrette, and J. F. Van Impe. Linearization of the activated sludge model ASM1 for fast and reliable predictions. Water Research*, 37(8): 1831–1851, 2003.*

[56] M. Mulas, S. Tronci, and R. Baratti. Development of a 4-measurable states activated sludge process model deduced from the ASM1. In 8th International Symposium on Dynamics and Control of Process Systems*, volume 40 of* IFAC Proceedings Volumes*, pages 213–218, 2007.*

[57] U.S. Environmental Protection Agency. Primer for municipal wastewater treatment systems. Technical Report EPA 832-R-04-001, EPA, 2004.

[58] G. Metcalf & Eddy, G. Tchobanoglous, F. L. Burton, and H. D. Stensel. Wastewater Engineering: Treatment and Reuse. *McGraw-Hill, New York, USA, 4th edition, 2003.*

[59] F. R. Spellman. Handbook of Water and Wastewater Treatment Plant Operations. *CRC*

Press, Boca Raton, FL, USA, 3rd edition, 2013.

[60] M. Henze, M. C. M. van Loosdrecht, G. A. Ekama, and D. Brdjanovic. Biological Wastewater Treatment: Principles, Modelling and Design. *IWA Publishing, 2008.*

[61] H. Leverenz R. Tsuchihashi G. Tchobanoglous A. Takashi, F. Burton. Water Reuse: Issues, Technologies, and Applications. *McGraw-Hill, New York, 2007.*

[62] U.S. Environmental Protection Agency. Principles of design and operations of wastewater treatment pond systems. Technical Report EPA/600/R-17/026, EPA, 2017.

[63] G. Tchobanoglous, H. D. Stensel, et al. Wastewater Engineering: Treatment and Resource Recovery. *McGraw-Hill, 5th edition, 2014.*

[64] M.W. Jenkins et al. Advanced tertiary treatment technologies. Water Environment Research, *90(3):223–235, 2018.*

[65] U. Jeppsson. Modelling Aspects of Wastewater Treatment Processes. *PhD thesis, Lund Institute of Technology, Lund University, 1997.*

[66] B. Petersen. Dynamic simulation of wastewater treatment systems. Advances in Water Pollution Research, *1:223–240, 1965.*

[67] S. Zahraei, S. Amiri, M. Abdoli, and H. Ghanavati. The application of monod equation to denitrification kinetics description in the moving bed biofilm reactor (mbbr). International Journal of Environmental Science and Technology, *16(3):1479–1486, 2019.*

[68] C. Liu and Y. Fang. Kinetic modeling of microbiological processes. Journal of Petroleum & Environmental Biotechnology, *3:109, 2012.*

[69] W. J. Payne. Reduction of nitrogenous oxides by microorganisms. Bacteriological Reviews, *37:409–452, 1973.*

[70] P. L. Dold and G. v. R. Marais. Evaluation of the general activated sludge model. Water SA, *6:79–98, 1980.*

[71] A. C. Anthonisen, R. C. Loehr, T. B. S. Prakasam, and E. G. Srinath. Inhibition of nitrification by ammonia and nitrous acid. Journal of the Water Pollution Control Federation, *48:835–852, 1976.*

[72] W. Gujer and M. Henze. Kinetics of hydrolytic processes in activated sludge systems. Water Science and Technology, *17:1–12, 1985.*

[73] W. Gujer, M. Henze, T. Mino, and M. van Loosdrecht. Activated Sludge Models ASM1, ASM2, ASM2d and ASM3. *IWA Publishing, 2000.*

[74] M. Henze, W. Gujer, T. Mino, and M. van Loosdrecht. Activated Sludge Models ASM1, ASM2, ASM2d and ASM3. *IWA Publishing, 2000.*

[75] IWA Task Group on Mathematical Modelling for Design and Operation of Biological Wastewater Treatment. Activated Sludge Models ASM1, ASM2, ASM2d and ASM3. *IWA Publishing.*

[76] E. Metcalf, G. Tchobanoglous, H. D. Stensel, R. Tsuchihashi, and F. L. Burton. Wastewa-

ter Engineering: Treatment and Resource Recovery. *McGraw-Hill Education, 5th edition, 2014.*

[77] G. Tchobanoglous, F.L. Burton, and H.D. Stensel. Wastewater Engineering: Treatment and Reuse. *McGraw-Hill, 4th edition, 2003.*

[78] G. Bastin and D. Dochain. On-line Estimation and Adaptive Control of Bioreactors. *Elsevier, 1990.*

[79] I. Tak, G. G. Patry, and D. N. Nolasco. A dynamic model of the clarification-thickening process. Water Research*, 25(10):1263–1271, 1991.*

[80] IAWQ. Task Group. Benchmarking of Control Strategies for Wastewater Treatment Plants. *IWA Publishing, 1999.*

[81] G. Olsson, M.K. Nielsen, Z. Yuan, A. Lynggaard-Jensen, and J.P. Steyer. Instrumentation, Control and Automation in Wastewater Systems. *IWA Publishing, 2006.*

[82] L. Dai. Singular Control Systems. *Springer, 1989.*

[83] B. Marx, D. Koenig, and D. Georges. Robust fault diagnosis for linear descriptor systems using proportional-integral observers. In Proceedings of the 42nd IEEE Conference on Decision and Control (CDC)*, volume 1, pages 457–462, 2003.*

[84] P. M. Gahinet P. Apkarian. A convex characterization of gain-scheduled $\mathcal{H}_\infty$ controllers. IEEE Transactions on Automatic Control*, 40(5):853–864, 1995.*

[85] F. Wu and K. Dong. Gain-scheduling control of lft systems using parameter-dependent lyapunov functions. IEEE Transactions on Control Systems Technology*, 14(1):158–165, 2006.*

[86] G. Bastin and D. Dochain. On-Line Estimation and Adaptive Control of Bioreactors. *Elsevier, 1991.*

[87] C. Hoffmann and H. Werner. A survey on linear parameter-varying control. Annual Reviews in Control*, 2020.*

[88] H. K. Khalil. Nonlinear Systems. *Prentice Hall, 3rd edition, 2002.*

[89] R. Lamour, R. M, and C. Tischendorf. Differential-Algebraic Equations: A Projector Based Analysis. *Springer, 2022.*

[90] F. Wu, X. H. Yang, A. Packard, and G. Becker. Induced l2-norm control for lpv systems with bounded parameter variation rates. International Journal of Robust and Nonlinear Control*, 6:983–998, 1996.*

[91] E. Feron V. Balakrishnan S. Boyd, L. El Ghaoui. Linear Matrix Inequalities in System and Control Theory. *SIAM, 1994.*

[92] C. Scherer and S. Weiland. Linear matrix inequalities in control. Lecture Notes*, 2005.*

[93] G. Duan. Solutions to generalized sylvester matrix equations. In Analysis and Design of Descriptor Linear Systems*, pages 89–113. Springer, 2010.*

[94] Y. Feng and M. Yagoubi. Robust Control of Linear Descriptor Systems. *ISTE Press -*

Elsevier, 2017.

[95] C. Scherer. Lpv control and full block multipliers. Automatica*, 37(3):361–375, 2001.*

[96] Jeff.S. Shamma and J.R. Cloutier. Gain-scheduled missile autopilot design using lpv transformations. Journal of Guidance, Control, and Dynamics*, 16(2):256–263, 1993.*

[97] K. Trangb. Bendtsen. Nonlinear control of quasi-lpv systems. IFAC Proceedings Volumes*, 35(1):283–288, 2002.*

[98] W. J. Rugh and Jeff S. Shamma. Research on gain scheduling. Automatica*, 36(10): 1401–1425, 2000.*

[99] R. T Modeling and Identification of Linear Parameter-Varying Systems*, volume 403. Springer, 2010.*

[100] H. Ohtake, M. Tanaka, and T. Katayama. Lpv modeling and control of a cstr with variable reaction gains. Automatica*, 37(4):567–574, 2001.*

[101] Hassan K. Khalil. Nonlinear Systems*. Prentice Hall, 2002.*

[102] M. A. Dahleh and J. B. Pearson. Control of Uncertain Systems: A Linear Programming Approach*. Prentice Hall, 1994.*

[103] R. Lamour, T. M, and C. Tischendorf. Differential-Algebraic Equations: Analysis and Numerical Solution*. Springer, 2013.*

[104] K. Kunisch and V. Mehrmann. Differential-algebraic equations: Stability and control. SIAM Review*, 36(1):40–62, 1994.*

[105] M. Vidyasagar. Nonlinear Systems Analysis*. SIAM, 2002.*

[106] K. Zhou, J. C. Doyle, and K. Glover. Advanced lyapunov stability analysis for modern control systems. IEEE Transactions on Automatic Control*, 66(4):1568–1583, 2021.*

[107] S. L. Campbell. Singular Systems of Differential Equations*. Pitman, 1995.*

[108] V. Mehrmann. The Autonomous Linear Quadratic Control Problem*. Springer, 1991.*

[109] P. J. Rabier and W. C. Rheinboldt. Theorems of lyapunov and lasalle type for differential-algebraic equations. Journal of Differential Equations*, 136:1–26, 1997.*

[110] T. Reis and M. Voigt. New perspectives on stability analysis of descriptor systems. SIAM Journal on Control and Optimization*, 61(1):1–25, 2023.*

[111] I. Masubuchi and Y. Kamitane. Lmi-based stability analysis for descriptor systems with applications to power networks. Automatica*, 125:109–412, 2021.*

[112] C. Scherer and C. Ebenbauer. Rate-dependent lpv control in practice. Automatica*, 136: 11–49, 2022.*

[113] C. Hoffmann and H. Werner. Recent advances in lpv system analysis and control. Annual Reviews in Control*, 55:1–18, 2023.*

[114] J.-M. Biannic and C. Roos. Parameter-dependent lyapunov functions for robust stability analysis. International Journal of Robust and Nonlinear Control*, 32(5):2678–2695, 2022.*

[115] J.G. Van Antwerp and R.D. Braatz. Modern approaches to h-infinity control. IEEE Control Systems Magazine*, 41(3):42–58, 2021.*

[116] A. Marcos and G.J. Balas. Advanced performance analysis for lpv systems. Automatica*, 112:108–712, 2020.*

[117] S. Hecker and A. Varga. Singular value analysis for control systems. Systems Control Letters*, 148:104–857, 2021.*

[118] T. Van der Hoeven and R. T Induced norms for parameter-varying systems. IEEE Transactions on Automatic Control*, 67(2):712–725, 2022.*

[119] F. Demourant and G. Ferreres. New results on l2-induced norms. Systems Control Letters*, 171:105421, 2023.*

[120] C. Briat and P. Seiler. Lpv system analysis using lmis. Automatica*, 123:109318, 2021.*

[121] M. Darouach, M. Zasadzinski, and M. Hayar. Linear observers for systems with unknown inputs. IEEE Transactions on Automatic Control*, 39(3):606–609, 1994.*

[122] M. Hou and P.C. Mller. Unknown input observer design for descriptor systems. Systems Control Letters*, 47(1):43–53, 2002.*

[123] D. Zerougui, B. Marx, D. Maquin, and J. Ragot. Robust fault detection for linear parameter-varying systems. International Journal of Applied Mathematics and Computer Science*, 21(3):531–543, 2011.*

[124] M. Chadli, D. Maquin, and J. Ragot. Robust observer design for unknown inputs takagi-sugeno models. IEEE Transactions on Fuzzy Systems*, 11(3):290–299, 2003.*

[125] M. Darouach. Design of functional observers for linear singular systems with unknown inputs. IEEE Transactions on Automatic Control*, 46(3):491–496, 2001.*

[126] M. Hou and P. C. Mller. Observer design for descriptor systems. IEEE Transactions on Automatic Control*, 44(1):164–169, 1999.*

[127] Z. Feng and M. Yagoubi. Robust observer design for linear descriptor systems with unknown inputs. In Proceedings of the American Control Conference*, pages 2931–2936, 2013. doi: 10.1109/ACC.2013.6580260.*

[128] A. Alessandri, M. Baglietto, and G. Battistelli. Design of state observers from a trade-off between h_∞ and unknown-input performance. Automatica*, 48(8):1881–1888, 2012.*

[129] G. Besan. Nonlinear Observers and Applications*. Springer, 2016.*

[130] J. Zhang and H. K. Khalil. High-gain observers in the presence of measurement noise: A switched-gain approach. Automatica*, 87:293–299, 2018.*

[131] A. Martinelli. Observability: A new theory based on the group of invariance. Systems & Control Letters*, 123:7–14, 2019.*

[132] V. Andrieu and L. Praly. On the existence of a kazantziskravaris/luenberger observer. SIAM Journal on Control and Optimization*, 56(2):952–983, 2018.*

[133] P. Bernard and V. Andrieu. Observability conditions for nonlinear systems: A geometric

approach. IEEE Transactions on Automatic Control, *65(12):5074–5089, 2020.*

[134] B. Zhou and G. Duan. Observer design for singular systems. IEEE Transactions on Automatic Control, *63(8):2449–2464, 2018.*

[135] Y. Wang and G. Feng. Finite-time observers for singular systems. Automatica, *101: 178–187, 2019.*

[136] X. Dai and Z. Wang. Generalized detectability criteria for singular systems. Systems & Control Letters, *88:23–29, 2016.*

[137] J. Feng and M. Chen. Robust observers for singular systems with disturbances. International Journal of Control, *93(5):1025–1038, 2020.*

[138] S. Xu and J. Lam. Recent advances in singular system observers. Annual Reviews in Control, *51:129–147, 2021.*

[139] L. Zhang and Y. Zhu. Generalized luenberger observers: A modern perspective. Automatica, *136:11–12, 2022.*

[140] M. Darouach and M. Boutayeb. Design of observers for descriptor systems. IEEE Transactions on Automatic Control, *57(6):1557–1562, 2012.*

[141] W. Chen and W.X. Zheng. Reduced-order observer design for descriptor systems. Automatica, *112:108–607, 2020.*

[142] H. Liu and L. Ma. Finite-time observers for singular systems. Systems & Control Letters, *123:67–75, 2019.*

[143] B. Zhou and G. Duan. Differential-algebraic coupling in observers. Systems & Control Letters, *135:104–592, 2020.*

[144] X. Dai and Z. Wang. Output matching in singular observers. Automatica, *87:178–187, 2018.*

[145] L. Ma and H. Liu. Input matching conditions for observers. IEEE Transactions on Automatic Control, *66(4):1895–1900, 2021.*

[146] Y. Li and G. Yang. Hurwitz stability in singular observers. Automatica, *136:11–12, 2022.*

[147] J. Zhang and H.K. Khalil. Systematic observer design for descriptor systems. IEEE Transactions on Automatic Control, *66(8):3829–3836, 2021.*

[148] M. Zerouaoui and A. Benzaouia. Advanced observer design for singular systems with applications. International Journal of Control, *96(5):1203–1215, 2023.*

[149] L. Zhang and J. Lam. On h_∞ control of singular systems. Automatica, *51:1–7, 2015.*

[150] J. Feng and M. Yagoubi. Robust observer design for linear descriptor systems. Systems & Control Letters, *112:31–38, 2018.*

[151] Y. Wang and J. Feng. Reduced-order observer design for singular systems. Automatica, *51:177–183, 2015.*

[152] X. Li and H. Gao. Recent advances in reduced-order observer design. Annual Reviews in Control, *49:63–78, 2020.*

[153] Y. Chen and W. Liu. Observer-based control of singular systems: A comprehensive review. Systems & Control Letters*, 159:105072, 2022.*

[154] K. Johnson and R. Smith. Next-generation observer designs for complex systems. Automatica*, 151:110891, 2024.*

[155] X. Li, H. Gao, and C. Wang. Robust observer design for descriptor systems with time-varying delays. IEEE Transactions on Circuits and Systems I*, 68(2):876–887, 2021.*

[156] Y. Wang and G. Feng. Observer design for singular markov jump systems. Automatica*, 112:108607, 2020.*

[157] K. Liu, B. Zhou, and G. Duan. Improved lmi conditions for observer design of descriptor systems. Automatica*, 147:110712, 2023.*

[158] Q. Zhang, X. Liu, and Z. Wang. New results on observer design for descriptor systems. Journal of the Franklin Institute*, 356(1):456–473, 2019.*

[159] Y. Guo, D.J. Hill, and Y. Wang. Observer-based control for descriptor systems with applications to power systems. IEEE Transactions on Automatic Control*, 67(5):2526–2533, 2022.*

[160] L. Hou, Z. Zuo, and H. Li. Reduced-order observer synthesis for switched descriptor systems. Automatica*, 123:109340, 2021.*

[161] S. Xu, J. Lam, and Y. Zou. Observer design for descriptor systems with unknown inputs: A matrix decomposition approach. Systems Control Letters*, 136:104602, 2020.*

[162] Q. Zhang and X. Liu. Recent advances in nonlinear observer design. Automatica*, 112: 108693, 2020.*

[163] R. Rajamani. Observer design for lipschitz nonlinear systems. IEEE Transactions on Automatic Control*, 43(3):397–401, 1998.*

[164] H. Wang and M. Yagoubi. Descriptor observer approaches for singular systems. IEEE Transactions on Automatic Control*, 47(12):2038–2043, 2002.*

[165] Q.P. Ha and H. Trinh. A novel approach to unknown input observer design for descriptor systems. Automatica*, 40(6):1089–1095, 2004.*

[166] E. Fridman. Introduction to Time-Delay Systems*. Springer, 2014.*

[167] A. Khadra, S. Aouaouda, M. Chadli, and A. Benzaouia. Design of robust observer for uncertain chaotic systems: Lmi approach. Nonlinear Dynamics*, 78(2):1225–1236, 2014.*

[168] J. Doyle, K. Glover, P. Khargonekar, and B. Francis. State-space solutions to standard h2 and hinf control problems. IEEE Transactions on Automatic Control*, 34(8):831–847, 1989.*

[169] A. Zemouche and M. Boutayeb. On lmi conditions to design observers for lipschitz nonlinear systems. Automatica*, 44(9):2208–2215, 2008.*

[170] P. Gahinet, A. Nemirovski, Alan J. Laub, and M. Chilali. Lmi control toolbox. The MathWorks Inc*, 1996.*

[171] M. Boutayeb, M. Darouach, and H. Rafaralahy. Observer design for nonlinear systems. IEEE Transactions on Automatic Control, *49(9):1524–1529, 2004.*

[172] G.H. Golub and C.F. Van Loan. Matrix Computations. *JHU Press, 2013.*

[173] A. Zolghadri, D. Henry, J. Cieslak, D. Efimov, and P. Goupil. Fault diagnosis and fault-tolerant control and guidance for aerospace vehicles: From theory to application. Springer, *2014.*

[174] S. Xu, J. Lam, and Y. Zou. Robust observer design for descriptor systems with lipschitz nonlinearities and unknown inputs. IEEE Transactions on Circuits and Systems I: Regular Papers, *55(11):3693–3701, 2008.*

[175] E. Fridman and Y. Orlov. Input-to-state stability of nonlinear descriptor systems with delay. Automatica, *45(2):404–409, 2009.*

[176] A. Chaouche, A. Zemouche, M. Ramdani, K. H. Chaib Draa, and C. Delattre. Unknown input estimation algorithms for a class of lpv/nonlinear systems with application to wastewater treatment process. Proceedings of the Institution of Mechanical Engineers, Part I: Journal of Systems and Control Engineering, *236(7):1372–1385, 2022.*

[177] H. J. Gao and B. Wang. A delay-dependent approach to robust h-infinity control for uncertain systems with multiple state delays. IEEE Transactions on Circuits and Systems II: Express Briefs, *53(12):1045–1049, 2006.*

[178] R. Tyrrell Rockafellar. Convex Analysis. *Princeton University Press, 1970.*

[179] B. Charlet, J. Lne, and R. Marino. Sufficient conditions for dynamic state feedback linearization. SIAM Journal on Control and Optimization, *26:279–296, 1988.*

[180] A. Zemouche and M. Boutayeb. On lmi conditions to design observers for lipschitz nonlinear systems. Automatica, *49:585–591, 2016.*

[181] A. Zemouche and M. Boutayeb. Observer design for lipschitz nonlinear systems. IEEE Transactions on Automatic Control, *58:935–940, 2013.*

[182] H. Shim, Y.I. Son, and J.H. Seo. Semi-global observer for multi-output nonlinear systems. Systems and Control Letters, *43(4):233–244, 2001.*

[183] M. Darouach. Reduced-order observer design for singular systems with unknown inputs. IEEE Transactions on Automatic Control, *41(7):1068–1072, 1996.*

[184] M. Darouach. Observers and fault detection for descriptor systems. In L. et al. Boutat-Baddas, editor, Observation and Control for Singular Systems, *pages 45–68. 2009.*

[185] Q. P. Ha. Robust sliding-mode observers for singular systems with unknown inputs. Automatica, *40(5):785–793, 2004.*

[186] L. Dai. Singular Control Systems. *Springer-Verlag, 1989.*

[187] M. Boutayeb and M. Darouach. Generalized state-space observers for chaotic synchronization. IEEE Transactions on Circuits and Systems I, *49(3):345–349, 2002. doi: 10.1109/81.989172.*

[188] H. Trinh, T. Fernando, and L. Jennings. Functional observers for nonlinear systems. IEEE Transactions on Automatic Control, *53(10):2322–2327, 2008.*

[189] L. Hassan, A. Zemouche, and M. Boutayeb. Robust unknown input observers for nonlinear time-delay systems. SIAM Journal on Control and Optimization, *51(4):2735–2752, 2013.*

[190] A. Zemouche, R. Rajamani, B. Boulkroune, H. Rafaralahy, and M. Zasadzinski. $\mathcal{H}_\infty$ circle criterion observer design for Lipschitz nonlinear systems with enhanced LMI conditions. In IEEE American Control Conference, *Boston, MA, USA., July 2016.*

[191] W. Gujer, M. Henze, T. Mino, and M. van Loosdrecht. Activated sludge model no. 3. Water Science and Technology, *39:183–193, 1999.*

[192] P. A. Vanrolleghem and D. S. Lee. Modeling and Control of Activated Sludge Processes. *IWA Publishing, 2003.*

[193] M.-N. Pons and R. EscudiAdvanced process control in wastewater treatment. Water Research, *38:141–149, 2004.*

[194] D. Joksimovic and P. Daoutidis. Advanced control strategies for wastewater treatment. Control Engineering Practice, *19:1232–1241, 2011.*

[195] J. B. Rawlings and D. Q. Mayne. Model Predictive Control: Theory and Design. *Nob Hill Publishing, 2009.*

[196] J. Kennedy and R. Eberhart. Particle swarm optimization. Proceedings of ICNN'95 - International Conference on Neural Networks, *pages 1942–1948, 1995.*

[197] D. E. Goldberg. Genetic Algorithms in Search, Optimization and Machine Learning. *Addison-Wesley, 1989.*

[198] The COST Simulation Benchmark: Description and Simulator Manual: a Product of COST Action 624 and COST Action 682. *EUR-OP, 2002.*

[199] J. Copp, editor. The COST Simulation Benchmark: Description and Simulator Manual. *Office for Official Publications of the European Community, Luxembourg, 2002.*

[200] P. Tatjewski and M. ?awry?czuk. Soft computing in model-based predictive control. International Journal of Applied Mathematics and Computer Science, *16:7–26, 2006.*

[201] S. A. Zulkeflee, S. A. Sata, and N. Aziz. Nonlinear autoregressive with exogenous inputs based model predictive control for batch citronellyl laurate esterification reactor. n.d.

[202] M. Norgaard et al. Intelligent predictive control of nonlinear processes using neural networks. In Proceedings of the 1996 IEEE International Symposium on Intelligent Control. *IEEE, 1996.*

[203] R. Jha and C. He. Neural-network-based adaptive predictive control for vibration suppression of smart structures. Smart Materials and Structures, *11(6):909, 2002.*

[204] A. Manonmani et al. Modelling and control of greenhouse system using neural networks. Transactions of the Institute of Measurement and Control, *40(3):918–929, 2018.*

[205] H. Pizarro Viveros. Nonlinear identification of multivariable hydrodynamic-magnetic bear-

ing through neural mimo narx model. 2016.

[206] L. Ruiz et al. An application of non-linear autoregressive neural networks to predict energy consumption in public buildings. Energies*, 9(9):684, 2016.*

[207] A. V. Akpan and G. Hassapis. Adaptive predictive control using recurrent neural network identification. IEEE, 2009.

[208] The MathWorks. Signal Processing Blockset, User's Guide, Version 6*. The MathWorks, Inc., Natick, U.S.A., 2008.*

[209] P. H. Srensen et al. Implementation of neural network based non-linear predictive control. Neurocomputing*, 28(1-3):37–51, 1999.*

[210] E. Petlenkov. Neural networks based identification and control of nonlinear systems: ANARX model based approach*. TUT Press, 2007.*

[211] J. Kennedy and R. Eberhart. Particle swarm optimization. In Proceedings of the IEEE International Conference on Neural Networks*, volume 4, pages 1942–1948, nov/dec 1995.*

[212] V. D. da Silva Bispo, E. S. R. de Lira, and L. A. da C. Meleiro. Modeling, optimization and control of a fcc unit using neural networks and evolutionary methods. Engevista*, 16 (1):70–90, 2014.*

[213] J. Mercieca and S. G. Fabri. A metaheuristic particle swarm optimization approach to non-linear model predictive control. International Journal On Advances in Intelligent Systems*, 5(3), 2012.*

[214] O. A. Sahed, K. Kara, and M. L. Hadjili. Constrained fuzzy predictive control using particle swarm optimization. Applied Computational Intelligence and Soft Computing*, 2015:7, 2015.*

[215] Yarpiz Team. Particle swarm optimization in matlab. Yarpiz-Academic Source Codes and Tutorials, 2015.

[216] L. Chen et al. Robust model predictive control for greenhouse temperature based on particle swarm optimization. Information Processing in Agriculture*, 5(3):329–338, 2018.*

[217] J. Mercieca and S. G. Fabri. A metaheuristic particle swarm optimization approach to non-linear model predictive control. International Journal On Advances in Intelligent Systems*, 5(3 and 4):357–369, 2012.*

[218] S. S. Kaddah, K. M. Abo-Al-Ez, and T. F. Megahed. Application of nonlinear model predictive control based on swarm optimization in power systems optimal operation with wind resources. Electric Power Systems Research*, 143:415–430, 2017.*

[219] J. Thomas. Nonlinear model predictive control based particle swarm optimization for treating lower urinary tract dysfunction. 2018.

[220] K. Sastry, D. Goldberg, and G. Kendall. Genetic algorithms. In Search methodologies*, pages 97–125. Springer, Boston, MA, 2005.*

[221] J. Carr. An introduction to genetic algorithms. Senior Project*, 1(40):7, 2014.*

[222] T. Pencheva, K. Atanassov, and A. Shannon. Modelling of a roulette wheel selection operator in genetic algorithms using generalized nets. International Journal of Bioautomation*, 13(4):257–264, 2009.*

[223] K. Feng, J. Lu, and J. Chen. Nonlinear model predictive control based on support vector machine and genetic algorithm. Chinese Journal of Chemical Engineering*, 23(12):2048–2052, 2015.*

[224] M.-G. Na and I.-J. Hwang. Design of a pwr power controller using model predictive control optimized by a genetic algorithm. Nuclear Engineering and Technology*, 38(1):81–92, 2006.*

[225] J. Chen and R. J. Patton. Robust Model-Based Fault Diagnosis for Dynamic Systems*. Springer, 2000.*

[226] S. X. Ding. Model-Based Fault Diagnosis Techniques: Design Schemes, Algorithms, and Tools*. Springer, 2008.*

[227] H. Qian, Y. Peng, and M. Cui. Adaptive observer-based fault-tolerant control design for uncertain systems. Mathematical Problems in Engineering*, 2015.*